Multiplex *in vitro* and *in vivo* RNAi screening to identify treatment response modifiers of targeted therapies in HCC

Von der Fakultät für Lebenswissenschaften

der Technischen Universität Carolo-Wilhelmina

zu Braunschweig

zur Erlangung des Grades

einer Doktorin der Naturwissenschaften

(Dr. rer. nat.)

genehmigte

D i s s e r t a t i o n

von Ramona Paulina Rudalska
aus Lodz / Polen

1. Referentin: Professorin Dr. Christiane Ritter
2. Referent: Professor Dr. Michael Steinert
eingereicht am: 26.08.2013
mündliche Prüfung (Disputation) am: 16.09.2014

Druckjahr 2014

Vorveröffentlichungen der Dissertation

Teilergebnisse aus dieser Arbeit wurden mit Genehmigung der Fakultät für Lebenswissenschaften, vertreten durch die Mentorin der Arbeit, in folgenden Beiträgen vorab veröffentlicht:

Publikationen

Kang, TW., Yevsa, T., Woller, N., Hoenicke, L., Wuestefeld, T., Dauch, D., Hohmeyer, A., Gereke, M., Rudalska, R., Potapova, A., Iken, M., Vucur, M., Weiss, S., Heikenwalder, M., Khan, S., Gil, J., Bruder, D., Manns, M., Schirmacher, P., Tacke, F., Ott, M., Luedde, T., Longerich, T., Kubicka, S., Zender, L.: Senescence surveillance of pre-malignant hepatocytes limits liver cancer development. Nature 479(7374): 547-551(2011).

Liu, L., Ulbrich, J., Mueller, J., Wuestefeld, T., Aeberhard, L., Kress, TR., Muthalagu, N., Rycak, L., Rudalska, R., Moll, R., Kempa, S., Zender, L., Eilers, M., Murphy, DJ.: Deregulated MYC expression induces dependence upon AMPK-related kinase 5. Nature 483(7391): 608-612 (2012).

Wuestefeld, T., Pesic, M., Rudalska, R., Dauch, D., Longerich, T., Kang, TW., Yevsa, T., Heinzmann, F., Hoenicke, L., Hohmeyer, A., Potapova, A., Rittelmeier, I., Jarek, M., Geffers, R., Scharfe, M., Klawonn, F., Schirmacher, P., Malek, NP., Ott, M., Nordheim, A., Vogel, A., Manns, MP., Zender, L.: A direct *in vivo* RNAi screen identifies MKK4 as a key regulator of liver regeneration. Cell 153(2):389-401 (2013).

Tagungsbeiträge

Rudalska, R., Dauch, D., McJunkin, K., Kang, TW., Wuestefeld, T., Geffers, R., Lowe, SW., Zender, L.: Multiplex *in vivo* RNAi screening instructs combination therapies to increase the therapeutic efficacy of the multikinase inhibitor Sorafenib. (Talk) AACR 103rd Annual Meeting, Chicago, USA (2012).

Rudalska, R., Dauch, D., McJunkin, K., Kang, TW., Wuestefeld, T., Geffers, R., Lowe, SW., Zender, L.: Multiplex *in vivo* RNAi screening instructs combination therapies to increase the therapeutic efficacy of the multikinase inhibitor Sorafenib. (Talk) Liver Cancer Conference, Heidelberg (2012).

Rudalska, R., Dauch, D., McJunkin, K., Kang, TW., Wuestefeld, T., Geffers, R., Schirmacher, P., Manns, M., Longerich, T., Lowe, SW., Zender, L.: Multiplex *in vivo* RNAi screening instructs combination therapies to increase the therapeutic efficacy of the multikinase inhibitor Sorafenib. (Poster) International Liver Cancer Association, 6th Annual Conference (ILCA), Berlin (2012).

Rudalska, R., Dauch, D., McJunkin, K., Kang, TW., Wuestefeld, T., Geffers, R., Schirmacher, P., Manns, M., Longerich, T., Lowe, SW., Zender, L.: Multiplex *in vivo* RNAi screening instructs combination therapies to increase the therapeutic efficacy of the multikinase inhibitor Sorafenib. (Poster) German Association of the Study of the Liver, 29th Annual Conference (GASL), Hannover (2013).

Moim Rodzicom

To My Parents

Table of contents:

Abbreviations

A	adenine/ ampere/ area
APS	ammonium persulfate
ATCC	american type culture collection
BCLC	barcelona clinic liver cancer
bp	base pair
BSA	bovine serum albumin
C	cytosine / celsius
cDNA	complementary DNA
CIP	calf intestine phosphatase
CLIP	cancer of the liver italian program
Dmso	dimethylsulfoxide
dNTP	2'-desoxynucleoside-5'-triphosphate
Dox	doxycycline
EDTA	ethylenediaminetetraacetic acid
e. g.	*exempli gratia* (for example)
F	farad
FCS	fetal calf serum
Fig	figure
G	guanine
GEMM	genetically engineered mouse models
gDNA	genomic DNA
H&E	haematoxylin and eosin
HBS	hepes buffered saline
HBV	hepatitis B virus
HCC	hepatocellular carcinoma
HCV	hepatitis C virus
HDI	hydrodynamic tail vein injection
HEPES	4-(2-hydroxyethyl)-1-piperazineethanesulfonic acid
HZI	helmholtz centre for infection research
IF	immunofluorescence
IRES	internal ribosomal entry site
IR/DR	inverted repeats/ direct repeats
IU	international unit
JIS	Japanese, integrated staging score
Kb	kilo base
LB	lysogeny broth
m/M	milli/molar
MAPK	mitogen-activated protein kinase
miR	microRNA
min	minute
mRNA	messenger RNA
MSCV	murine stem cell virus
n	number
NASH	nonalcoholic steatohepatitis
NGS	normal goat serum
nt	nucleotide
NTP	nucleoside-5'-triphosphate
P	phosphate/ p-value
PAA	polyacrylamide
PBS	phosphate buffered saline
PBST	phosphate buffered saline with tween
PCR	polymerase chain reaction
PEI	percutaneous ethanol injection
PFA	paraformaldehyde
qPCR	quantitative PCR
RFA	radiofrequency ablation
RNAi	RNA interference
ROMA	representation oligonucleotide microarray analysis
SB	sleeping beauty
SDS	sodium dodecyl sulfate
sec	second
Ser/S	serine
shRNA	short hairpin RNA
siRNA	small interfering RNA
SIRT	selective internal radiation therapy
SOC	super optimal broth with catabolite repression
std. dev.	standard deviation
Tab	table
TACE	transarterial chemoembolization
TAE	transarterial embolization
Taq	*Thermus aquaticus*
TBS	tris-buffered saline
TBST	tris-buffered saline with tween
Tet	tetracycline
Thr/T	threonine
T	thymine
TNM	tumor, node and metastasis
Tris	tris-(hydroxymethyl)-aminomethan
TUNEL	terminal deoxynucleotidyl transferase dUTP nick end labeling
U	uracil / units
V	volt
v/v	volume/ volume
Vs	versus
WB	western blot
w/v	weight/ volume
WT	wild type

Summary

Hepatocellular carcinoma (HCC), the third leading cause of cancer death worldwide, represents a highly chemoresistant tumor and only recently the multikinase inhibitor Sorafenib was approved as the first active systemic treatment against HCC. This illustrates that targeted therapies can be effective and therefore heralds a new era in HCC treatment. However, Sorafenib monotherapy increases survival of HCC patients by less than 3 months, thus emphasizing the strong need to understand the molecular mechanisms of Sorafenib sensitivity and resistance in order to inform new combination therapies with higher therapeutic efficacy.

Activation of the Ras/MAPK signaling pathway was reported to play a major role in liver tumor development and progression. Taking advantage of genetically defined mosaic liver cancer mouse models, it was shown that Sorafenib treatment of $Nras^{G12V}$; $p19^{Arf-/-}$ driven murine liver carcinomas results in moderate but distinct treatment responses resembling the response rates of Sorafenib treated human HCCs.

To identify genes mediating resistance or sensitivity towards Sorafenib, we conducted an *in vivo* RNAi screen. Pools of shRNAs targeting genes found amplified in human hepatocellular carcinomas were applied and $p19^{Arf-/-}$ mice harboring $Nras^{G12V}$ expressing liver carcinomas with stable expression of shRNA library pools were either treated with Sorafenib or carrier (control). After 5 weeks of treatment, shRNA distribution was quantified in tumors from both cohorts using deep sequencing, whereas depleted shRNAs pinpoint potential resistance genes towards Sorafenib treatment.

Functional validation experiments were performed with multiple independent single shRNAs against a possible "sensitizing" target (Mapk14 or p38α) and confirmed a significant survival benefit over Sorafenib treated tumors that express non-targeting control shRNAs.

Cell proliferation and cell death assays pinpoint inhibition of proliferation as the main mechanism responsible for the synergism between Sorafenib and Mapk14 inhibition.

Using mouse models and conditional RNAi technology, the sensitizing effect of Mapk14 knockdown towards Sorafenib treatments could also be shown in advanced tumors in a preclinical treatment study.

Importantly, Mapk14 represents a kinase and, taking advantage of readily available pharmacological inhibitors, it could be shown that combination therapy with Sorafenib results in a significant survival advantage of tumor bearing mice. Some of the used inhibitors (Skepinone-L and PH 797804) are believed to have a high potential to enter the clinic.

The identified new combination treatment was also expanded to murine HCC cell lines with additional genetic backgrounds. In these cell lines, therapeutic efficacy as a result of Sorafenib and p38 blockade was also found, but not every Mapk14 inhibitor worked efficiently in the tested cell lines. Additionally, it was shown that the newly identified combination therapy significantly decreased proliferation and induced cell death in a panel of well established human hepatoma cell lines (PLC/PRF/5, Huh7, Hep3B).
To characterize how Mapk14 blockade sensitizes for towards Sorafenib treatment, microarray based mRNA expression analyses were performed and were analysed by Ingenuity pathway analysis. This analysis along with genetic validation experiments identified the Mapk14 downstream target and transcription factor ATF2 as relevant for Mapk14 mediated resistance towards Sorafenib treatment.

In summary, our study establishes a new Sorafenib-based combination therapy for the treatment of hepatocellular carcinoma.The study highlights the potential of *in vivo* RNAi screens to identify genes that modulate the treatment response of targeted therapies. Additionally, the screen was performed in a mosaic mouse model that resembles the natural, spontaneous cancer development and could be used to identify other treatment options in HCC.

1. Introduction

1.1. Development of hepatocellular carcinoma (HCC)

Hepatocellular carcinoma is the sixth most common cancer and the third most common cause of cancer mortality worldwide. In 2008, around 700,000 new cases were identified and there were 696,000 deaths from HCC worldwide. Reasons accounting for the high lethality rate are HCC detection at advanced stages and also liver dysfunction due to liver cirrhosis [1;2]. The majority of HCCs arise in Eastern Asia and sub-Saharan Africa with the highest incidence rate (50 %) occurring in China. In contrast, the occurrence of HCCs is lower for North and South America, Northern Europe, Oceania and shows a more moderate rate for Southern Europe [3]. HCCs arise mainly from adult hepatocytes (80 %) and to a lesser extent from bipotential liver progenitor cells [4;5]. The highest risk of HCC development occurs in patients with chronic liver diseases which trigger rounds of cell death and proliferation that further give rise to nodules surrounded by collagen deposition and liver scarring, so-called cirrhosis. Cirrhotic nodules can further progress into hyperplastic and dysplastic nodules, and as a result into HCCs which can be categorized into well differentiated, moderately differentiated and poorly differentiated tumors (Fig. 1) [6].

Major risk factors for liver cancer development are viral infection with hepatitis B and C, alcohol abuse, and infection with aflatoxin-B1 containing food [7]. Although normally higher risk for HCC is associated with cirrhosis, HBV infection can also elicit hepatocarcinogenesis in noncirrhotic liver disease. HBV is a DNA virus that can directly integrate into the host genome. HBV integration can cause chromosomal instability as a result of deletions, amplifications or translocations and can integrate into the genes coding for oncogenes or tumor suppressor genes, responsible for control of cell proliferation [8]. By contrast, HCV is an RNA virus that does not integrate into the genome but rather regulates cell cycle via direct interaction with proteins, like p53 or Rb tumor suppressor proteins. Aflatoxin B, a mycotoxin from *Aspergillus flavus* or *Aspergillus parasiticus* can exert its carcinogenic effects via generation of DNA mutations, for example in *TP53* gene that may further decrease its tumor suppressive function [9]. Alcohol is also an important risk factor for development of HCC which may act synergistically with viral hepatitis to further increase risk of HCC. Hereditary hemochromatosis, an inherited liver disorder that increases the risk for HCC in individuals homozygous for *HFE* mutation.

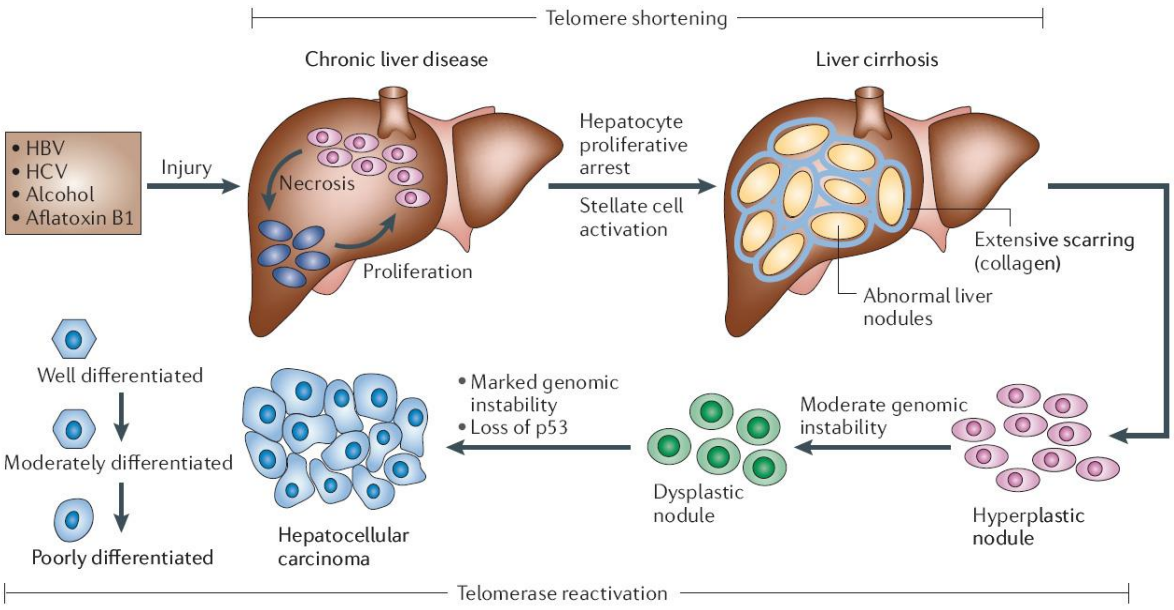

Figure 1 Hepatocellular carcinoma development

Different risk factors and liver diseases induce cycles of cell death and proliferation that may ultimately give rise to HCCs (adopted from [6]).

There are other rare cases that may predispose for HCC development, such as Wilson's disease (copper accumulation), α_1-antitrypsin deficiency and type1 glycogen-storage disease [7]. Moreover, a nonalcoholic fatty liver disease with its most aggressive form known as nonalcoholic steatohepatitis (NASH) can also contribute to HCC carcinogenesis. Among the risk factors for NASH to develop are obesity, diabetes and iron deposition [10;11].

1.2. Molecular pathogenesis of hepatocellular carcinoma

The exposure to different risk factors influences signaling pathways and consequently the gene expression profile. Some of the most important key signal transduction pathways that are implicated in hepatocarcinogenesis are Ras/MAPK signaling pathway, Akt/mTOR pathway, IGF and EGF signaling cascades, c-MET pathway and Wnt-βcatenin pathway [12].

Signaling molecules like epidermal growth factor (EGF), hepatocyte growth factor (HGF), platelet-derived growth factor (PDGF) and vascular endothelial growth factor (VEGF) can activate Ras/MAPK cascade by binding to receptor tyrosine kinases (RTK) [12]. Upon binding of those ligands, RTKs undergo activation as a result of phosphorylation of their tyrosine (Tyr) residues which further signal via SOS to Ras (Fig. 2a). Ras works as a molecular switch that relays the signals only when in its active, GTP-bound status.

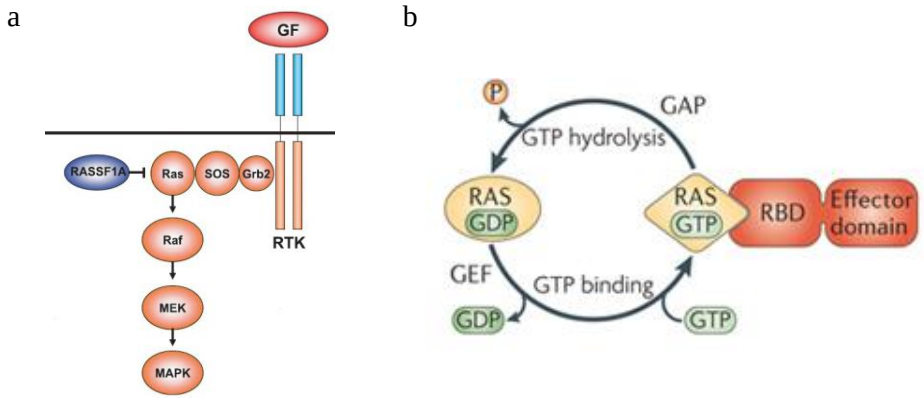

Figure 2 Signal relay along the Ras/MAPK cascade

Upon activation of tyrosine kinase receptors, Ras conveys the signal by firstly activating Raf-1 which in turn phosphorylates and activates Mek (MAP2K1 and MAP2K2) which subsequently activates Erk to influence cell cycle processes (a). Inactive, GDP-bound Ras is activated by GEF (guanine nucleotide exchange factor) which releases GDP and allowes GTP to bind to Ras, thereby forming its active GTP-bound state (b) (adopted from [13]).

Guanine nucleotide exchange factors (GEFs) catalyse the replacement of GDP-bound, inactive state with GTP. Contrary, GTPase activating proteins (GAPs) catalyse the hydrolysis of bound GTP into inactive GDP-bound conformation via induction of GTPase activity of Ras itself (Fig. 2b) [14].

Activated Ras binds and activates the kinase activity of Raf proteins (c-Raf1, B-Raf and A-Raf). Further downstream, Raf phosphorylates and activates mitogen-activated protein kinase kinases 1 and 2 (MAP2K1 and MAP2K2 or also known as Mek1 and Mek2) which proceed in phoshorylation and consecutive activation of extracellular-signal regulated kinase (Erk1 and Erk2). Ras/MAPK pathway regulates many transcription factors which control the genes implicated in apoptosis, cell growth and differentiation [13].

Deregulation of the Ras/MAPK pathway may occur as a consequence of activating mutations in *RAS* which in case of HCC account for ~7 % in *KRAS* and ~4 % in *NRAS* [14]. These mutations normally influence the GTPase activity of Ras which by avoiding the hydrolysis of GTP makes Ras to accumulate in its active, GTP-bound conformation [15]. Additionally, deletion of *NF1* (neurofibromin), *RASAL1* or *DAB2IP*, GTPase activating proteins with tumor suppressive role may promote Ras/MAPK upregulation and indeed are found depleted or downregulated in human HCCs [16]. Another frequently mutated gene in HCC (9.6 %) is *RPS6KA3* encoding for the ribosomal S6 protein kinase 2 (RSK2) which exerts its inhibitory role on Ras/MAPK pathway by phosphorylating SOS [17].

Ras also regulates p38 MAPK pathway [18;19], also known as stress activated protein kinase pathway that is often found deregulated in cancers [20]. P38 MAPKs encompass 4 genes: *MAPK14* (p38α), *MAPK11* (p38β), *MAPK12* (p38γ) and *MAPK13* (p38δ). Although, p38α and p38β are much related in function and sequence, with p38α being mostly abundant and mostly characterized. The other two, p38γ and p38δ share more similarity and are more constrained in expression [20]. Interestingly, in cancer cell lines p38α can either have anti-proliferative functions or can positively regulate cell proliferation [21;22]. For example, mice with liver specific deletion of Mapk14 showed stronger hepatocyte proliferation and enhanced chemically induced tumor development [23].

The MAPK pathway can stimulate the growth of new vessels upon activation of vascular-endothelial growth factor receptor (VEGFR). This process, termed angiogenesis, stimulates the tumor vascularization and therefore plays an important role in regulating tumor growth and metastatic potential. The major angiogenesis stimulant is VEGF that binds to two different receptors on endothelial cells, namely VEGFR-1 and VEGFR-2 that further transduce the signal along MAPK pathway proteins [24]. Aberrant VEGF expression occurs often in HCC and is associated with HCC tumour invasion and metastasis [25] and may also be involved in the development of the stroma in HCC [26].

The PI3K (phospatidylinositol-3 kinase)/Akt pathway also plays a crucial role in hepatocarcinogenesis and importantly its catalytic subunit *PIK3CA* is found somatically mutated in 26 of 73 human hepatocellular carcinomas [27]. PI3Ks are capable of phosphorylating the inositol ring 3'-OH group in inositol phospholipids to induce the production of second messengers like PIP3, phosphatidylinositol-3,4,5-triphosphate. PIP-3 activates the kinase PDK1 3-phosphoinositide-dependent protein kinase-1 which in turn phosphorylates and activates Akt kinase, also known as protein kinase-B. Akt modulates the activity of numerous downstream targets involved in the regulation of cell cycle progression, like NF-kappa B, mTOR (mammalian target of rapamycin) and GSK3β. A negative regulator of PI3K/Akt pathway is Pten (phosphatase and tensin homolog deleted on chromosome 10). Pten is a tumor suppressor gene and its loss of function constitutively activates its downstream elements such as Akt and mTOR [28;29]. Deregulation of *PTEN* in HCC occurs mainly via epigenetic silencing and it is localized in a region of frequent loss of heterozygosity (LOH) [30;31].

A very important target of the Ras/MAPK- and PI3K/Akt pathways is the family of *MYC* protooncogenes (*C-MYC*, *L-MYC* and *N-MYC)*. Myc is a pleiotropic transcription factor which coordinates many cellular processes like cell proliferation, angiogenesis or apoptosis.

Its overexpression in almost half of human cancers occurs as a result of epigenetic alterations. Interestingly, Ras can signal to Myc via two different cascades which influence Myc stability. If Ras conveys a signal through the classical MAPK pathway (along Raf and Erk) it becomes phosphorylated at Ser62 extending its half life. On contrary, Ras signals through phosphoinositide-3-kinase to block the activity of Gsk-3 (glycogen synthase-3) to further phosphorylate Myc at Thr58 that normally targets it for proteolytic degradation [32;33]. Myc activates the expression of high number of genes and has around 25,000 binding sites in the genome, called E-boxes with CANNTG sequence. Monomers of Myc have not been found, instead it forms dimers with its partner, Max. Concurrently, Max forms homodimers and heterodimers with other proteins, like Mad1, Mxi1, Mad3, Mad4 or Mnt. Interestingly, Myc-Max dimers are typical for proliferating cells, whereas Mad-Max or Mnt-Max complexes are frequently found in resting or differentiated cells [34;35]. Myc regulates the pRb-E2F pathway, one of major cellular barriers to cancer development in which tumor suppressor retinoblastoma protein Rb controls the E2F transcription factor (Fig. 4) [36].

In normal cells with wild type Rb, hypophosphorylated Rb binds and thereby sequesters E2F1, 2, and 3. However, phosphorylation of Rb by cyclin-dependent kinases (CDKs) together with their catalytic subunit cyclins causes release of E2F which can in turn induce the transcription of E2F responsive genes important for progression through G1/S transition. Complexes between Rb and E2F repress E2F responsive promoters by mainly recruiting histone deacetylases (HDACs) which silence genes upon deacetylation of nucleosomes [37;38]. The inhibition of CDKs by the INK4 proteins ($p16^{INK4a}$, $p15^{INK4b}$, $p18^{INK4c}$ and $p19^{INK4d}$) prevents the phosphorylation of Rb [39].

The gene locus of $p16^{INK4a}$ *(CDKN2a)* also encodes for the alternative reading frame protein $p19^{Arf}$ in mice ($p14^{ARF}$ in humans). Arf stands for an alternative reading frame since it shares two exons with $p16^{INK4a}$ but in another reading frame [40]. $P19^{Arf}$ is an important tumor suppressor that regulates p53, which is another potent tumor suppressor responsible for inducing cellular pathways of tumor suppression (apoptosis or growth arrests) upon oncogene activation, DNA damage or hypoxia (Fig. 3). P53 is negatively regulated by Mdm2 that targets it for proteosome-mediated degradation. In contrast, p53 is positively activated by $p19^{Arf}$ which binds to Mdm2 to antagonize its functions [41]. Rb and p53 are important mediators of cellular senescence, which act as a barrier to tumorigenesis and can be induced in response to oncogenic activation.

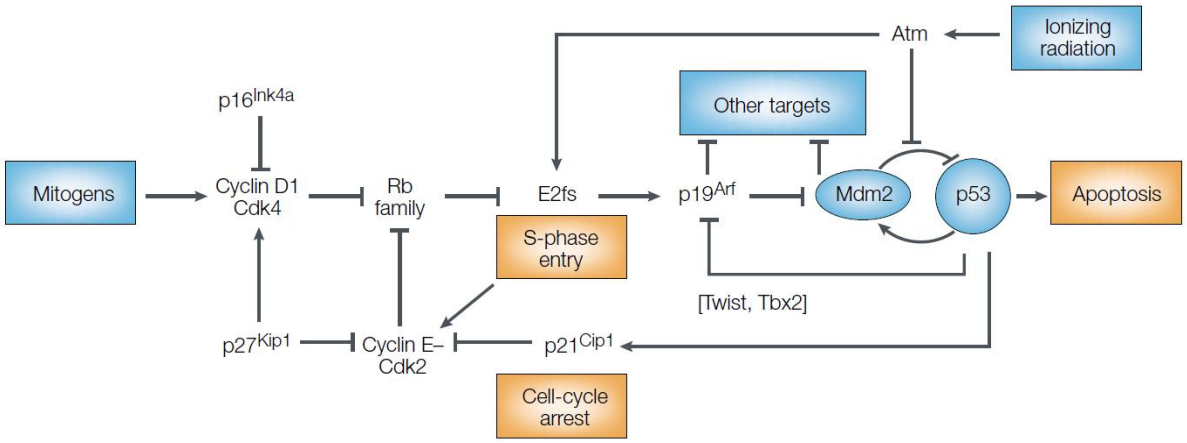

Figure 3 Scheme for the interaction between Rb and p53 pathways

$P19^{Arf}$ is induced upon oncogenic activation and activates as well as stabilizes the tumor suppressor p53 via inhibition of p53 negative regulator Mdm2. $P19^{Arf}$ is also a target of E2F transcription factor that in turn is activated upon deactivation of tumor suppressor Rb by dephosphorylation. Rb protein is inhibited by Cdk4, the activity of which can be blocked by $p16^{Ink4a}$, another important tumor suppressor gene (adopted from [41]).

P16 and p21 are both cyclin-dependent kinase inhibitors (CDKIs) which keep Rb in its active, hypophosphorylated state which in turn curtails proliferation by not allowing for transcription of E2F target genes. Interestingly, p53 induces the expression of p21 and E2F constrains proliferation by inducing $p19^{Arf}$ transcription which implicates p53 [42]. The *TP53* gene encoding for p53 is inactivated by genetic alteration in around half of human cancers [43]. It is also found mutated in 30 – 40 % cases of human HCCs [44;45]. Mutations of $p14^{Arf}$ are not common in HCC but rather found inactivated by promoter methylation in approximately 15 % of HCCs [46].

Additionally, $p16^{INK4A}$ gene is also found inactivated usually by promoter methylation in around 65 % of HCCs, and sometimes by homozygous deletion [46]. Similarly, the expression of *RB1* coding for Rb is reduced in 25 % of HCCs by promoter methylation [47].

Another important pathway that is implicated in HCC is the Wnt signaling pathway. The Wnt signaling cascade is activated when Wnt ligands bind to their target Frizzled (Fz) receptors to interfere with the multi-protein destruction complex (including Axin, adenomatosis polyposis coli (APC) and GSK3β), resulting in the activation of transcription of β-catenin target genes. The presence of this complex is necessary for GSK3-mediated phoshorylation of β-catenin that targets it for proteasomal degradation. Upon pathway activation, the complex is disassembled and thus β-catenin cannot undergo phosphorylation and consequently can accumulate in the nucleus and activate TCF/LEF transcription factors which in turn activate specific oncogenes such as *c-Myc* and *cyclin D* [48]. Overexpression and mutations of β-

catenin arise particularly in HCV-related HCCs [44;49]. Furthermore, β-catenin has also been implicated in HBV-related HCC due to stabilization of β-catenin by HBx protein [50]. According to some studies, β-catenin overexpression or mutations are associated with early-stage HCCs [51] and according to others, with HCC progression [52]. In HCCs, activating mutations in the β-catenin gene *CTNNB1* occur in 17 % of all cases and inactivating mutations in the negative regulator of Wnt pathway, Axin gene *AXIN1* arise in 7 % of HCCs [53]. Moreover, Wnt signaling cascade can also be activated by aberrant promoter hypermethylation of Apc [54].

1.3. Treatment of hepatocellular carcinoma

So far several staging systems for HCC have been defined, such as Barcelona Clinic Liver Cancer (BCLC), Cancer of the Liver Italian Program (CLIP), TNM (tumor, node and metastasis), Okuda, and Japanese Integrated Staging Score (JIS). However, BCLC came up as a standard classification system for the management of HCC in the clinic in which tumor staging is associated with recommended treatment options [2]. BCLC distinguishes three main stages: early stage (0-A), intermediate-advanced stage (B-C) and end stage (D). The very early stage 0 is characterized by one single nodule ≤ 2 cm and by lack of invasion into surrounding tissue. In stage A the tumor is defined as a single nodule 2-5 cm, or by 3 nodules each of which is ≤ 3 cm in size. Patients that are classified among 0-A stage have a well preserved liver function and are suitable for curative treatments such as: liver transplantation, surgical resection, or local ablation approaches, encompassing percutaneous ethanol injection (PEI) and radiofrequency ablation (RFA) [55]. The performance in terms of survival is usually good with 5-year survival rates between 50 - 70 % when using the aforementioned treatment options [56]. Patients with intermediate, stage B HCC are asymptomatic with multinodular tumors without an invasive pattern [57]. For those patients, transarterial embolization (TAE) or transarterial chemoembolization (TACE) are applicable [55]. Normally, a median survival of 16 months is typical for untreated patientsin this stage that can be further expanded up to 19 - 20 months upon application of chemoembolization [58]. On contrary, untreated patients with advanced stage C HCC exhibit symptomatic tumors with additional presence of vascular invasion or extrahepatic spread [57] and a median survival of 6 months. Systemic treatments such as Sorafenib, systemic chemotherapy, immunotherapy or hormonal blockade can be applied to stage C patients. Here, however, only Sorafenib shows a significant increase in survival and there is no survival benefit for other therapy options.

Patients with stage D HCC do not benefit from antitumor therapies, show very severe tumor-related symptoms and exhibit a median survival of 3 - 4 months [59].

Surgical resection to remove the tumor while preserving enough liver tissue is mostly suitable for non-cirrhotic patients with one nodule. Tumor recurrence after resection arises in 70 % of patients at 5 years. It occurs as a result of true recurrence (up to 2 years) or after 2 years due to growth of *de novo* tumors. The risk of recurrence correlates with tumor size and the number of tumors, and vascular invasion increases with nodule size. Thus, surgical resection is not recommended for patients with vascular invasion or metastasis [60]. Interestingly, microscopic tumor invasion occurs in 20 % of nodules with 2 cm in size, 30 - 60 % in 2 - 5 cm nodules and reach 60 - 90 % in nodules that exceed 5 cm in size [59]. Taking into account these criteria, only 10 - 15 % of patients are suitable for resection [1].

Liver transplantation seems to be the best curative treatment since it fully replaces the diseased liver with a living donor graft. HCC patients eligible for liver transplantation are those with a solitary nodule smaller or not larger than 5 cm, or up to 3 nodules each of 3 cm or smaller, and additionally without vascular invasion or extrahepatic spread. These patients achieve a 4-year survival of 75 % with a recurrence rate below 15 %. The major disadvantage of this treatment is the shortage in donors and thus the number of candidates undergoing liver transplantation is small compared with the total number of patients with HCC [1;61].

Image-guided tumor ablation is based on direct application of chemical or thermal treatment to tumor(s). Ablation itself should significantly destroy the tumor as a consequence of induced necrosis either upon injection of chemicals (e.g. ethanol, acetic acid) or temperature change (e.g. cryoablation, or ablation by laser, or by radiofrequency). Most often used ablation procedures in HCC treatment are percutaneous ethanol injection (PEI) and radiofrequency ablation (RFA), both recommended for patients who are not good candidates for surgical resection or liver transplantation due to comorbidities or non-functional liver. PEI and RFA have an excellent outcome with complete necrosis in most HCCs with nodules < 2 cm in size and a survival benefit comparable with surgical resection or liver transplantation. Both procedures are not suitable for patients with nodules bigger than 5 cm [62]. The major drawback of PEI is high local recurrence rate that accounts for 33 % in nodules smaller than 3 cm, and 43 % in nodules greater than 3 cm [63]. RFA is regarded as having higher anticancer effect than PEI [64] and being more effective against nodules

bigger than 2 cm [62]. However, the occurrence of side effects is higher for RFA-treated patients (4.1 %) compared to 2.7 % for PEI-treated patients [65].

Progression of HCC is accompanied by intense angiogenesis, and TACE (transarterial chemoembolization) is performed by injecting chemotherapeutic drugs (e.g. cisplatin, doxorubicin) mixed with an embolizing agent (e.g. gelfoam) into arterial vessels supplying the tumor. The same procedure but without the introduction of chemotherapy is called transarterial embolization (TAE). The aim of embolization is to cause tumor necrosis via arterial occlusion. It is mostly recommended for patients with multinodular disease, without vascular invasion or extrahepatic spread, and those being ineligible local for ablative procedures [62]. Another type of TAE for non-resectable liver tumors is selective internal radiation therapy (SIRT). SIRT is a means of delivery microspheres containing radioactive substance into hepatic artery which are selectively directed into liver tumors as a result of hepatic arterial supply to tumors [66;67].

HCC is a highly chemoresistant tumor and although many chemotherapeutic agents have been tested in HCC, no single or combination chemotherapy appeared to have a significant survival advantage. Doxorubicin is probably the most commonly used agent in HCC with a response rate ranging from 10 % to 15 %, but without survival benefit. Patients treated with this agent encounter grade 3 or 4 toxicities. Low response rates and no survival benefit were also observed for other chemotherapeutic drugs like cisplatin, epirubicin, 5-fluorouracil or etoposide, as well as their combinations. Newer chemotherapeutic agents like gemcitabine, paclitaxel, irinotecan, capecitabine, and pegylated liposomal doxorubicin did not yield better results. Given the disappointing results with single agents, different combination treatments were tested. Even if initially some of them showed interesting results in II phase trial, many of them did not succeed in phase III studies [68]. Combination chemotherapy with doxorubicin, cisplatin and 5-fluorouracil with or without interferon showed a moderate response rate of 13 % to 39 % without any influence on survival [69]. The combination of gemcitabine and oxaliplatin displayed a response rate of only 19 % in patients with advanced HCC [70].

In fact, resistance to chemotherapy is linked to different drug resistance mechanisms occurring in HCCs. Doxorubicin targets DNA topoisomerase II and its frequent overexpression in HCC may be the reason for resistance to doxorubicin-based therapy [71]. Resistance to 5-fluorouracil is usually accounted for by high levels of dihydropyrimidine dehydrogenase present in HCC [72]. Moreover, overexpression of P-glycoprotein is

associated with poor response to paclitaxel [73]. Since p53 is important for induction of apoptosis, tumors with an impaired p53 pathway become refractory to chemotherapy. Cirrhosis plays also a role in responsiveness to chemotherapeutic agents. Cirrhotic tissue causes changes in liver architecture, and thus changes in blood flow and drug metabolizing enzymes [74].

Other randomized trials employing anti-hormonal treatment with, tamoxifen, did not improve the overall survival of HCC patients [68].

Similarly, immunotherapy with interferon appeared also to be ineffective. Studies conducted using a 3 times weekly scheme of interferon (dose of $3x10^6$ IU) did not demonstrate any survival benefit [68].

1.4. Molecular targeted therapies in HCC

Although resection and liver transplantation are considered as the standard curative treatments for HCC, they are not suitable for patients with advanced stage HCC and poor liver function. Additionally, a problem is the waiting time due to a lack of liver donors that delays transplantation and also contributes to tumor progression during that time. Cancer development is regulated by a complex molecular network of signaling cascades comprising a multitude of proteins such as extracellular ligands, transmembrane receptors, intracellular proteins and transcription factors. Many standard anticancer agents affect rapidly growing cells (e.g. chemotherapy) in general, thus resulting in significant toxicities to rapidly dividing tissues such as bone marrow or intestine. In contrast, molecular targeted therapies are designed to specifically inhibit signaling pathways that are induced in cancer cells and hold the promise to allow for a more efficient and less toxic cancer therapy [75].

Some hope for the patients with advanced HCC came with the development of Sorafenib (Nexavar). Many other molecular targeted therapies are under development for the treatment of HCC, but so far only Sorafenib showed a significant benefit that led to its approval for HCC treatment. Sorafenib is an oral multityrosine kinase inhibitor which was originally selected based on its high Raf (wild-type Raf1, and mutant and wild type B-Raf) inhibitory effect (Fig. 4). Additionally, it targets the vascular endothelial growth factor receptor 2 (VEGFR-2) and VEGFR-3, platelet-derived growth factor receptor PDGFR-β, Fms-like tyrosine kinase 3 (Flt-3), Ret, and c-KIT [76]. Sorafenib exhibits antiproliferative effects *in vitro* in HCC cell lines (e.g. PLC/PRF/5 (also called Alexander), HepG2) and strong

antitumor effects in HCC xenograft models [77]. It demonstrates also a broad antitumor role in a panel of other human tumor xenograft models representing human colon, lung, breast, melanoma, ovarian, and pancreatic cancers [78;79]. Sorafenib showed improvement of overall survival in patients with advanced HCC in two phase III trials. One of them was carried out in 121 centres for which 299 patients were randomly assigned into Sorafenib treatment (200 mg twice daily) and 303 patients to placebo group with no difference between the groups with respect to tumor stage, prognosis or demographic features. In this trial, patients who received Sorafenib had an almost 3-month median survival benefit over patients in the placebo group, with overall survival reaching 10.7 months for Sorafenib arm versus 7.9 months for placebo group (Fig. 5). Time to progression differed between the groups, with 5.5 months for Sorafenib treated patients and 2.8 months for placebo treated patients [80]. These results were also reproduced by another randomized trial in Asia in which the median overall survival was 6.5 months in the Sorafenib group compared to 4.2 months in the placebo group [81].

The most common adverse effects associated with drug administration were diarrhea and hand-foot skin reaction [80]. These promising results led to approval of Sorafenib for the treatment of advanced hepatocellular carcinoma.

Since Sorafenib shows only a moderate survival benefit, there is a strong need to further improve molecular targeted therapy against HCC. One other target for molecular inhibition within Raf/MAPK pathway is Mek (Fig. 4).

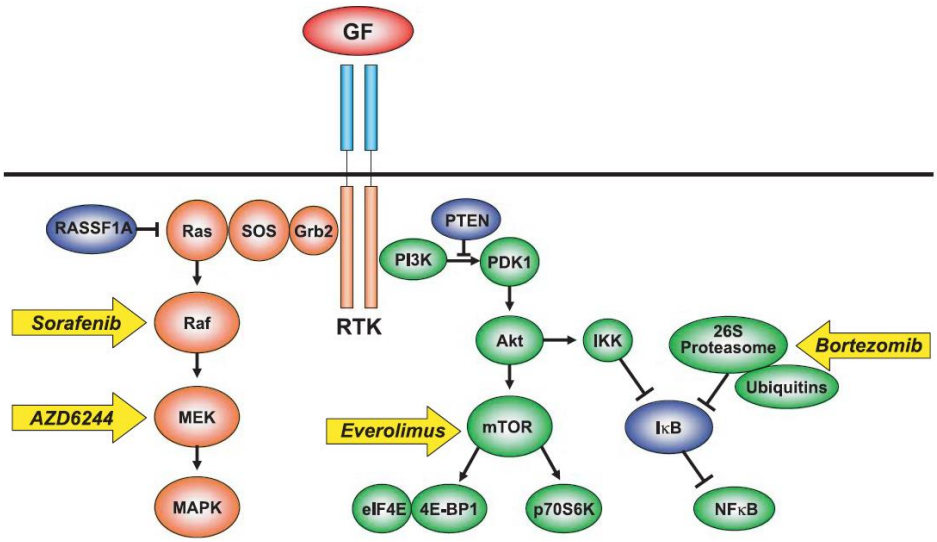

Figure 4 Molecular therapies targeting the Ras/MAPK and PI3K/Akt pathway

Within Ras/MAPK pathway targets for Sorafenib and AZD6244 are shown, furthermore targets for Everolimus and Bortezomib are depicted (adopted from [82]).

AZD6244 is an oral Mek inhibitor which was evaluated in HCC patients in a phase II study, however, as a single agent did not show any survival advantage. It was tested in 19 HCC patients [83].

As described before, also the PI3K/Akt pathway contributes to hepatocarcinogenesis. Therefore, several targeted therapies against this pathway have been developed (Fig. 4). The most common one is rapamycin (sirolimus), an mTOR inhibitor with antiproliferative and antiangiogenic functions. Rapamycin and its derivative, Everolimus, showed antitumor effects in preclinical studies and in xenograft HCC models [84;85]. A small study with 21 HCC patients who underwent treatment with Sirolimus showed a partial response for five patients and disease stabilization for at least 3 months in 24 % of patients. The median overall survival was 6.5 months, without severe side effects [86]. Bortezomib is a proteasome inhibitor that was approved for the treatment of multiple myeloma and a phase I and II in patients with HCC is under way [82].

Other molecular therapies for HCC aimed to improve antiangiogenic efficacy underwent clinical evaluation (Fig. 6). One of them is Sunitinib. It is also an inhibitor of different kinases such as VEGFR-1, -2, PDGFR-α, -β, c-Kit, Flt-3 and RET [87].

Sunitinib showed antitumor efficacy in xenograft models of HCC by inducing apoptosis, decreasing microvessel density and inhibiting cell proliferation [88]. A phase III trial that aimed at comparing Sunitinib with Sorafenib in patients with advanced HCC was dismissed due to more frequent severe adverse effects in the sunitinib group than Sorafenib group [83].

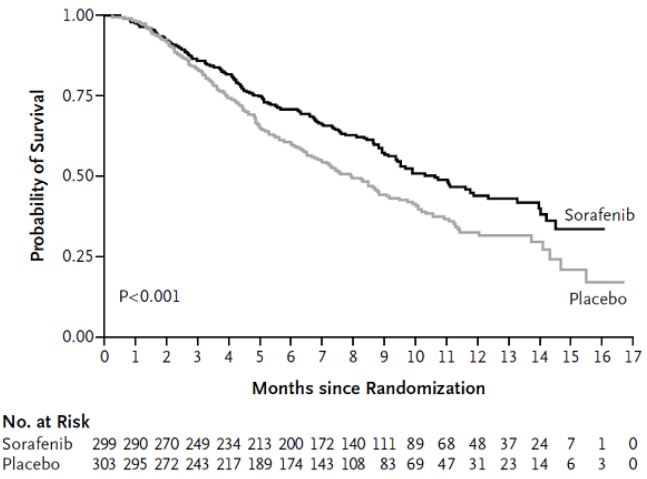

Figure 5 Overall survival of patients with advanced HCC assigned to Sorafenib or placebo treatment

Randomized placebo controlled trial in patients with advanced hepatocellular carcinoma in which Sorafenib group shows an almost 3-month survival benefit over placebo group (adopted from [80]).

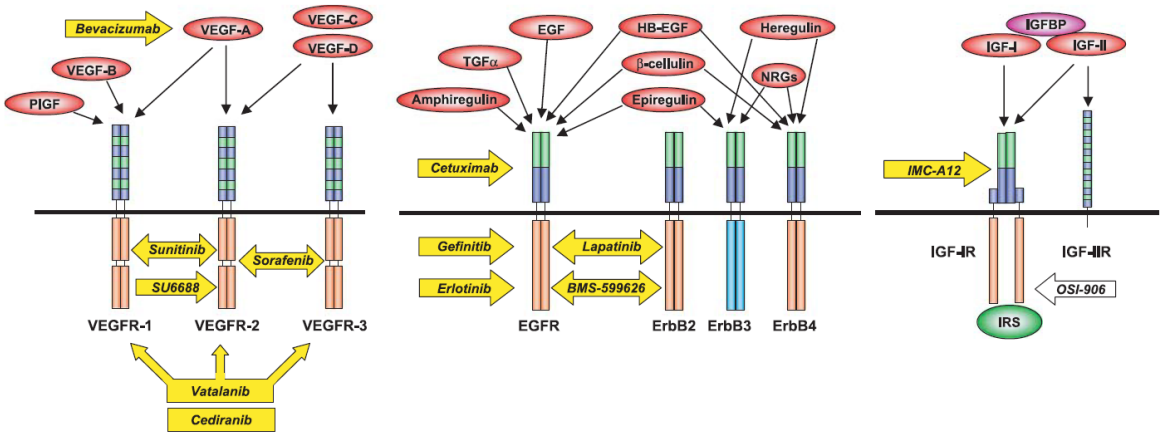

Figure 6 Molecular-targeting agents for VEGFR-, EGFR-, ErbB2-, and IGFR-induced signaling

Shown are targeted therapies for pathways stimulated mainly by VEGF, EGF, and IGF (adopted from [82]).

Bevacizumab (Avastin), a humanized monoclonal antibody that targets all VEGF isoforms showed antiangiogenic effects in orthotopic models based on the human HCC cell line Hep3B [89]. In a phase II study, 13 % of patients had a partial response and 65 % patients achieved stable disease [90]. Similar results were obtained in a second phase II study in which partial response was observed in 12.5 % and stable disease in 29 % [83].

A frequent deregulaton of signaling via EGFR in HCCs prompted the development of targeted therapies blocking its signaling (Fig. 6). One of them is Gefinitib (Iressa) that blocks EGFR. In a phase II study with 31 HCC patients , 3 % of patients showed a partial response and 22.6 % a stable disease. Later on, Gefinitib was considered as being inactive in patients with advanced HCC [83]. Erlotinib, another EGFR inhibitor was evaluated in two phase II studies in patients with advanced HCC. The first study with 38 patients demonstrated a partial response for 3 patients, and progression-free survival at 6 months for 12 patients, with a median overall survival of 13 months [91]. In another study with 40 patients, 17 patients experienced a progression-free survival at 16 weeks [92]. Cetuximab, a monoclonal antibody against EGFR underwent two phase II studies. In the first study with 30 HCC patients, a stable disease was observed for five patients, with a median overall survival of 9.6 months and with a progression-free survival of 1.4 months. In another study with 32 patients, no responses were reported and the median time to progression was 8 weeks [82].

Taken together, Sorafenib improves the survival of patients with advanced HCC in a significant but moderate way. Although Sorafenib is approved as a standard treatment for advanced HCC, there is a strong need for combining Sorafenib with other therapies to

enhance the response rate and the overall survival benefit for patients with advanced HCC. Preliminary results for combination of Sorafenib with doxorubicin were promising but doxorubicin causes severe toxicities, and hence trials with novel chemotherapeutic drugs are ongoing [1]. Inhibiton of Mek by AZD6244 enhanced the anticancer activity of Sorafenib in both orthotopic and ectopic HCC xenograft models [93]. Combination of Sorafenib with sunitinib failed due to toxicity; other combinatorial trials are underway [1].

1.5. Mouse models for studying hepatocellular carcinoma

The study of human cancers by characterizing cell lines, which were isolated from human tumors have made important contributions to the understanding of signaling and molecular mechanisms of tumorigenesis, however, cell lines they do not recapitulate the microenviroment and vascularization of tumors. Furthermore, these models do not reflect the complex interaction of tumors with the surrounding tissue and the immune system.

Also the significance of tumors based on human cancer cells, which were inoculated subcutaneously or orthotopically in different organs of immunodeficient mice (xenograft models) is limited, because these tumors show a different vascularization and microenvironment. Furthermore, the implantation of human tumor cells necessitates the usage of immunodeficient mice, however, it has been shown that the immune system plays an important role in tumor development. Although almost each anticancer agent was subjected to testing in these xenograft models, treatment studies are limited because immunomodulatory agents cannot be tested and as a result the tested drugs may demonstrate a response in xenograft models but may be much less effective in the clinical evaluation [94-96].

Mice and humans share a high similarity in genetics and physiology [97] and 99 % of murine genes have a direct human counterpart [97]. Therefore, mouse models with an orthotopic and autochtonous tumor initiation are highly valuable to study the molecular mechanisms as well as potential treatment options of cancer [94].

To study hepatocellular carcinoma in mice, HCCs can be developed as a result of exposure to carcinogenic chemicals, like N-nitrosodiethylamine (DEN) to induce hepatocarcinogenesis [98;99]. However, arising tumors are not genetically defined, restricted in type and grade with variable latency [100].

To establish genetically defined liver cancer mouse models, genetically engineered mouse models (GEMM) can be used which harbor hyperactive oncogenes and/or lack functional

tumor suppressor genes. To allow for oncogenic expression in specific organs, tissue specific promoters can be used (e. g. albumin promoter in the liver [101;102]) or hyperactive oncogenes can be activated by the Cre-lox system (using a lox-stop-lox sequence 5' of gene of interest), whereas Cre is activated by a tissue specific promoter (Alb-Cre for the liver [103]). Additionally, tumor suppressor genes can be deleted by Cre activation, when the corresponding genes are flanked by lox sequences (lox-p) [104].

To avoid developmental compensation or embryonic lethality, conditional expression of transgenes as well as conditional loss of tumor suppressor genes is possible by using tetracycline responsive elements (TeT-Off or TeT-On systems), which induce Cre activation dependent on tetracycline or doxycycline administration [105].

However, mouse models based on tissue specific expression of oncogenes pose a limitation due to the genetic field effect of expressing an oncogene in every cell of the tissue where the surrounding environment carries the same genetic event [106]. Importantly, this expression pattern does not reflect human carcinogenesis, where cancer development is based on the transformation of a single cell in the context of a normal microenvironment [100].

In order to induce oncogenic activation only in a subfraction of cells, which are sourrounded by non malignant cells (mosaic mouse model), Cre recombinase can be delivered manually into the corresponding organ of mice (e.g. using adenoviral gene transfer in the liver).

Another mosaic liver cancer mouse model is based on a transplantation of liver progenitor cells (chimeric mouse model). Embryonic hepatoblasts can be isolated from $p53^{-/-}$ fetal livers and subjected to *ex vivo* viral gene transfer via MSCV-based retroviruses expressing different oncogenes. Such models were already efficiently used to identify new genes implicated in hepatocarcinogenesis via oncogenomic approaches [107;108]. Although this model closer resembles the physiological, spontaneous tumor developement, the requirement for *ex vivo* genetic manipulation may cause some unfavourable genetic alterations. Additionally, 80 % of HCCs are induced from hepatocytes, and this model relies on the usage of progenitor cells which account only for 20 % of HCCs [4;5].

Interestingly, DNA, proteins and viruses can be delivered to adult hepatocytes using a hydrodynamic tail vein injection [109;110]. Furthermore, the delivery of transposable elements in combination with a transposase (sleeping beauty) allows for efficient integration of target genes into the genome [111;112].

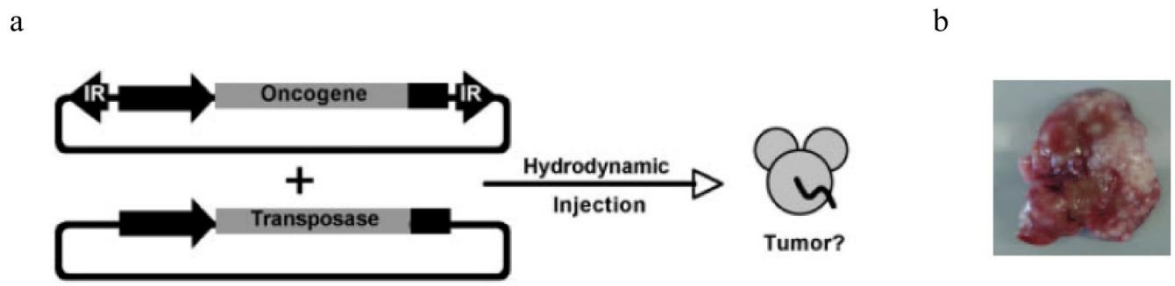

Figure 7 Hydrodynamic tail vein injection delivers DNA into the liver and efficiently induces tumor development

Injection of transposable elements encoding oncogenes together with transposase (a). Stably transfected $Nras^{G12V}$ triggers HCC in $p19^{Arf-/-}$ mice (adopted from [113]).

The delivery of oncogenes into hepatocytes with different genetic background allows for investigating the molecular mechanisms of liver cancer in adult hepatocytes [113-115]. Therefore, the delivery of oncogenic $Nras^{G12V}$ into $p19^{Arf}$ deficient mice elicits a high number of liver tumors within several weeks, which is an efficient genetic background to study hepatocarcinogenesis (Fig. 7) [113]. This mosaic mouse model is very attractive, as it allows for oncogenic transformation of a target cell that has never been taken out of its natural environment.

1.6. RNAi screening for the discovery of novel modulators of cancer

RNA interference (RNAi) emerged as a mechanism to silence gene expression and can be used to delineate gene function. RNAi can suppress gene expression at both transcriptional and posttranscriptional level [116;117] by different types of small non-coding RNAs, as small interfering RNA (siRNA), microRNA (miRNA) or Piwi-interacting RNA (piRNA).

Availability of RNAi technology led to the development of high-throughput screens with RNAi-based libraries for elucidating signaling cascades and revealing cancer vulnerabilities. The libraries can contain either synthetic siRNAs or shRNAs that are expressed by DNA precursors. SiRNAs can be directly transfected into cells, whereas shRNA libraries are mainly available in the form of viral vectors (retrovirus, lentivirus). The application of siRNAs is most suitable for easily transfectable cells and a transient silencing of gene expression because siRNAs do not replicate simultaneously with DNA of the host cells and are therefore lost with time.

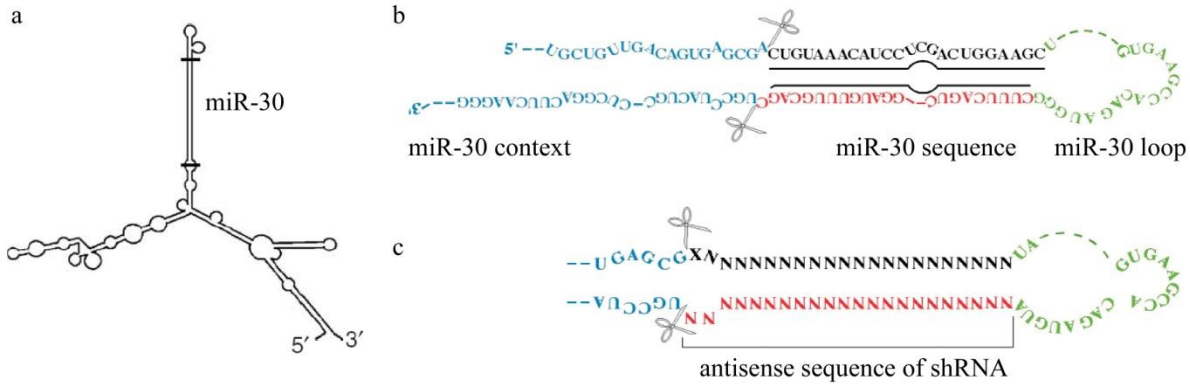

Figure 8 miR30-based shRNAs

Schematic representation above depicts an example of secondary structure of miR30-based shRNA hybrid (a) (adopted from [118]), primary transcript of the miR30 miRNA (b), and shRNA embedded within the miR30 context (c) (adopted from [119]).

On the contrary, shRNAs are chosen if the cells are difficult to transfect and if a longer silencing of gene expression is needed. Since retroviruses expressing shRNAs are integrated into the genome of the host cell, they are copied along with the host cell DNA and consequently ensure stable gene silencing [120].

Classical stem loop stem shRNAs are expressed from polymerase III (pol III) promoters such as U6 or H1. However, the discovery of microRNAs (miRNAs) has also stimulated the generation of shRNAs that resemble the endogenous miRNA transcripts. These shRNAs were embedded within the context of microRNAs (e. g. miR30) which allows for transcription from a polymerase II promoter (pol II) (Fig. 8). These microRNA-based shRNAs are shown as physiological and allow for efficient gene silencing even when present as single copy in the genome [119;121].

RNAi screens can be divided into genome-wide screens, aimed at identifying all likely modulators of a cellular process or can be focused with respect to a specific pathway or a specific process. Both approaches have been widely used in cell culture and can be used either as arrayed format in multi-well plates or as high-complexity pools in bulk.

In pooled shRNA screens, positive or negative selection screens are distinguished. In a positive screen, RNAi-mediated gene silencing gives rise to a phenotype that confers an advantage due to shRNA expression, whereas in a negative screen the expression of the shRNAs confers a disadvantage.

Taking advantage of the commonly available collections of siRNAs and shRNAs, a number of different RNAi screens have been performed to dissect cellular pathways, or identify new therapeutic targets, or modulators of drug resistance and sensitivity [120].

As an example, RNAi screens can be performed to search for genes that are required only in the context of specific cancer-causing mutations, so called 'synthetic lethal' screens. Such a screen was performed to delineate genes necessary for the viability of cells with deregulated Myc. In this screen AMPK-related kinase 5 (Ark5) was found to be important for survival of Myc driven HCCs [122].

In another study, a genome-wide pooled lentiviral RNAi screen identified essential viability genes in 12 different human cancer cell lines. Among them were some known and probable oncogenes: Kras, Myc, Crkl or Cdk4. Those genes are involved in basic cellular processes like ribosomal function, mRNA processing, further underscoring the possibility for identifying the genes that are essential [123].

RNAi screens in the presence of drugs could reveal new mechanisms of drug resistance and sensitivity, and as such identify targets for combination therapies. For instance, such a screen was performed in breast cancer cells with siRNAs in the presence of PARP inhibitor and identified new genes (e.g. CDK5, STK22c) whose inhibition sensitizes to the drug [124]. Other screens took advantage of siRNAs to identify sensitizing genes to paclitaxel or genes modulating the response to gemcitabine [125;126]. A retrovirally encoded miR30-based shRNA library containing 2,300 shRNAs was used to screen lymphoma cells for new genes mediating doxorubicin resistance [127].

Although there have been many different *in vitro* RNAi screens in the arrayed, as well in the pooled format, so far there is only a limited number of conducted *in vivo* screens. One of them is a positive screen for shRNAs that promote tumorigenesis in a mouse model of hepatocellular carcinoma. This model was generated via *ex vivo* genetic manipulation of isolated liver progenitor cells which afterwards were transduced with miR30-based shRNAs and transplanted into mice. It revealed new genes with potential tumor suppressive functions involved in HCC development [108]. Another positive *in vivo* RNAi screen relies on the same model in which isolated fetal liver hematopoietic stem cells from Eμ-Myc transgenic mice were *ex vivo* infected with a complex shRNA library and transplanted into mice. In this lymphoma mouse model, analysis of enriched hairpins indicated new tumor suppressor genes like Numb, or Mek1, likely involved in lymphomagenesis [128]. In a negative selection *in vivo* RNAi screen, Eμ-Myc cells were *ex vivo* transduced with a pool of around 900 shRNAs,

transplanted and analyzed for depleted hairpins. This screen revealed new modulators of lymphoma cell motility such as Rac2 and Twf1. Suppression of those two candidate genes impaired lymphoma cell migration to the lymph nodes and other common organs of lymphoid metastasis [129].

Taken together, RNAi screens have emerged as an efficient technology for identification of genes to identify molecular mechanisms of cancer development. Additionally, identified candidates can serve as potential therapeutic targets in cancer therapy. Genes which are identified as modulators of drug sensitivity or resistance may serve as therapeutic targets for combinatorial therapies.

1.7. Aim of the study

Considering the significant but moderate responses to Sorafenib treatment in the clinic, there is an urgent need to search for new treatment options that could improve the responsiveness towards Sorafenib. The aim of this study was to identify potential candidates for such a combinatorial therapeutic approach in a mosaic cancer mouse model. As a first step, it is necessary to determine an *in vivo* response to Sorafenib in a newly developed transposon-based mosaic HCC model. Furthermore, an *in vivo* negative selection screen should be established to identify new modulators of response towards Sorafenib. A possibility of recapitulation the *in vivo* screen in the *in vitro* set-up under the same genetic conditions ($Nras^{G12V}$; $p19^{Arf-/-}$) should be further explored. Ultimately, the mechanism of synergism between Sorafenib and identified candidate should be delineated as well as the possibility of using this candidate as a target for combination therapy together with Sorafenib.

2. Materials

2.1. Chemicals

If not stated otherwise, all chemicals were purchased from the following companies: Amersham, Bioscience, BioRad, Boehringer Mannheim, Fermentas, GE Healthcare, Invitrogen, Life Technologies, Merck, Millpore, New England Biolabs, PAA, Promega, Qiagen, Roche, Roth, Sigma-Aldrich, Serva.

2.2. Buffers

The buffers which were used for this study are listed in Table 1.

Table 1 Buffers

name	composition
PBS (10x)	100 mM $Na_2HPO_4x2H_2O$, 20 mM KH_2PO_4, 1.37 M NaCl, 27 mM KCl; pH 7.4
TBS (10x)	500 mM Tris-HCl, 1.5 M NaCl; pH 7.4
PBST	0.1 % Tween 20 in 1xPBS
TBST	0.1 % Tween 20 in 1xTBS
NP40 Lysis Buffer	50 mM Tris-HCl (pH 7.5), 150 mM NaCl, 0.5 % NP40, 1 tbl. Complete Mini (Roche)
NP40 Phospho Lysis Buffer	50 mM Tris-HCl (pH 7.5), 150 mM NaCl, 0.5 % NP40, 1 tbl. Complete Mini (Roche), 1 tbl. PhosphoSTOP (Roche)
gDNA Extraction Buffer	20 mM Tris-HCl (pH 8.0), 100 mM EDTA, 100 mM NaCl, 1% SDS, 0.5 mg/ml Proteinase K
SDS Running Buffer (10x)	250 mM Tris base, 1.92 M glycine, 1 % SDS
Protein Loading Buffer (5x)	150 mM Tris-HCl (pH 6.8), 6 % SDS, 15 mM DTT, 50 % glycerol, 0.25 % bromophenolblue
Transfer Buffer	48 mM Tris-HCl (pH 8.3), 39 mM glycine, 20 % methanol, 0.037 % SDS
Stripping Buffer	65.5 mM Tris-HCl (pH 6.7), 2 % SDS, 100 mM β-mercaptoethanol
PFA	4 % paraformaldehyde in PBS; pH 7.4
TAE (50x)	2 M Tris base, 1 M glacial acetic acid, 50 mM EDTA; pH 8.3
DNA loading buffer (5x)	0.25 % orange G, 15 % Ficoll type 400
Normal Goat Serum Blocking Solution	5 % NGS, 0.2 % Triton X-100, 0.1 % Tween 20 in PBS
HBS (10x)	7.5 mM Na2HPO4 (pH 7.0), 1.4 M NaCl, 250 mM HEPES, 60 mM dextrose, 50 mM KCl

2.3. Cell culture reagents and placticware

Cell culture media and additives were purchased from Gibco, Invitrogen, PAA or Sigma unless stated otherwise. Plasticware was obtained from Corning, Falcon, Nunc and PAA.

2.4. Enzymes and reagents for molecular biology

All restriction endonucleases, alkaline calf intestinal (CIP), DNase I, DNA polymerase I, and T4 DNA ligase were used from New England Biolabs (NEB). *Taq* DNA polymerase and Platinum *Pfx* DNA polymerase were purchased from Applied Biosystems and Invitrogen, respectively.

2.5. Plasmids

Sleeping beauty (SB13) transposase was provided by Dres. David Largaespada and Mark Kay. Further expanded plasmids with transposable elements carrying $Nras^{G12V}$ were provided by Daniel Dauch (unpublished data). Murine stem cell virus (MSCV) plasmids containing IRES and GFP, MSCV plasmid with rtTA3 and MSCV plasmid with TREtight promoter were provided by Scott Lowe.

2.6. Bacterial cultures

The *Escherichia coli* bacteria DH5α and MegaX DH10B T1 Electrocomp from Invitrogen were used.

2.7. Cell lines

Cell lines applied to this study are listed in Table 2. All cell lines were abtained from the American Type Culture Collection.

Table 2 Cell lines

name	species	source
Phoenix amphotropic	*Homo sapiens*	embryonic kidney (ATCC)
Phoenix ecotropic	*Homo sapiens*	embryonic kidney (ATCC)
PLC/PRF/5 (Alexander)	*Homo sapiens*	hepatocellular carcinoma (ATCC)
Hep3B	*Homo sapiens*	hepatocellular carcinoma (ATCC)
Huh7	*Homo sapiens*	hepatocellular carcinoma (ATCC)

2.8. Oligonucleotides

Oligonucleotides used for this study are listed in Table 3. They were obtained from MWG. The sequences of hairpins from the used RomaAmplicon library are listed in Table 14.

Table 3 Oligonucleotides

name	sequence	application
5'miR30 XhoIF	cagaaggctcgagaaggtatattgctgttgacagtgagcg	PCR
3'miR30 EcoRIF	ctaaagtagccccttgaattccgaggcagtaggca	PCR
Mir30fw	tgtttgaatgaggcttcagtac	Sequencing
GFP_mid_seq1	acggcgtgcagtgct	Sequencing
p7+Loop	caagcagaagacggcatacgatagtgaagccacaga	Illumina seq
p5+mir30	aatgatacggcgaccaccgactaaagtagcccctg	Illumina seq
ARF 1:	agtacagcagcgggagcatgg	Arf genotyping
ARF 2:	tttgaggaggaccgtgaagccg	Arf genotyping
ARF 3:	accacactgctcgacattggg	Arf genotyping
shMapk14.1095	tgctgttgacagtgagcgaaagatgaacttcgcaaatgtatagtgaagccacagatgtatacatttgcgaagttcatcttctgcctactgcctcgga	Cloning of shRNAs
shMapk14.2590	tgctgttgacagtgagcgactcctttactatctttctcaatagtgaagccacagatgtattgagaaagatagtaaaggagctgcctactgcctcgga	Cloning of shRNAs
shAtf2.1136	tgctgttgacagtgagcgcaccaatggtgatactgtaaaatagtgaagccacagatgtattttacagtatcaccattggtatgcctactgcctcgga	Cloning of shRNAs
shAtf2.1362	tgctgttgacagtgagcgacagcttcaagatgccgacaaatagtgaagccacagatgtatttgtcggcatcttgaagctgctgcctactgcctcgga	Cloning of shRNAs
shcontrol	tgctgttgacagtgagcgcaggaattataatgcttatctatagtgaagccacagatgtatagataagcattataattcctatgcctactgcctcgga	Cloning of shRNAs
b-actin for	ccaccgatccacacagagta	qPCR
b-actin rev	ggctcctagcaccatgaaga	qPCR
ATF2 for	aaactccggcttctccag	qPCR
ATF2 rev	actgaacccacactttcct	qPCR

2.9. Antibodies

Primary antibodies used in this study are listed in Table 4. Secondary antibodies are listed in Table 5.

Table 4 Primary antibodies

name	species	antigen	application	source
2125	rabbit	α-tubulin	WB (1:3000)	Cell Signaling
2401	rabbit	phospho-Hsp27 (Ser82)	WB (1:1000)	Cell Signaling
sc-31	mouse	N-Ras(F155)	WB (1:1000)	Santa Cruz Biotechnology
4370	rabbit	phospho-p44/42 MAPK (Erk1/2) (Thr202/Tyr204)	WB (1:2000)	Cell Signaling
ab15580	rabbit	Ki67	IF (1:200)	Abcam
ab7952	rabbit	p38	WB (1:200)	Abcam
ab28848	rabbit	p-ATF2 (T69 + T51)	WB (1:1000)	Abcam
sc-596	rabbit	Cyclin A	WB (1:200)	Santa Cruz Biotechnology

Table 5 Secondary antibodies

name	species	species antigen	application	conjugation	source
4Ac	goat	mouse	WB (1:2000)	peroxidase (PO)	Dianova, Hamburg
B4c	goat	rabbit	WB (1:2000)	peroxidase (PO)	Dianova, Hamburg
A-11037	goat	rabbit	IF (1:1000)	Alexa 594	Invitrogen

2.10. Kits

All kits used in this study are listed in Table 6.

Table 6 Kits

name	company
QIAquick Gel Extraction	Qiagen
QIAprep Spin Miniprep	Qiagen
Qiagen Plasmid Maxi	Qiagen
Qiagen Plasmi Midi	Qiagen
Rapid DNA Ligation	Roche
Platinum Pfx DNA Polymerase	Invitrogen
Rneasy Mini Kit	Qiagen
TaqMan Reverse Transcription Reagents	Applied Biosystems

2.11. Culture media

All cell lines were maintained and propagated in DMEM medium (Gibco) supplemented with 10 % FCS, 1 mM sodium pyruvate, 0.1 mM Non-Essential Amino Acids Solution (in Minimum Essential Medium Eagle) (Gibco) and 1x PenStrep (Gibco). Cells were frozen in DMEM freezing medium containing 50 % FCS and 10 % dmso.

Bacteria were cultured in LB Medium, containing 10 g/l bacto-tryptone 5 g/l bacto-yeast extract, 20 mM NaCl (pH 7.5) and ampicillin (50 µg/ml). Transformed bacteria were incubated in SOC medium (Invitrogen). Agar plates were made with LB medium containing 15 g/L agar and ampicillin (50 µg/ml).

2.12. Mouse strains

Wild type C57 Bl/6 mice were purchased from Harlan or Janvier. $P19^{Arf-/-}$ mice have been generated by Charles Sherr [130] and were obtained in a C57 BL/6 background from Scott Lowe.

3. Methods

3.1. Molecular biology techniques

3.1.1. PCR cloning of shRNAs

DNA fragments were amplified and restriction sites were added to their ends by standard cloning PCRs with the Platinum *Pfx* DNA Polymerase Kit from Invitrogen. For the reaction 10-300 ng template DNA was used and incubated in the supplemented buffer with: 0.02 - 0.1 Unit/µL polymerase, 0.3 mM dNTP mixture (Peqlab), 0.3 µM of forward and reverse cloning primers, and 1 mM $MgCl_2$ (Invitrogen). The following PCR protocol was used (Tab. 7):

Table 7 PCR protocol with *Pfx* Polymerase

94 °C	2 min	
94 °C	15 sec	25-35 cycles
X °C	30 sec	
68 °C	1 min per kb	
68 °C	5 min	
4 °C	∞	

3.1.2. Digestion of DNA with endonucleases

For analytical digests approximately 0.2 to 1 ug DNA was used. Preparative digests were performed with 10-15 µg DNA. Digestions with restriction endonucleases (NEB) were carried out with 0.1 - 1 Units/µl in 37 °C for 2 to 4 hours in corresponding reaction buffers (NEB).

3.1.3. Dephosphorylation of digested DNA

To avoid religation of digested plasmids, 10 - 15 µg DNA was dephosphorylated with 0.1 - 1 Units/µl of Calf Intestinal Alkaline Phosphatase in the corresponding buffer (NEB) for 1 to 3 hours at 37 °C.

3.1.4. Agarose gel electrophoresis

The separation of DNA fragments was done via agarose gel electrophoresis. The corresponding agarose gels were prepared with 1 - 2 % agarose, dissolved in 1x TAE buffer and supplemented with 0.01 % ethidium bromide. The DNA was separated together with the peqGOLD low range DNA ladder or the 1kb DNA ladder (Peqlab) under 50 - 120 V in 1x TAE and visualized under UV light. In some cases DNA was extracted from the gels by using the QIAEX II Agarose Gel Extraction Kit (Qiagen).

3.1.5. Ligation

For standard ligations the T4 DNA Ligase (NEB) was used. 100 - 1000 ng DNA was ligated usually in a 5:1 molar ratio of insert to backbone DNA. The reaction was performed with 20 U/µL T4 DNA ligase in T4 DNA ligase reaction buffer for 1 - 3 hours at 16 °C.
For cloning of high complexity shRNA libraries the Rapid Ligation Kit from Roche was used. 300 - 500 ng of DNA was used in a 5:1 molar ratio of insert to backbone DNA. Ligation was run overnight starting at 4 °C with warming up to room temperature. All ligation reactions were also performed without insert as a negative control.

3.1.6. Transformation of recombinant DNA

For cloning of single constructs DH5α Competent Cells (Invitrogen) were used for transformation. 1 - 10 ng of DNA were incubated with bacteria on ice for 30 minutes and subjected to a 20 second heat shock at 42 °C.
For transformation of bacteria with DNA containing shRNA libraries, MegaX DH10B T1 electrocompetent bacteria (Invitrogen) were used. The transformation with 1-10 ng DNA was performed by electroporation with 2 kV, 200 Ω and 25 µF. Transformed bacteria were incubated with 950 µL SOC medium (Invitrogen) at 37°C for 1 hour shaking at 225 rpm and afterwards plated on LB-agar plates with ampicillin (50 µg/µL). The plates were then incubated for 12-16 hours at 37 °C.

3.1.7. Sequencing

Standard DNA capillary sequencing was processed in the HZI array and genome analysis facility (Head: Robert Geffers) with corresponding sequencing primers (10 µM) which are listed in Table 4.

3.1.8. DNA purification

DNA was purified via the QIAquick Gel Extraction Kit from Qiagen using the DNA purification protocol. Additionally, in some cases (e. g. cloning of shRNA libraries) DNA was purified via Phenol-Chloroform extraction and ethanol precipitation. Phenol-chloroform extractions were performed either with a mixture of phenol, chloroform and isoamylalcohol (25/24/1) or, for small DNA fragments, with phenol (both from Roth). These solutions were mixed with DNA in the same volume and centrifugated (17.000 x g, 10 minutes) to separate a DNA containing phase. Subsequently ethanol precipitation was done with 3 M sodium acetate (1/10 volume of DNA solution), ethanol (three times volume of DNA solution) as well as 1 µL pellet paint (Novagen). The solution was incubated at -20 °C (1- 4 hours) and centrifuged (17.000 x g; 30 minutes). The pellet was washed twice with 70 % ethanol, dried and dissolved in water.

3.1.9. Plasmid DNA preparation

DNA plasmids were amplified by overnight bacteria cultures, shaking at 37 °C in LB medium with 50 µg/ml ampicillin. The bacteria were centrifuged with 3.500 – 6.000 x g for 10 min and the DNA was extracted using either the Qiagen Plasmid Maxi Kit (for high amounts of DNA) or the Qiagen Miniprep Kit (for small amounts of DNA). For hydrodynamic tail vein injection or cell transfection the EndoFree Qiagen Plasmid Maxi Kit from Qiagen was used for DNA preparation.

3.1.10. Isolation of DNA from cells and mouse tissues

Genomic DNA was isolated from cells, smashed mouse livers or tails. The samples were incubated overnight with a corresponding volume of gDNA extraction buffer (7,5 ml for whole liver extraction, 750 µL for tails and cells). Subsequently, proteinase K was inactivated at 90 °C for 10 minutes. 1/3 volume of 5 M NaCl solution was added to the solution, which was incubated for 5 minutes at 55 °C and centrifuged with 17000 x g for 10 minutes. Afterwards, 2/3 volume of isopropanol was added to the supernatant incubated at -20 °C and centrifuged with 17000 x g for 30 minutes. The pellet was washed with 70 % ethanol and after a drying step dissolved in water. In some cases (e.g. Solexa PCR) the DNA was additionally purified by phenol-chloroform extraction and ethanol precipitation (see DNA purification).

3.1.11. RNA isolation and RNA purification

RNA was isolated from cells by using TRIZOL RNA isolation protocol (Invitrogen). Contaminating DNA was digested via DNase I (NEB) (0.05 U/µL) in a 30 minutes reaction at room temperature in the corresponding reaction buffer (NEB). Afterwards the reaction was purified by the RNeasy Mini Kit (Qiagen) using the RNA cleanup protocol.

3.1.12. cDNA synthesis

cDNA synthesis from mRNA templates was performed with the TaqMan Kit (Applied Biosystems) using the corresponding protocol. 2 µg of RNA and random hexamer primers were used. The reaction was performed at 25 °C for 10 minutes, at 48 °C for 30 minutes and at 95 °C for 5 minutes.

3.1.13. Nucleic acid concentration measurement

DNA and RNA concentrations were determined with the NanoDrop 1000 from peqlab.

3.1.14. Quantitative polymerase chain reaction (qPCR)

The primers for qPCR were designed by means of Pearl Primer software. As a template, 2 µL cDNA was used with 0.3 µM of both forward and reverse primers. Primers were used either for the gene of interest or for beta-actin [108] that served as a control (Tab. 4). qPCR was performed with the 7500 real-time PCR system cycler (Applied Biosystems) using SYBR green detection (passive reference rox dye) and the SYBR green PCR Master Mix (Applied Biosystems). The used PCR protocol is shown in Table 8.

Table 8 qPCR protocol

95 °C	10 min	
95 °C	15 sec	45 cycles
56 °C	1 min	
60 °C	1 min	
95 °C	15 sec	
60 °C	1 min	
95 °C	15 sec	
60 °C	15 sec	

To analyze the size of PCR fragments a dissociation curve was performed subsequent to the PCR reaction. The calculation of mRNA concentrations was done via manual cT values (hhreshold 0.2 in cycles 3-15). The fold expression was calculated with dilution rows.

3.2. Cell culture methods

3.2.1. Cell culture

Cells were cultured in DMEM medium containing 10 % FCS at 37 °C, 90 % humidity and 7 % CO_2. Cells were splitted using Trypsin/EDTA solution (Gibco). Cells were frozen in DMEM freezing medium and stored in liquid nitrogen.

3.2.2. Isolation of cells from tumor nodules

Cell lines were generated from murine tumor tissues. Mice were euthanized and sterilized with 70 % ethanol for 10 minutes and tumor nodules were cut out from adhering tissue under sterile conditions, smashed and incubated with Dispase (1000 U/ml) and Collagenase (0.1 U/ml) (Roche) in DMEM medium, containing 1xHBS buffer for 30 minutes at 37 °C with gentle shaking. The cells were filtrated with nylon mesh filter (100 µm), centrifuged at 80 x g for 10 min and washed twice with medium. The cells were placed on a 0.1 % gelatin solution and maintained in culture as long as remaining contaminating fibroblasts were removed.

3.2.3. Calcium-phosphate-mediated transfection

Eucaryotic cells were transfected using calcium phosphate transfection. 20 - 30 µg DNA was used for 70 - 80 % confluent cells in 10 cm plates. The cells were incubated for 15 minutes with DMEM medium, containing 25 µM chloroquine. 500 µL of DNA solution, containing 2 M $CaCl_2$ was dropwise added by bubbling to 500 µL 2x HBS buffer. The received precipitate was added dropwise to the cells and incubated with the chloroquin containing medium for 14-16 hours.

3.2.4. Retroviral gene transfer for generation of stable cell lines

Retroviral gene or shRNA transfer was accomplished using phoenix packing cells which produce viral particles with retroviral vector DNA. The phoenix cells were transfected with retroviral DNA via calcium phosphate-mediated transfection. The viral supernatant was collected every 6 hours during 24-72 hours after transfection [131]. The viral supernatant was filtered through a syringe filter (0.45 µM) and 100 – 1000 µL of viral supernatant was applied directly to the medium of 30 % confluent target cells. To improve the infection efficiency of differently infectable target cells, the infection was accompanied by addition of polybrene (1-10 µg/ml). Target cells were selected by addition of corresponding antibiotics, either puromycin (1 - 10 µg/ml) or hygromycin (300 - 1000 µg/ml).

3.2.5. *In vitro* drug treatment

Sorafenib was dissolved in dmso (stock concentration: 4.3 mM) and added to different final concentrations into the medium of the corresponding cells.
BIRB 796 (stock concentration: 15.76 mM), SB 202190 (stock concentration: 25.15 mM) Skepinone-L (stock concentration: 10mM) and PH 797804 (stock concentration: 10.4mM) were also dissolved in dmso and added to different final concentrations into the medium of the corresponding cells.

3.2.6. Crystal violet staining

Cells were washed with PBS and fixed with 10 % formaldehyde solution for 30 - 60 minutes. After fixation, the cells were washed with water and dried and stained with a 0.07 % crystal violet solution for 30 – 60 minutes. The cells were washed again and dried.

3.2.7. Cell doubling assay

The quantification of cell proliferation rates was evaluated by cell doubling assay. For this, the cell number (cells / µL) was counted using Guava flow cytometer and Guava EasyCyte Plus software. For counting, trypsinized cells were resuspended in medium and measured in a corresponding dilution with PBS. The doubling time was calculated as fold-changes in comparision to an intial point measurement.

3.2.8. Trypan blue staining

To estimate the percentage of dead cells, tryphan blue staining of cells was performed. For staining, the medium containg floating cells, PBS after cell washing as well as the trypsinized cells were collected and centrifuged at 80 x g for 10 – 15 minutes. The pellet was resuspended in 1-2 mL medium and mixed with tryphan blue solution (0.4 %) (Sigma) in a 1:1 ratio. The total number of cells and tryphan blue positive cells were counted by means of Neubauer hemocytometer.

3.3. Biochemical methods

3.3.1. Preparation of protein extracts from cultured cells

NP40 lysis buffer or NP40 phospho lysis buffer were used to extract proteins from cultured cells and mouse tissue. Culture cells were washed twice with PBS and the NP40 lysis buffer was added directly to the cells, which were removed from the dish using a cell scraper. Tissues were also washed with PBS and homogenized in the NP40 buffer. Cells and homogenized tissue were incubated with shaking for 10 min at 4 °C, and centrifuged for 10 min at 11000 x g at 4 °C. The supernatant with the proteins was separated from the pellet.

3.3.2. Measurement of protein concentration

Protein concentration was determined using the Precision Red Advance protein assay (Cytoskeleton) according to the manufacturer's manual.

3.3.3. Sodium dodecyl sulfate polyacrylamide gel electrophoresis

Sodium dodecyl sulfate polyacrylamide gel electrophoresis (SDS-PAGE) was performed essentially according to Laemmli (Laemmli, 1970). SDS-PAGE gels were run in BIO-RAD apparatures with 1mm spacers. 20 - 80 µg of proteins were incubated with protein loading buffer at 95 °C for 5 minutes and seperated with the prestained protein marker broad range (NEB) on SDS stacking gels with 30 mM and on separation gels with 35 mA. (Tab 9, 10).

Table 9 10 % seperating gel
10 % Acrylamid
0.27 % Bisacrylamid
375 mM TrisHCl (pH 8.8)
0.1 % APS
0.01 % TEMED

Table 10 5 % stacking gel
5 % Acrylamid
0.13 % Bisacrylamid
125 mM TrisHCl (pH 6.8)
0.1 % APS
0.01 % TEMED

3.3.4. Western blotting

Proteins from SDS-PAGE gels were transferred onto nitrocellulose membrane (Amersham Hybond ECL Nitrocellulose Membrane) usind a semidry blotting system and a transfer buffer for 30 min at 15 V. Membranes were blocked for 30 min at room temperature or at 4 °C overnight with 5 % BSA (Roth) in TBS-Tween. Afterwards, membranes were incubated for 1 hour at room temperature or overnight at 4 °C in TBS-Tween buffer containing primary antibodies. Membranes were washed 3 times in TBS-Tween buffer 15 min and then incubated for 1h at room temperature in TBS-Tween buffer containing the corresponding secondary antibodies (1:1000) (Tab. 7). Membranes were again washed 3 times with TBS-Tween buffer and incubated for up to 4 min with Lumi-Light Western Blotting Substrate (Roche) and exposed to Hyperfilm ECL (Amersham Biosciences).

3.4. Mouse experimental methods

3.4.1. Mouse husbandry

All animal experiments have been approved by the German legal authorities. All mice were housed and maintained under pathogen free conditions in accordance with the institutional guidelines of the Helmholtz Centre for Infection Research.

3.4.2. Genotyping

The genotype of $p19^{Arf}$ mice was analysed via PCR of genomic tail DNA. The PCR was performed with *Taq* polymerase (Applied Biosystems) (0.04 - U/µL) in the corresponding buffer and 0.16 mM dNTPs, 4 % dmso, and three primers, Arf-1 (0.4 µM), Arf-2 (0.96 µM) and Arf-3 (0.96 µM). The following PCR programs were used (Tab. 11).

Table 11 p19^{Arf} genotyping PCR

95 °C	5 min	
95 °C	1 min	37 cycles
65 °C	1 min	
72 °C	1 min	
72 °C	5 min	
4 °C	∞	

Genotyping PCRs were analyzed on agarose gels which identified the wildtype allele with a 415 bp and a mutant allele with 250 bp PCR product.

3.4.3. Hydrodynamic tail vein injection

DNA for hydrodynamic tail vein injection was prepared, using the Qiagen EndoFreeMaxi Kit and disolved in 0.9 % NaCl solution to a final volume of 10 % of body weight. Animals were injected within ten seconds with 25 µg transposon plasmids and 5 µg transposase.

3.4.4. Orthotopic transplantation of tumor cells

Mice were anasthesized with rompun/ketamin solution (450µl ketamine + 50µl rompun + 4500µl NaCl) and dosed intraperitoneally as 10µl/g body weight and subjected to laparotomy. 1,000,000 murine hepatoma cells were injected into the left murine liver lobe. To avoid the extravasation of tumor cells the abdominal cavitiy was washed with prewarmed deoinized water.

3.4.5. Doxycycline administration

Doxycycline hyclate (Sigma) was added to the drinking water of mice to a final concentration of 2 mg/ml. Additionally, saccharose (Roth) was added to a final concentration of 1 g/100 ml water. Doxycycline containing water was prepared fresh and changed once per week.

3.4.6. Drug treatment of mice

The treatment of mice with Sorafenib, BIRB 796 or the corresponding vehicles was performed by oral gavage every second day.

The mice were treated with 100 mg/kg body weight Sorafenib (Nexavar), which was freshly dissolved in a Cremophor EL / 95 % ethanol / water solution (12.5:12.5:75). BIRB 796 was dissolved in 25 % ethanol and delivered to mice in a dose of 50 mg/kg body weight.

3.4.7. Dissections of murine livers

Mice were harvested either due to a critical tumor burden (survival plots) or at defined time points. Livers were photographed, sampled and processed for further analysis.

3.4.8. *In situ* GFP detection

In vivo GFP Imaging of mice and tumor bearing livers was done using the Hamamatsu Imaging system.

3.5. Histological methods

3.5.1. Sections of paraffin embedded tissues

The corresponding samples were fixed overnight with 4 % PFA in PBS. They were embedded in paraffin and cut by Nina Struever (Hannover Medical School) or Anna Rinkel (HZI histopathology core facility).

3.5.2. Haematoxylin and eosin staining

Hämatoxylin and eosin (H&E) stainings were performed by the HZI histopathology core facility.

3.5.3. Preparation of frozen sections frozen tissue samples.

Sections were made with the HM 560 cryostat (Microtom) at -20 °C. Snap frozen tissue embedded in Tissue-Tec OCXT compound (Sakura) were used.

3.5.4. Ki67 staining

Ki67 stainings were performed with 8 µm sections of snap frozen tissues. The slides were fixed with 4 % paraformaldehyde (in PBS) for 10 minutes at RT and then washed three times for 5 min with PBS. The slides were blocked with normal goat serum (NGS) blocking solution for 1 hour at RT. After rinsing the sections shortly in PBST, the primary Ki67 antibody was applied (1:200) in 1 % NGS in PBST and the samples were incubated overnight at 4 °C. After washing tree times with PBST the slides were incubated with the rabbit secondary antibody (1:1000) and 1 µg/ml DAPI in PBST with 1 % NGS for 1 hour at room temperature in the dark. Finally, the sections were washed three times in PBST in the dark and mounted with Vectashield H-1000. The sections were stored at 4°C.

3.5.5. Terminal deoxynucleotidyl transferase dUTP nick end labeling (TUNEL)

Apoptotic cells were detected by using of the Terminal deoxynucleotidyl transferase dUTP nick end labeling (TUNEL) Kit from Roche. The staining was performed on 8 µm sections of snap frozen tissues. Additionally, DNA was stained by 1 µg/ml DAPI for 1 hour at 37°C.

3.5.6. Microscopy

All stainings were photographed with the Zeiss Photomicroscop Axiophot2. Pictures were taken with the ORCA-ER camera from Hamamatsu and the Simple PCI software.

3.6. Microarray and deep sequencing analysis

3.6.1. PCR-based amplification of shRNA cassettes

Genomic DNA was isolated from corresponding mouse livers. The hairpin sequences of genomic tumor DNA and plasmid pools were amplified with primers harboring the Illumina adapter sequence and a sample identifier (3 bp barcode). The PCR was done with *Taq* polymerase (Applied Biosystems). Up to 64 samples were pooled and subjected to Illumina deep sequencing. (Nature protocols)

3.6.2. Determination of shRNA abundance by deep sequencing analysis

Deep sequencing was carried out in HZI array and genome analysis facility (Head: Robert Geffers). Illumina GA IIx with a 46 bp single end run was applied to deep sequencing analysis. Base calling and export of the sequencing results were performed with FASTA files via Illumina Pipeline Vers.1.8. The data analysis was accomplished by Michael Jarek (HZI array and genome analysis facility) using a Perl-Script. The data were separated using the corresponding barcodes and the unique reads of the separated samples were determined. The sequences were further aligned to the shRNA library data (Tab. 14) (only 100 % matches) and summarized.

3.6.3. Expression array

mRNA gene expression microarray analyses were performed by Robert Geffers and the HZI array and genome analysis facility by using Affymetrix GeneChip MOE430 2.0. The image analysis was done using the GCS3000 Scanner and the GCOS1.2 Software Suite (Affymetrix). Analysis of microarray data was performed using GeneSpring 11.5.1 (Agilent Technologies). Upstream factors were analysed by Ingenuity pathway analysis software (Ingeuity Systems, Inc)

3.7. Statistics and bioinformatical methods

3.7.1. *De novo* design and synthesis of shRNAs

DSIR and Biopred algorithms/webtools were used to design hairpin sequences as 21 nucleotide RNAs [132]. These sequences were combined with common hairpin sequences to obtain 97mer oligonucleotides with a stem loop stem sequence (Tab. 3).

3.7.2. Statistical analysis

Two-tailed student's *t*-test or log-rank test were applied to statistical analyzes.

4. Results

4.1. Sorafenib treatment results in moderate but distinct treatment responses of aggressive murine hepatocellular carcinomas (HCCs)

To study the therapeutic efficacy of Sorafenib *in vivo*, we treated murine HCCs that were generated in a new mosaic liver cancer mouse model. In this model, a transposon-mediated delivery of oncogenes and marker genes was applied into adult hepatocytes. Transposons were delivered together with the sleeping beauty transposase (SB13) in a 5:1 ratio into hepatocytes via hydrodynamic tail vein injection (HDI). In a recent study, it had been shown that two transgenes can be integrated via single transposon where both genes are expressed bicistronic, separated by an internal ribosome entry site (IRES).

We took advantage of a transposon construct, wherein oncogenic $Nras^{G12V}$ and GFP were expressed by the Caggs promoter (pCaggs-$Nras^{G12V}$-IRES-GFP) (Dauch and Zender, unpublished data) (Fig. 9a). As described before transposon-mediated delivery of pCaggs-$Nras^{G12V}$ into $p19^{Arf}$ deficient hepatocytes induces aggressive hepatocarcinogenesis [113]. Additionally, the tumors can be imaged by GFP expression in the liver (Dauch and Zender, unpublished data).

To study the effect of Sorafenib on these tumors, a cohort of mice was injected with $Nras^{G12V}$-IRES-GFP and treated with Sorafenib or carrier, respectively (Fig. 9a). The mice were subjected to a dose of 100 mg/kg body weight every second day, starting 7 days after injection. The Sorafenib treated, as well as the carrier treated groups developed a high amount of liver tumors which were identified as hepatocellular carcinomas by experienced pathologists (Thomas Longerich and Peter Schirmacher, University of Heidelberg) (Fig. 9b,c). The mice treated with the carrier manifested a comparable tumor development to non treated mice and died after median survival of 33 days. Interestingly, the number of tumors in Sorafenib treated mice was not lower than in carrier treated mice but these mice exhibited in general tumors with smaller size (Fig. 9b). These mice died after a median survival of 41 days upon injection and showed therefore a moderate but significant survival benefit to carrier treated mice ($p = 0.0239$) (Fig. 9d).

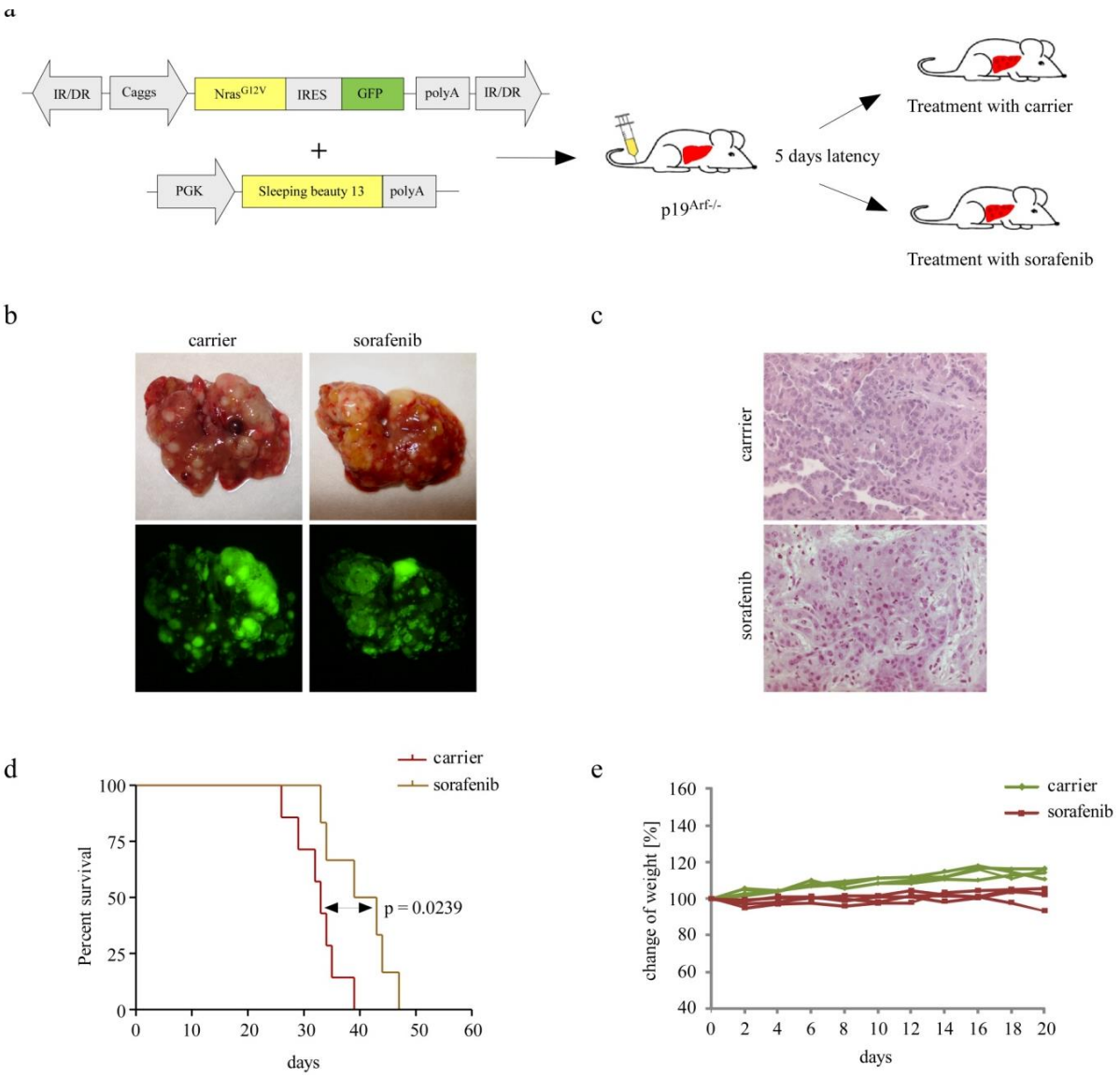

<u>Figure 9</u> A mosaic cancer mouse model allows for studying the *in vivo* response to Sorafenib in HCC

Shematic outline of a transposable element carrying oncogenic Nras^{G12V} and GFP which was delivered together with the sleeping beauty transposase into p19^{Arf} deficient mice, which were subsequently treated with Sorafenib or carrier, respectively (a). Intrahepatic tumor burden with GFP imaging of p19^{Arf} deficient livers of carrier and Sorafenib treated mice, 33 days upon Nras^{G12V} injection (b). H&E staining for Sorafenib and carrier treated mice (c). Survival curves of Sorafenib and carrier treated mice upon Nras^{G12V}-IRES-GFP injection (d). Weight development for Sorafenib and carrier treated mice over a period of 3 weeks (e).

To uncover potential side effects of Sorafenib, a weight analysis was recorded over a 3-week period. This analysis identified a stable but slightly lower weight of Sorafenib treated mice in contrast to carrier treated mice (Fig. 9e).

Tumorigenic cells in cancer mouse models can be used as a source to establish cell lines which then allow for investigating cancer related mechanisms *in vitro*. HCCs derived from transposon-based delivery of Nras^{G12V} into p19^{Arf} deficient hepatocytes were used to isolate

cell lines in a defined genetic background (Fig. 10a,b). Importantly, these cells could be retransplanted into the livers of immuncompetent wild type mice where they again formed HCCs (Fig. 10c).

These cells were also subjected to Sorafenib treatment in order to determine the Sorafenib response in an *in vitro* model, carrying the same genetic leasions as the *in vivo* model.

As described before, Sorafenib targets specifically Raf/Mek/Erk pathway (MAPK pathway) by inhibiting Raf kinases (C-Raf, also known as Raf1 and B-Raf) which is reflected by a downregulation of downstream target Erk.

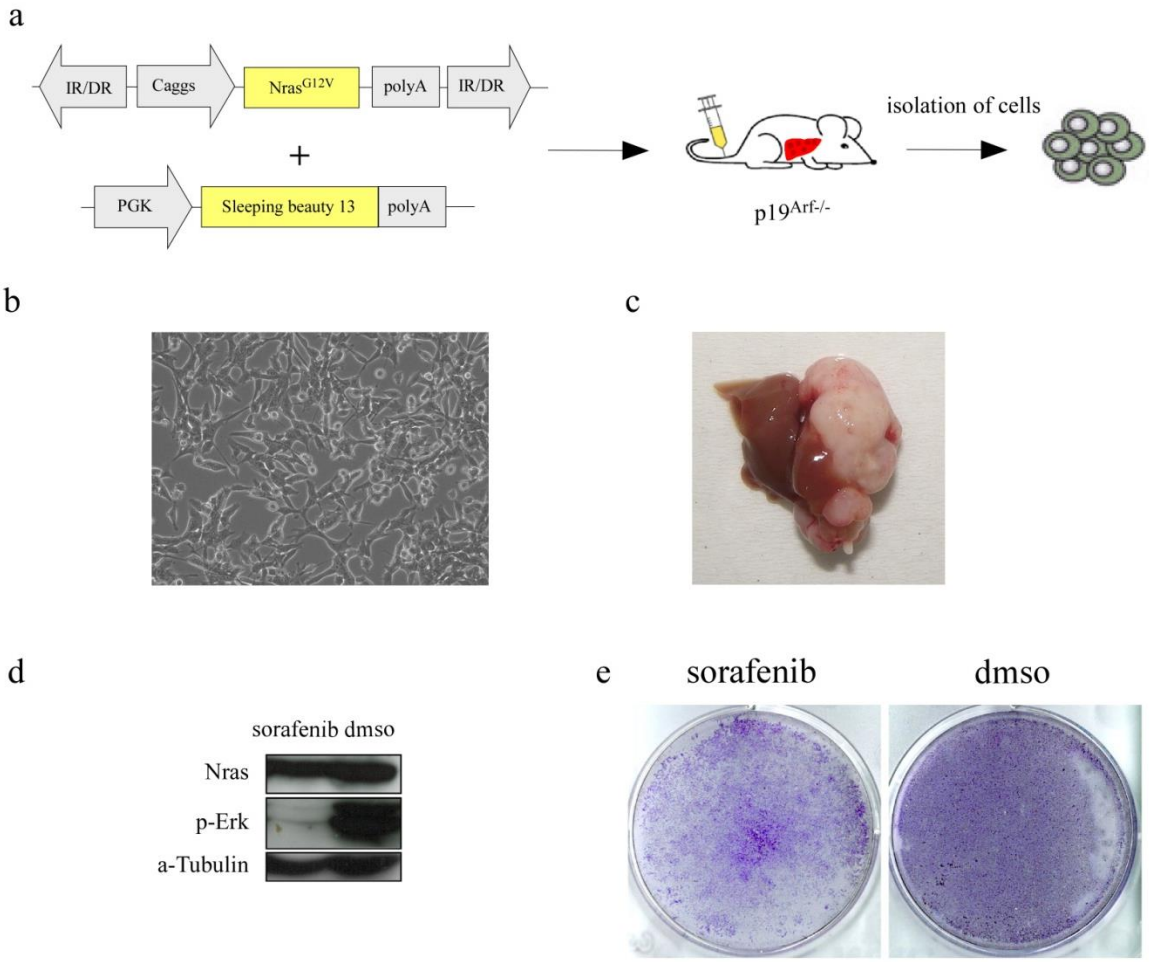

Figure 10 Treatment of Nras^{G12V} driven p19^{Arf} deficient HCC cells *in vitro*

Schematic outline of a transposable element carrying oncogenic Nras^{G12V} that was injected with the sleeping beauty transposase into p19^{Arf} deficient mice to generate tumors for isolation of cells (a,b). *In situ* injection of Nras^{G12V}; p19$^{Arf-/-}$ cells (1 million) into the liver of wild type mice allows for *in situ* tumor development (c). Western blot against phosphorylation status of the Raf downstream target Erk upon Sorafenib or dmso treatment (d). Visualization of crystal violet staining of Sorafenib (8 µM) or dmso treated Nras^{G12V}; p19$^{Arf-/-}$ cells (e).

Indeed, western blot analysis identified a lower amount of phosphorylated Erk upon a 3-day treatment with Sorafenib compared to a dmso (carrier) treatment (Fig. 10d). Furthermore, a visualization of cells by crystal violet staining shows a lower amount of cells after a 3-day treatment by Sorafenib compared to dmso treatment, implying a visual but also moderate effect of Sorafenib on those cells (Fig. 10e).

Taken together, an established *in vivo* mouse model as well as an *in vitro* HCC model carrying the same genetic background allow for studying the response towards Sorafenib.

4.2. *In vivo* and *in vitro* RNAi screens identify putative genes involved in resistance towards Sorafenib

To improve treatment of human HCCs towards Sorafenib it is of high importance to identify new candidate genes involved in mediating resistance to this therapy. Such candidate genes could be potential targets for a combination therapy with Sorafenib which may improve the survival of patients compared to Sorafenib monotherapy. As desribed before, a mosaic liver cancer mouse model was established that reveals a significant but moderate response to Sorafenib treatment. This model was used to apply high throughput functional genetics by an *in vivo* RNAi screen. Expanded transposable elements were used, wherein transgenic expression of oncogenes and marker genes were combined with miR30-based shRNA technology. In these constructs transgenes and shRNAs were transcribed on a single transcript (expressed by Caggs promoter) which allows for an efficient intrahepatic gene knockdown in a physiological manner (Fig. 11a), (Dauch and Zender, unpublished data).

To conduct the screen, we took advantage of an shRNA library targeting genes found amplified in human HCCs (Powers, McJunkin, Zender and Lowe, unpublished data). Genetic amplifications in 200 human HCCs were identified by representative oligonucleotide microarray analysis (ROMA). Hairpins were designed against 70 target genes (~250 shRNAs) using the BIOPREDsi algorithm [133], pooled and cloned into TRMPV vector [134] (Tab. 14). To allow expression of genes and shRNAs on one transcript we took advantage of hairpins, which were embedded into the sequence of microRNA 30 [118]. To transfer the Roma Amplicon library into the $Nras^{G12V}$-IRES-GFP transposon plasmid, the shRNAs from TRMPV were first shuttled via the restriction enzymes XhoI and EcoRI into MSCV plasmid, which contain the miR30 sequence [108;118]. Next, the shRNAs were shuttled together with the 3`miR30 sequence via the restriction enzymes XhoI and MluI/AscI into the $Nras^{G12V}$-

IRES-GFP vector containg the 5` miR30 precusor sequence. To ensure the transfer of all shRNAs, both cloning steps were performed with a 1000 fold overrepresentation of colonies.

The transposable elements, carrying $Nras^{G12V}$, GFP and the ROMA Amplicon library were delivered by HDI into $p19^{Arf}$ deficient hepatocytes (Fig. 11a). 7 days upon injection, mice were subjected to Sorafenib or carrier treatment (n = 8-10) every second day. After 5 weeks, the mice were sacrificed and genomic DNA was extracted from tumor bearing livers (Fig. 11b). To determine the abundance of each individual hairpin in these livers of treated and non-treated mice, deep sequencing analysis was performed. The integrated hairpin sequences were amplified via PCR, which also added a 3-base barcode sequence that allows for analyzing multiple samples in a high-throughput manner.

To make a thorough analysis, the abundance of consecutive hairpins was compared between the average of Sorafenib treated mice and the average of carrier treated mice (Tab. 1).

The differences of invidual hairpins between both groups were determined by the quotient of average hairpin abundance of Sorafenib treated mice over the average hairpin abundance of carrier treated mice.

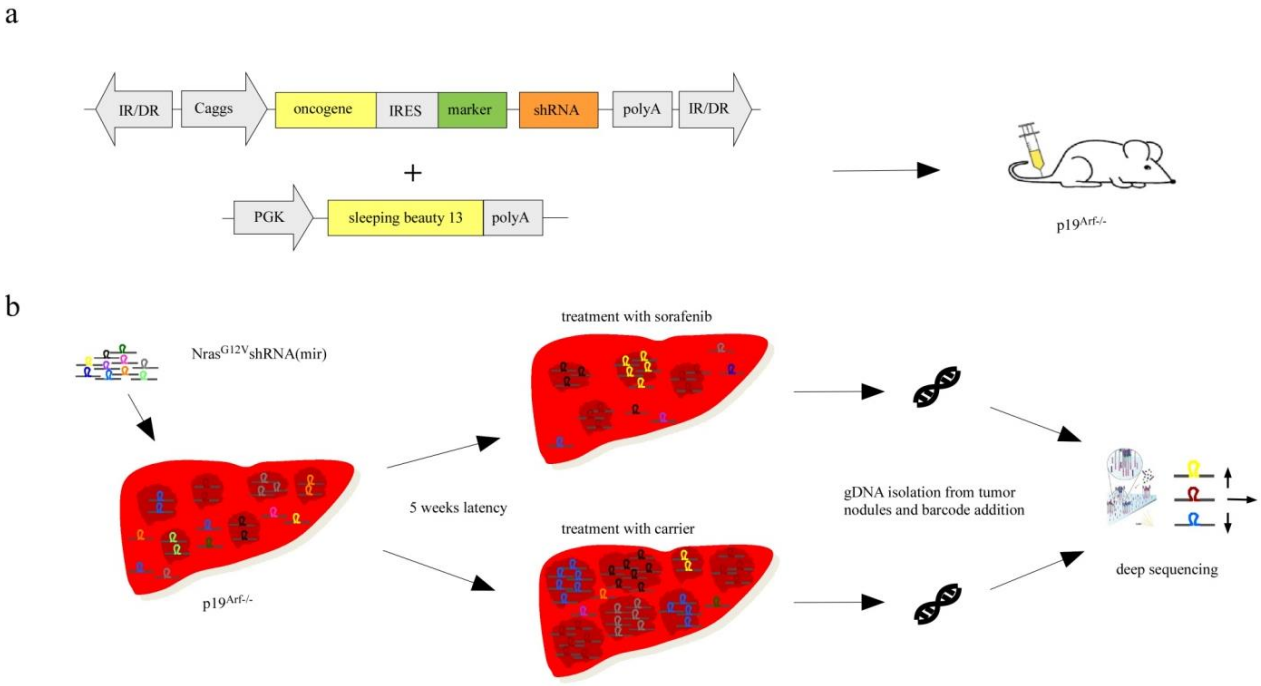

Figure 11 Schematic outline of an *in vivo* RNAi screen to identify genes mediating resistance to Sorafenib

Transposable elements, carrying oncogenes, marker genes and miR30-based shRNAs (a). Schematic outline of an *in vivo* RNAi screen in tumors growing in $p19^{Arf}$ deficient mice, which were injected with $Nras^{G12V}$-IRES-GFP in combination with a shRNA library. Mice were treated either with Sorafenib or carrier (n = 8-10) and the hairpin distribution in the liver tumors was evaluated via deep sequencing of extracted gDNA (b).

This overview identifies the abundance of the majority of shRNAs not influenced by Sorafenib treatment (63.2 % of all shRNAs have a fold-change compared to carrier group < 5). However, some hairpins were shown to be enriched or depleted after Sorafenib treatment (Tab. 15). In total, 19 hairpins were found depleted more than 10 fold and 3 hairpins are depleted more than 100 fold compared to the carrier group (Tab. 12).

Interestingly, among the group of hairpins with a more than 100 fold depletion rank two hairpins targeting the Mitogen Activated Pathway Kinase 14 (Mapk14 or p38alpha) with the hairpins Mapk14.1095 (depletion 138.28 fold) and Mapk14.2590 (depletion 324.16 fold).

Table 12 Most depleted shRNAs under Sorafenib treatement (*in vivo* RNAi screen)

hairpin	average carrier	std. dev. carrier	average Sorafenib	std. dev. Sorafenib	depletion
Stk32c.2014	0,014	0,038	0,003	0,004	-5,599
268893_Gstp1	0,695	1,951	0,122	0,150	-5,671
Bcl2l1.101	0,004	0,013	0,001	0,001	-5,912
Fkbp5.2813	1,327	1,902	0,218	0,295	-6,088
Pim2.1464	0,019	0,040	0,003	0,005	-6,508
Neu1.452	0,037	0,066	0,006	0,011	-6,710
Rxra.2278	0,132	0,351	0,019	0,056	-6,874
Mmp8.2236	0,031	0,090	0,004	0,005	-7,385
Stk32c.2134	0,174	0,492	0,023	0,053	-7,611
CYP27B1.1252	0,174	0,340	0,018	0,034	-9,698
Mmp3.1478	0,459	1,316	0,047	0,071	-9,836
Mmp7.256	0,008	0,023	0,001	0,001	-10,405
Ccnd1.3415	0,661	1,532	0,062	0,091	-10,711
Sparc.1758	0,009	0,021	0,001	0,001	-10,861
Pld1.2050	0,267	0,564	0,022	0,061	-12,052
RNASE4.499	0,210	0,409	0,017	0,024	-12,578
Tmprss2.1667	0,354	0,699	0,026	0,046	-13,777
Oat.136	2,553	4,642	0,169	0,172	-15,116
Rxra.2109	0,056	0,086	0,004	0,004	-15,450
Neu1.1710	0,151	0,432	0,007	0,010	-20,524
Acy3.902	0,999	2,524	0,048	0,081	-20,606
Mapk13.417	0,018	0,051	0,001	0,001	-23,589
Mettl1.259	0,107	0,259	0,003	0,004	-37,513
Met.3642	0,236	0,392	0,005	0,011	-44,385
Hck.420	0,845	2,323	0,012	0,018	-69,178
Mmp8.708	0,983	2,909	0,013	0,016	-76,167
BAK1.1809	0,361	1,081	0,005	0,010	-79,266
Mapk14.1095	2,014	5,832	0,015	0,029	-138,285
PMPCA.1841	1,910	5,655	0,012	0,019	-163,065
Mapk14.2590	0,616	1,823	0,002	0,003	-324,163

As described before, Mapk14 is a member of the MAP kinase pathway, and involved in several cell regulatory mechanisms and is described to have pro and anti proliferative functions. A possible role of Mapk14 in resistance to Sorafenib treatment may be interesting due to the fact that it is a good target for pharmacological inhibition and inhibitors are already available [135;136].

To address whether this candidate could only be depleted in an *in vivo* RNAi screen and therefore to address the general significance of *in vivo* RNAi screens, the screen was repeated under *in vitro* conditions. For this screen, the already described $Nras^{G12V}$; $p19^{Arf-/-}$ cells were used. These cells were stably transduced with retroviral particles of Murine Stem Cell Virus (MSCV) which carries the pool of 250 shRNAs of the ROMA Amplicon library that was also used for the *in vivo* screen. Secreted viral particles were applied on target cells to allow for a viral-based gene transfer (Fig. 12a) [131]. The infection rate was kept low (< 25 % of GFP positive cells) to assure a population of cells with single copy integration of viral vectors. Targeted cells were selected with puromycin to achieve a pure population (> 99 % of GFP positive cells).

Several independently infected populations (n = 4) were expanded after selection and divided into different flasks, for Sorafenib and dmso treatment, respectively.

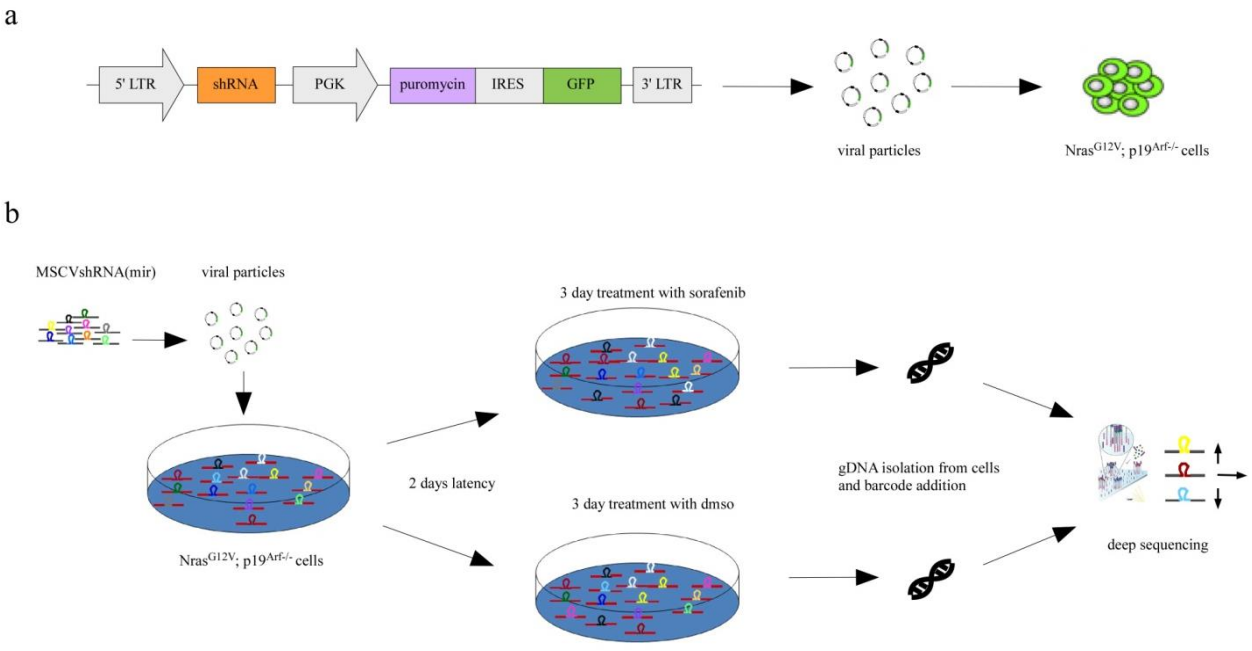

Figure 12 Layout of *in vitro* RNAi screen in $Nras^{G12V}$; $p19^{Arf-/-}$ liver cancer cells

MSCV construct used for viral gene transfer into $Nras^{G12V}$; $p19^{Arf-/-}$ cells (a). Draft of screening procedure, where $Nras^{G12V}$; $p19^{Arf-/-}$ cells were infected with viral particles, harboring the corresponding hairpin pool (ROMA Amplicon). Infected cells were selected to pure populations and subjeted to Sorafenib (8 µM) or dmso treatment. The hairpin distribution of both sets was determined by deep sequencing analysis (b).

After a 3-day treatment, genomic DNA was extracted to analyze hairpin distribution by deep sequencing analysis (Fig. 12b).

Similar to the *in vivo* screen analysis the presence of hairpins was compared between the average value of Sorafenib treated cells and the average value of dmso treated cells (Tab. 15). A pattern with a majority of shRNAs being non-affected hairpins (81,6 % have a fold-change compared to dmso group < 5) was comparable to the *in vivo* screen (Tab. 15). However, although depleted hairpins were found in the *in vitro* setup, the hairpins in general did not deplete that pronounced as in the *in vivo* system (Fig. 13a,b). Therefore, only 14 hairpins are found depleted more than 10 fold, and only one hairpin depletes more than 100 fold compared to dmso group (Tab. 13).

Table 13 Most depleted shRNAs under Sorafenib treatement (*in vitro* RNAi screen)

hairpin	average dmso	std. dev. dmso	average Sorafenib	std. dev. Sorafenib	depletion
Bcl2l1.974	0,090	0,110	0,016	0,025	-5,729
Itfg1.1897	0,049	0,069	0,008	0,011	-5,825
Ndufv1.221	1,623	2,876	0,265	0,436	-6,117
NUDT3.1284	0,079	0,165	0,012	0,025	-6,360
FGF12.1241	0,292	0,591	0,045	0,079	-6,457
Stk32c.724	0,322	0,377	0,046	0,061	-6,932
Rpo1-1.311	0,217	0,451	0,031	0,064	-6,995
CLIC1.1126	0,171	0,219	0,024	0,023	-7,069
Mmp7.256	0,072	0,161	0,010	0,012	-7,097
Mmp8.2236	0,035	0,067	0,004	0,006	-8,070
Ehhadh.1876	0,031	0,032	0,004	0,005	-8,702
NDUFS8.807	0,673	1,296	0,077	0,072	-8,772
FGF12.1933	0,410	0,459	0,046	0,072	-8,870
BRMS1.1002	0,228	0,409	0,025	0,040	-9,205
Pim1.602	0,350	0,819	0,037	0,063	-9,501
Mmp7.170	0,044	0,088	0,004	0,003	-10,762
Brd3.1245	0,353	0,480	0,030	0,061	-11,871
Sparc.1196	0,413	0,433	0,035	0,048	-11,937
Cdkn1a.639	0,250	0,253	0,020	0,019	-12,339
Sparc.1898	0,740	1,347	0,060	0,047	-12,347
Ehhadh.2855	0,205	0,323	0,015	0,015	-14,082
LIPH.291	0,025	0,046	0,002	0,002	-15,123
CYP27B1.1244	0,580	1,361	0,028	0,036	-20,959
Grhpr.361	0,048	0,097	0,002	0,003	-22,233
Pim1.685	0,311	0,640	0,013	0,025	-24,115
Mapk14.1095	0,530	1,288	0,011	0,020	-49,379
Ccnd1.1856	0,039	0,091	0,001	0,001	-50,624
Parp2.574	0,517	0,856	0,009	0,009	-58,230
Bcl2l1.2091	0,060	0,146	0,001	0,001	-81,355
Mmp8.708	0,462	1,098	0,005	0,005	-101,143

The most depleted hairpin was Mmp8.708 (101.143 depletion), targeting Matrix Metallopeptidase 8 (Tab. 13). Although the depletion was lower, the top-scored candidate from the *in vivo* screen (Mapk14) was also found clearly depleted *in vitro* (Mapk14.1095) for which depletion accounted for 49.379 fold.

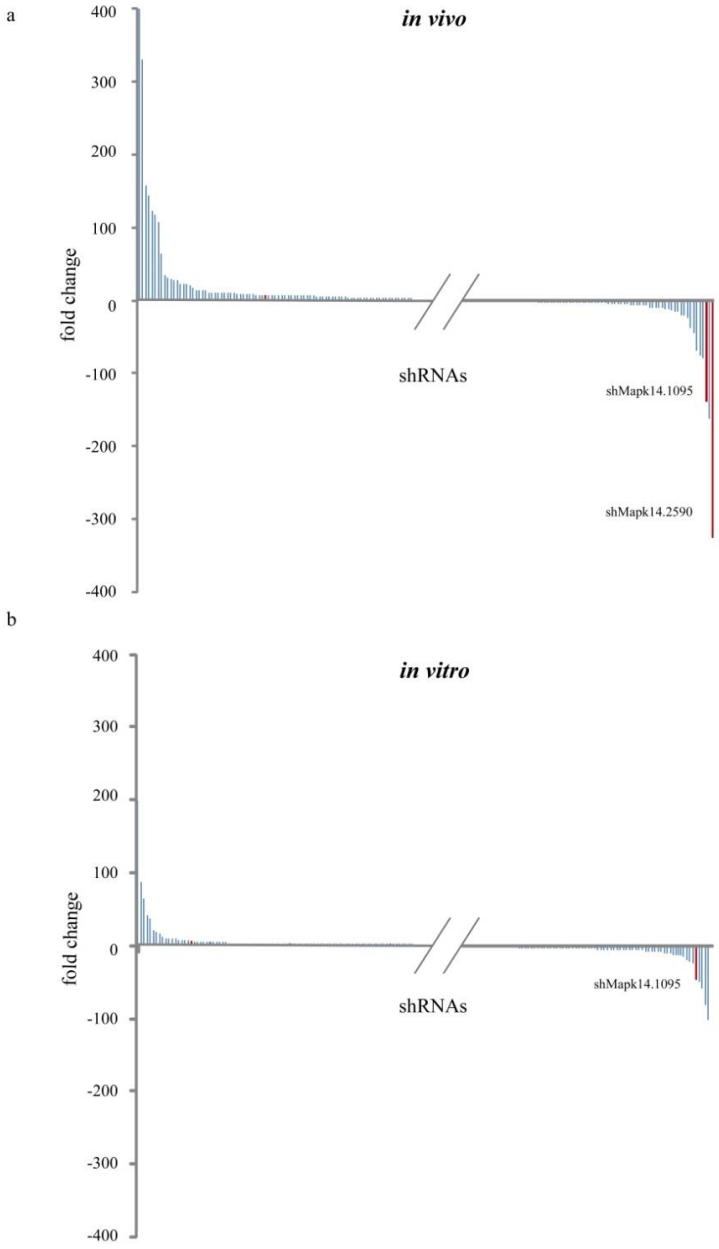

Figure 13 Identification of a potentially therapeutic target for Sorafenib treated HCCs by different RNAi screens

Enrichment and depletion of shRNAs in the *in vivo* RNAi screen after Sorafenib treatment compared to carrier treated mice. Plotted are quotients of average values for Sorafenib treated and carrier treated mice (n = 8-10) (a). Enrichment and depletion of shRNAs in the *in vitro* RNAi screen after Sorafenib treatment of $Nras^{G12V}$; $p19^{Arf-/-}$ cells in comparison to dmso treated cells, plotted are also quotients of average values for Sorafenib treated and carrier treated dishes of cells (n = 4) (b) (Mapk14 hairpins = red, remaining hairpins = blue).

However, if candidate selection had been based on *in vitro* screening alone, four other candidates would have been prioritized for functional testing before MAPK14 and it is unclear whether these other candidate would have shown robust effects in vivo. Nevertheless, comparing the screening results from both systems, Mapk14 was found depleted in both screens (Fig. 13a,b). This target could be a potential candidate gene for mediating resistance to Sorafenib. However, this candidate would not have been selected from an *in vitro* shRNAi screen alone, indicating the significance of screens perfomed in an *in vivo* model.

4.3. Knockdown of Mapk14 sensitizes towards Sorafenib treatment in HCC

The *in vivo* and *in vitro* RNAi screens implied Mapk14 as a potential mediator of resistance towards Sorafenib. To validate this candidate, the effect of single hairpin introduction under Sorafenib treatment was determined by *in vivo* and *in vitro* follow-up experiments. Therefore, the two Mapk14 hairpins (Mapk14.1095 and Mapk14.2590) that were found depleted were cloned as single constructs into MSCV and transposon plasmids.

For this purpose, the hairpin sequences were ordered as 97mer oligonucleotides to which the restriction sites XhoI and EcoRI were added via PCR amlification. The amplified DNA was then cloned with XhoI and EcoRI into MSCV plasmid and next shuttled via XhoI and MluI/AscI restriction sites into transposon plasmid.

Next, the knockdown efficiency of the Mapk14 hairpins was determined, which is important to identify whether the hairpins hit their target and to exclude off-target effects. For this knockdown test $Nras^{G12V}$; $p19^{Arf-/-}$ cells were used. The Mapk14 hairpins as well as non-targeting control hairpin were introduced into those cells by MSCV-based viral gene transfer. After puromycin selection, proteins and mRNA were extracted to determine Mapk14 expression level.

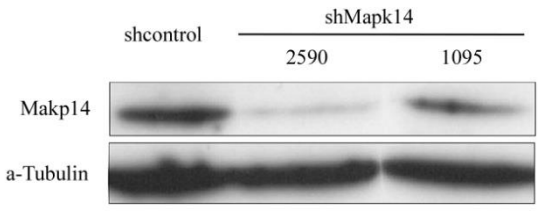

Figure 14 Knockdown efficiency of different Mapk14 hairpins

Western blot analysis of knockdown efficiency of Mapk14.2590 and 1095 shRNAs and a control shRNA after stable transdution of $Nras^{G12V}$; $p19^{Arf-/-}$ cells, measured by whole cell extracts of proteins.

Western blot analysis identified lower protein level of Mapk14 in the presence of respective hairpins and therefore both hairpins exerted a significant knockdown in contrast to a control hairpin (Fig. 14).

For *in vivo* validation of this candidate, several cohorts of $p19^{Arf-/-}$ mice were injected with transposable elements carrying $Nras^{G12V}$-IRES-GFP and either Mapk14 hairpins (Mapk14.1095 and Mapk14.2590) or non-targeting control hairpin. 7 days after injection the treatment with Sorafenib or carrier was commenced with standard treatment protocol.

One cohort of mice was harvested simultaneously 5 weeks after injection to compare the liver cancer development between consecutive groups (n = 4) (Fig. 15a). The other cohort was sacrificed due to critical tumor burden to determine the differences in survival for individual groups (Fig. 15b).

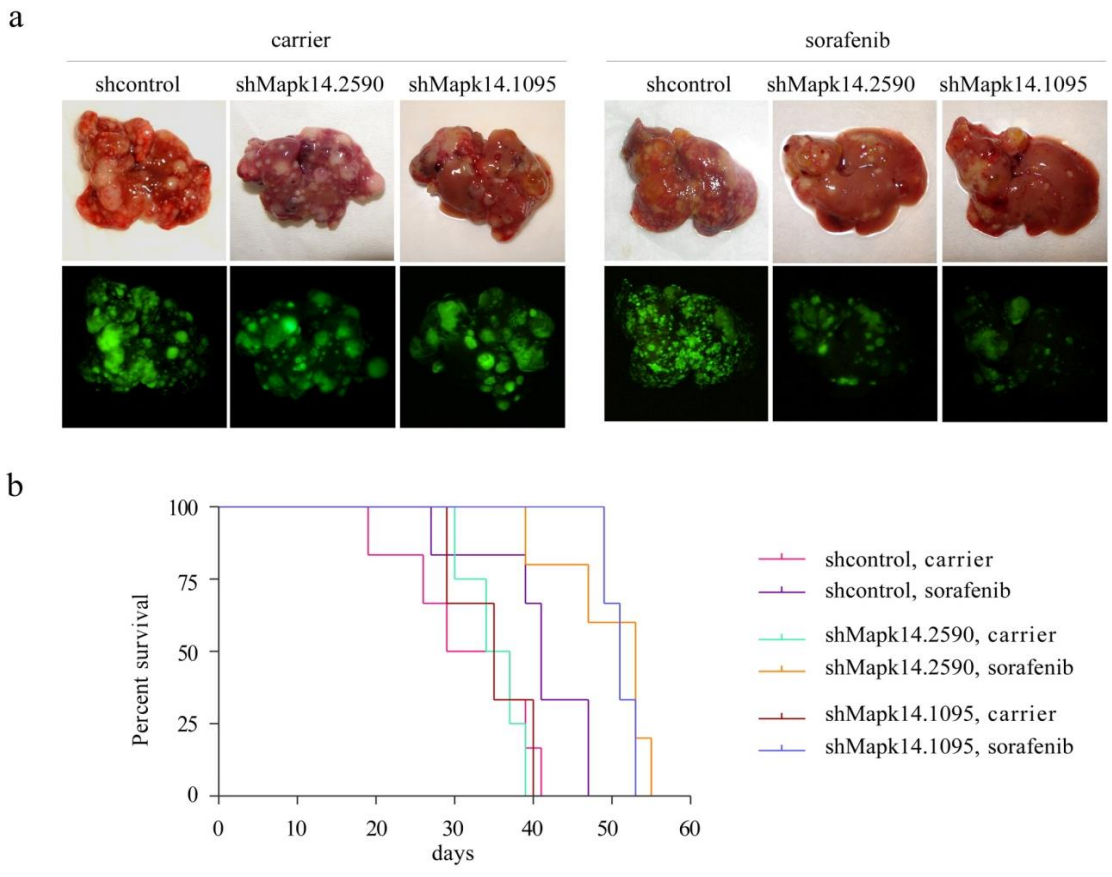

Figure 15 Knockdown of Mapk14 gives rise to smaller tumor burden and a survival benefit for mice under Sorafenib treatment

Intrahepatic tumor burden of $p19^{Arf-/-}$ deficient mice, 5 weeks after injection of transposons containing $Nras^{G12V}$-IRES-GFP and two different hairpins against Mapk14 or control after treatment with Sorafenib or carrier (n = 4) (a). Survival curve of $p19^{Arf}$ deficient mice after injection of $Nras^{G12V}$-IRES-GFP in combination with 2 different Mapk14 or control hairpins for Sorafenib and carrier group, respectively (b).

Carrier treated mice carrying a control hairpin showed massive tumor burden after 5 weeks and had to be sacrificed due to liver failure with a median survival of 33 days. Administration of Sorafenib reduced tumor growth in a moderate way and prolonged median survival up to 41 days. These data were in accordance with prior observations of the initial treatment study. Carrier treated mice harboring Mapk14 hairpins showed a similar pattern of tumor burden and survival as carrier treated mice with control hairpin (with median survival of 35 days for both shMapk14.2590 and shMapk14.1095), indicating no general impact of Mapk14 knockdown on tumor development.

Interestingly, knockdown of Mapk14 in combination with Sorafenib showed smaller tumor burden after 5 weeks and also significantly extended survival compared to Sorafenib treated mice (with control hairpin) with a median survival of 53 days for shMapk14.2590 and median survival of 51 days for Mapk14.1095 ($p = 0.0466$ between shcontrol and shMapk14.2590; $p = 0.0125$ between shcontrol and Mapk14.1095, under Sorafenib treatment). These data indicate that knockdown of Mapk14 induces survival benefit under Sorafenib treatment.

To allow for *in vitro* experiments, which may be relevant to get mechanistic input, cells harboring transposons carrying $Nras^{G12V}$-IRES-GFP and either Mapk14 hairpin (shMapk14.1095) or control hairpin were isolated by collagenase/dispase digestion of tumors from $p19^{Arf}$ deficient mice. To estimate whether cells carrying Mapk14 hairpin are more sensitive to Sorafenib treatment than cells with a control hairpin, a colony formation assay was performed. For this, 5000 cells were plated onto 10-cm dish plates, allowed to seed and subjected to Sorafenib or dmso treatment on next day. After 8 days, the size and number of colonies were visualized by crystal violet staining of cells (Fig. 16).

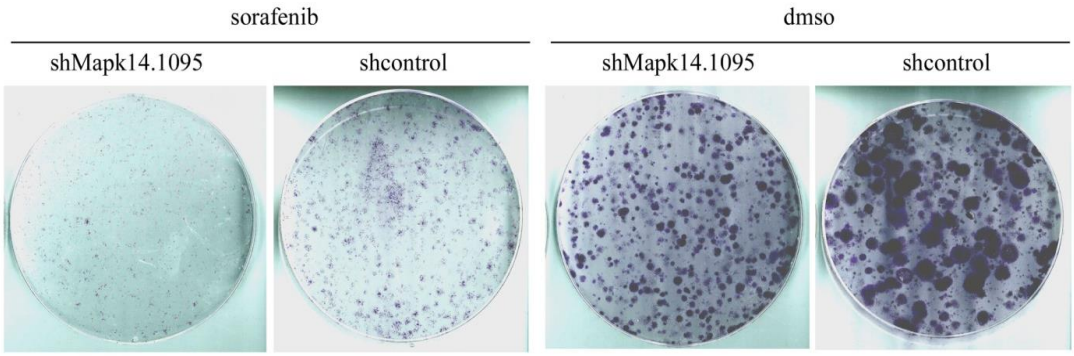

Figure 16 Knockdown of Mapk14 reduced proliferation of $Nras^{G12V}$; $p19^{Arf-/-}$ cells under Sorafenib treatment

Colony formation assay of $Nras^{G12V}$; $p19^{Arf-/-}$ cells, carrying Mapk14 or control hairpin (5000 cells were plated for each condition). Shown is visualization of cells stained with crystal violet 9 days later, after an 8-day Sorafenib (8 µM) or dmso treatment.

Due to the fact that dmso treated cells with shMapk14 showed slightly smaller colonies than dmso treated cells with shcontrol, a small difference between both cell lines was observed. However, Sorafenib treatment diminished colony formation in cells with Mapk14 hairpin much stronger than in cells with control hairpin, supporting the important role for Mapk14 under Sorafenib treatment and implies Mapk14 as a potential target for combinatorial therapy.

4.4. Sorafenib treatment and Mapk14 knockdown act synergistically by inhibition of proliferation

As described above, Mapk14 knockdown improves the response of HCC to Sorafenib treatment. Next, it was determined whether the slower tumor growth under Mapk14 knockdown is caused by a decreased proliferation rate or a higher amount of cell death. Therefore, $Nras^{G12V}$; $p19^{Arf-/-}$ murine HCCs were analysed by Ki67 staining to evaluate the proliferation rate and by Terminal Deoxynucleotidyl Transferase dUTP Nick End Labeling (TUNEL) to count the rate of apoptotis. These stainings were conducted 5 weeks after injection, with Sorafenib or carrier treatment and with Mapk14 or control hairpins, respectively.

The percentage of Ki67 positive cells was comparable between all carrier treated mouse livers, with 22.6 ± 4.9 % for shcontrol mice, 23.3 ± 5.8 % for shMapk14.1095 mice and 23.4 ± 7.0 % for shMapk14.2590 mice. In contrast, the number of Ki67 positive cells was in general lower for Sorafenib treated mice. Interestingly, mice with Mapk14 hairpins showed lower percentages of Ki67 positive cells with 13.9 ± 1.9 % for shMapk14.1095 mice and 10.6 ± 3.6 % for shMapk14.2590, compared to the control hairpin with 18.4 ± 4.2 % of positive cells ($p < 0.05$) (Fig. 17a).

The number of apoptotic, TUNEL positive cells was in general not higher than 5 % for both Sorafenib and carrier treated mice. In the Sorafenib group, the average percentage of dead cells was 5.1 ± 2.5 % for the control hairpin, and 4.4 ± 0.7 % or 4.2 ± 2.9 % for shMapk14.1095 and shMapk14.2590, respectively. The percentages were similar for carrier treated groups, with 3.8 ± 3.8 % for the control hairpin, and 4.9 ± 2.9 % or 4.9 ± 1.6 % for shMapk14.1095 and shMapk14.2590, respectively (Fig. 17b).

These data suggest that smaller tumor burden under Mapk14 knockdown in Sorafenib treated mice is due to a decreased proliferation rate of murine HCCs.

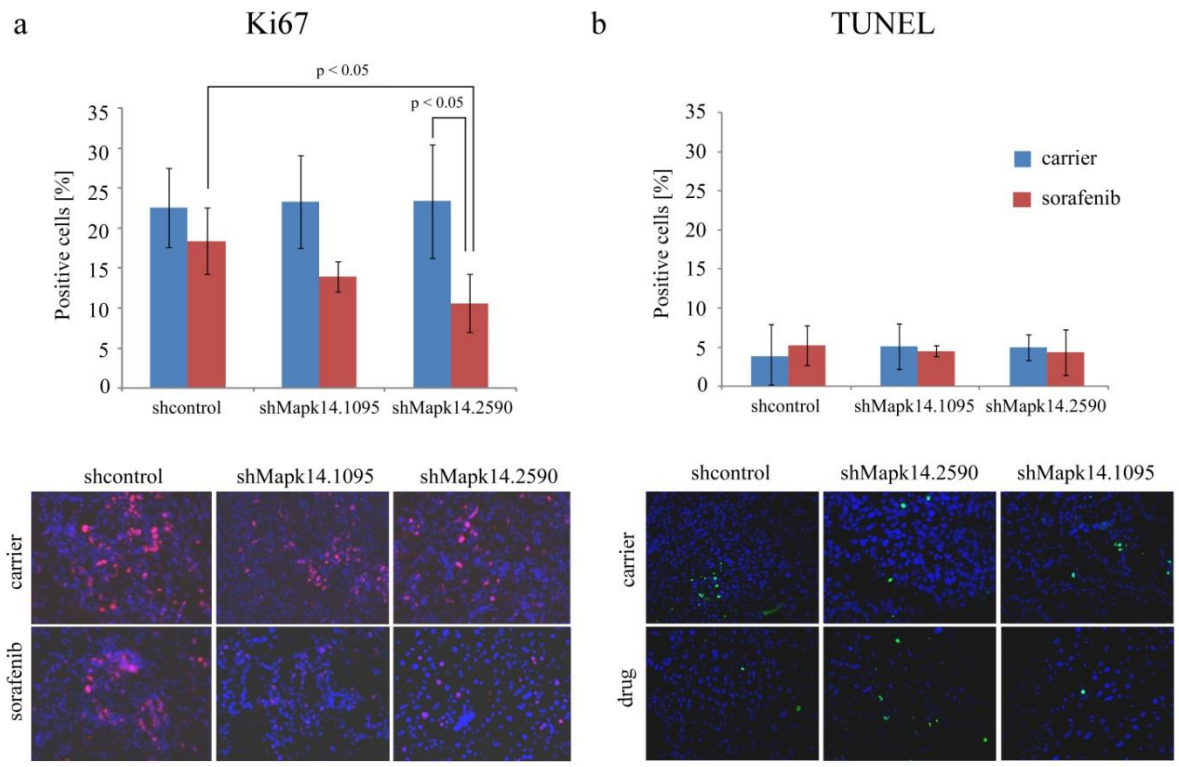

Figure 17 Reduced level of Mapk14 in murine Nras^{G12V} driven p19$^{Arf-/-}$ tumors results in a decreased proliferation rate but has no significant effect on apoptosis upon Sorafenib treatment

Quantification of cell proliferation rates by staining tumor samples against proliferation marker Ki67. Shown is the number of Ki67 positive cells in tumors treated with Sorafenib or carrier , 5 weeks after injection of Nras^{G12V} and shMapk14 or shcontrol into p19^{Arf} deficient mice with representative pictures of stained liver tumors (400 x) (a). Evaluation of cell death by TUNEL staining of tumor samples 5 weeks after injection of Nras^{G12V} and shMapk14 or shcontrol into p19^{Arf} deficient mice, and treatment with Sorafenib or carrier. Shown are also representative pictures of stained liver tumors (400 x) (b).

Apart from the effect of the combinatorial treatments on murine HCCs, it was shown that Mapk14 knockdown also reduced the size of Sorafenib treated colonies of Nras^{G12V}; p19$^{Arf-/-}$ cells in an *in vitro* assay. To determine whether this result is also based on a decreased proliferation rate under Mapk14 knockdown and not due to induced cell death, a cell doubling assay was carried out in combination with trypan blue staining under Sorafenib or dmso treatment.

120,000 of Nras^{G12V}; p19$^{Arf-/-}$ cells carrying shMapk14.1095 or control hairpin were seeded per plate and subjected to either Sorafenib or dmso treatments after 24 hours. The number of attached cells was subsequently measured everyday for a 4-day time period and compared to the initial point (day 0) to calculate a fold-change.

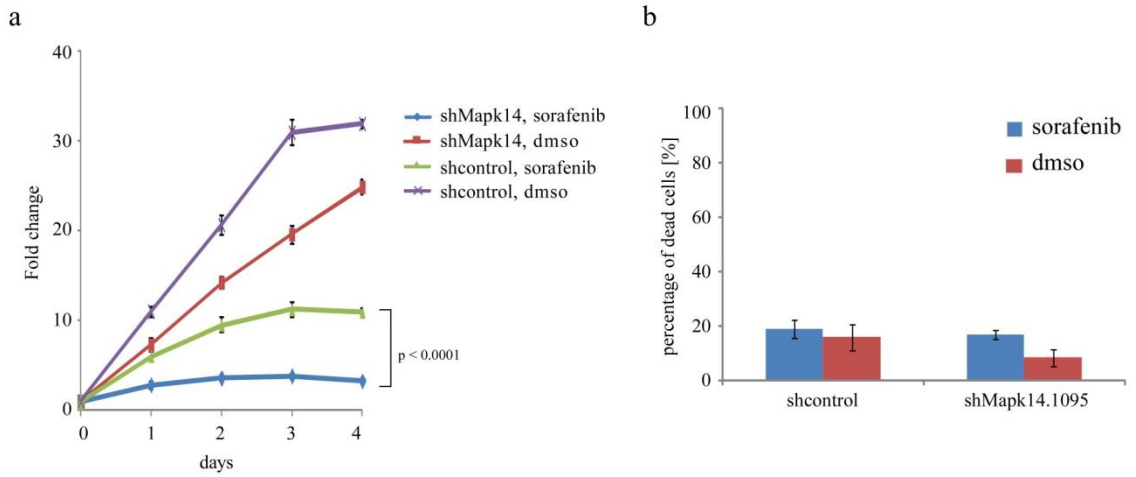

Figure 18 Knockdown of Mapk14 in combination with Sorafenib treatment decreases proliferation rate in $Nras^{G12V}$; $p19^{Arf-/-}$ cells

Cell proliferation rates of $p19^{Arf-/-}$ cells carrying shMapk14.1095 or control hairpin upon treatment with 8 µM Sorafenib. Plotted are averages of fold-changes in comparison to the initial point (day 0). 120,000 cells were plated, subjected to treatment a day later and the number of cells was determined by Guava FACS measurements (a). Quantification of cell death evaluated by trypan blue staining after 4 days of treatment with 8 µM Sorafenib. Depicted are percentages of trypan blue positive cells, counted by the Neubauer hemocytometer upon mixing cell suspension with trypan blue solution in a 1:1 ratio (b).

The proliferation profile identified dmso treated cells growing in general faster than Sorafenib treated cells. Shcontrol cells reached after 4 days a fold-change in cell number of 32 ± 0.5, slightly more than shMapk14 cells with a fold-change in cell number of 24.9 ± 0.8. The proliferation rate of cells expressing a control hairpin was diminished by Sorafenib treatment to a fold-change in cell number of 11.0 ± 0.5 after 4 days. However, Sorafenib treated shMapk.1095 cells showed a significantly lower amount of cells with only a fold-change in cell number of 3.3 ± 0.2 after 4 days ($p < 0.0001$ shMapk14 vs. shcontrol, both Sorafenib treated) (Fig. 18a). At this timepoint the number of dead (trypan blue positive) cells reached 16 ± 4.8 % for dmso treated shcontrol and 8.5 ± 3.2 % for dmso treated shMapk14 cells. Sorafenib treated cells showed a slightly higher amount of dead cells with 19.1 ± 3.4 % for shcontrol and 16.7 ± 1.8 % for shMapk14 cells (Fig. 18b).

Taken together, these *in vivo* and *in vitro* observations indicate that a decreased proliferation rate is responsible for the observed tumor inhibitory effect of combinatorial treatment.

4.5. Combination of Mapk14 knockdown together with Sorafenib treatment can be applied to treat advanced HCCs

Due to the fact that our transposon-based shRNA-mediated gene knockdown is constitutively active, the knockdown is directly induced upon transposon-based gene delivery. Although this setup allows for tracking genes involved in reducing tumor development, it does not allow to distinguish whether this inhibition influences advanced HCC tumors in an intervention setting.

However, recent systems allow for a regulatable induction of gene knockdown, based on tetracycline responsive elements (TRE) [137]. In this system, a tetracycline/doxycycline binding protein (rtTA3) is constitutively expressed, which regulates expression from a TRE promoter and as a result, of a gene or a shRNA of interest. Therefore, the expression of a gene/shRNA of interest occurs upon addition of tetracycline (Tet) or doxycycline (Dox) (Tet-on system).

To determine whether a tumor inhibiting effect by knockdown of Mapk14 in combination with Sorafenib can be seen in an intervention setting, this tet-on system was used where GFP and miR30-based shRNAs against Mapk14 were expressed by a TREtight promoter (a modified version of TRE promoter resulting in further reduced basal expression of gene/shRNA of interest [138]). Therefore, $Nras^{G12V}$; $p19^{Arf-/-}$ HCC cells were double transduced with an MSCV vector expressing rtTA3 and a second MSCV vector expressing TREtight–GFP carrying either shMapk14.1095 or shcontrol.

Each vector contains its own selection marker, which allows for generating homogenous cell populations containing both vectors as single copy integrants. These cells (1 million) were transplanted into the livers of wild type mice followed by doxycycline administration 7 days after injection in combination with Sorafenib administration (Fig. 19a).

Mice with activated Mapk14 or control hairpin (+ Dox) as well as mice with non-activated Mapk14 hairpin (- Dox) were followed up for intrahepatic tumor development under Sorafenib therapy. Mice harboring an activated control or non-activated Mapk14 hairpin died with a comparable median survival of 20 days (shcontrol) or 22 days (shMapk14). Interestingly, mice carrying an activated shMapk14 lived significantly longer with a median survival of 49 days ($p = 0.033$ shcontrol vs. shMapk14.1095, +Dox) (Fig. 19b). Phenotypic analyses revealed intrahepatic tumor burden to be the cause of lethality (Fig. 19c).

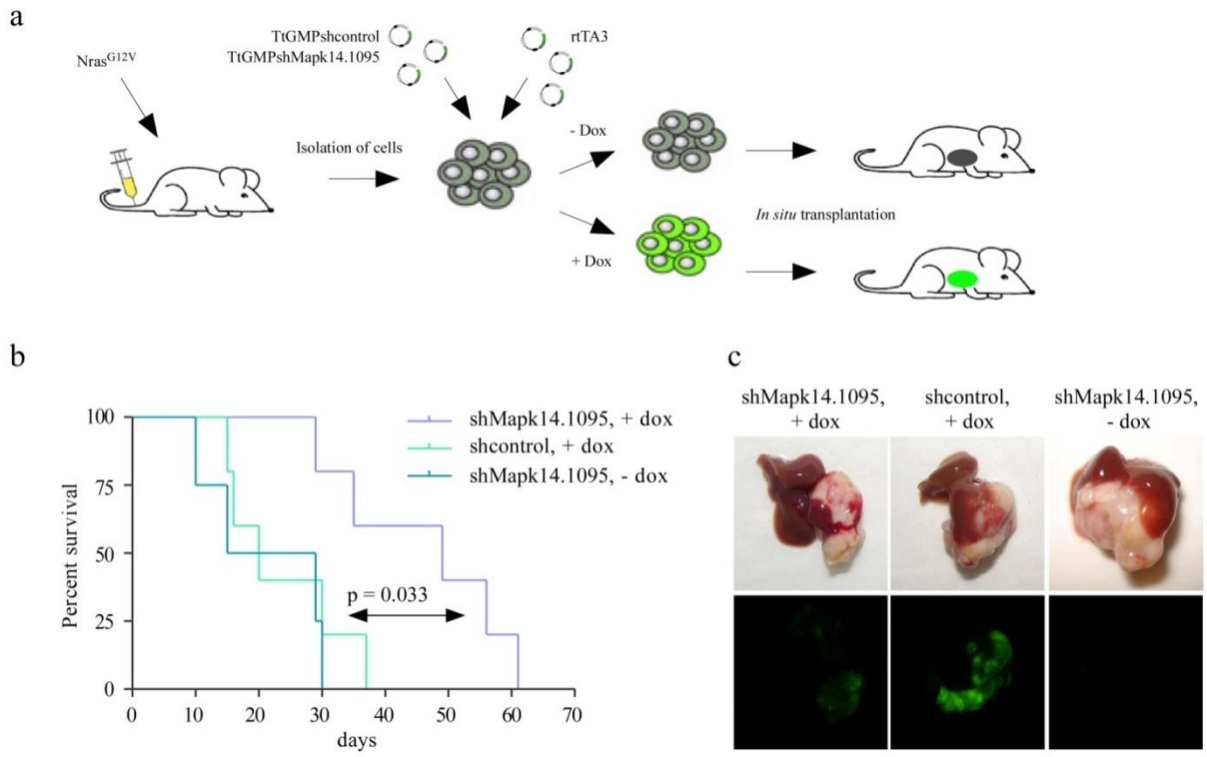

Figure 19 Knockdown of Mapk14 sensitizes towards Sorafenib treatment also in a therapeutic intervention setting

Schematic representation of inducible gene/shRNA expression in the tet-on system upon *in situ* transplantation (a). Survival curves for wild type mice after *in situ* transplantation of double transduced $Nras^{G12V}$; $p19^{Arf-/-}$ cells with an MSCV vector expressing rtTA3 and a second MSCV vector expressing TRETight-GFP carrying either shMapk14.1095 or shcontrol. Injection of 1 million cells was followed by doxycycline administration for the corresponding groups, together with Sorafenib treatment 7 days later (b). Representative pictures of developed tumors after transplantation of $Nras^{G12V}$; $p19^{Arf-/-}$ cells (1 million) also followed by doxycycline administration for the corresponding groups, together with Sorafenib treatment 7 days later (c).

In general, GFP imaging of livers showed that tumors with activated hairpins are GFP positive, whereas tumors with non-activated hairpins did not show GFP signal. However, in HCCs with activated Mapk14 hairpin the intensity of GFP signal was frequently weaker than in tumors with activated shcontrol (Fig. 19c). These findings imply a selection against activated Mapk14 hairpin under Sorafenib treatment.

Taken together, these data show that knockdown of Mapk14 improves the response of murine $Nras^{G12V}$; $p19^{Arf-/-}$ HCCs towards Sorafenib even when Mapk14 hairpin is activated to a later time point in already advanced tumor cells. Due to the fact that there was a selection against cells with active Mapk14 hairpins under Sorafenib treatment, the resultant data are likely to underestimate the response to advanced HCCs.

4.6. A pharmacological inhibition of Mapk14 phenocopies the shRNA-mediated knockdown of Mapk14

Based on the finding that knockdown of Mapk14 improves Sorafenib treatment of HCC also in an intervention setting, the question arises whether a pharmacological inhibition of Mapk14 (p38α) could recapitulate the effect of shRNA-mediated knockdown and therefore improve the efficacy of Sorafenib therapy.

The kinase activity of Mapk14 can be inhibited by different pharmacological inhibitors. Some of them were developed as agents against cancer and inflammation diseases. Several Mapk14 inhibitors are in clinical trials, however, none of them are at the moment approved for patient treatment [20].

For pharmacological inhibition of Mapk14, two different inhibitors were applied, BIRB 796 and SB 202190 (Fig. 20a,b). Since BIRB 796 was already investigated in clinical trials, it shows a putative potential for Mapk14 inhibition in *in vivo* systems [139;140]. However, although SB 202190 was often exploited in *in vitro* assays, it was never applied for clinical studies [140].

To determine the inhibitory efficiency of these compounds in mice, a short-term *in vivo* treatment study was performed. $P19^{Arf}$ deficient mice were injected with $Nras^{G12V}$ transposons and daily treated for 3 days with the inhibitors. The inhibition was tested by analyzing the efficiency of the Mapk14 kinase to phosphorylate its downstream target Hsp27. Western blot analysis identified a lower level of phosphorylated Hsp27 upon administration of BIRB 796 and SB 202190, confirming a target specific inhibition by these compounds (Fig. 20c).

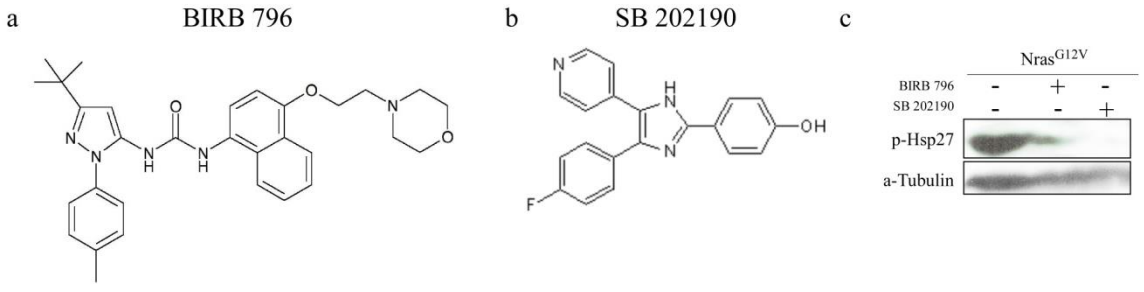

Figure 20 The p38 inhibitors BIRB 796 and SB 202190 efficiently inhibit Mapk14 activity in mouse livers

Schematic structure of BIRB 796 (a) and SB 202190 (b). Western blot analysis of phosphorylation level of Mapk14 downstream target, Hsp27 upon 3-day treatment with BIRB 796 and SB 202190 in murine livers of $p19^{Arf-/-}$ mice directly upon injection of $Nras^{G12V}$ (c).

The described *in vitro* system of $Nras^{G12V}$; $p19^{Arf-/-}$ cells was used to determine the effect of pharmacological inhibition of Mapk14 for Sorafenib treatment. Therefore, $Nras^{G12V}$; $p19^{Arf-/-}$ cells were treated with Sorafenib, BIRB 796/SB 202190 alone, or the combination thereof. Dmso treated cells were run in parallel for each condition. The effect of these treatments to the cells was determined by cell doubling assays and crystal violet staining to identify cell proliferation and by trypan blue staining to detect cell death.

As described before, the cell doubling assay was carried out to evaluate the proliferation rate of the cells by daily measurements of the cell number over a 4-day period time. This assay, using SB 202190 as a Mapk14 inhibitor revealed dmso treated cells with comparable growth activities (fold-change in cell number was between 30.6 and 34.6). The administration of Sorafenib reduced the cell growth to fold-change in cell number of 8.6 ± 3.6. Interestingly, in contrast to shRNA-mediated knockdown, the chemical inhibition of Mapk14 by SB 202190 caused also a reduced proliferation rate (fold-change in cell number 9.2 ± 1.1). However, a combination treatment with Sorafenib and SB 202190 together induced a much stronger decline in proliferation rate than either treatment alone (fold-change in cell number 2.7 ± 0.3, $p < 0.0001$ combinatorial treatment vs. Sorafenib) (Fig. 21a). These results were confirmed by cell doubling assay in which BIRB 796 was used as a Mapk14 inhibitor. Within a 4-day time period, dmso treated cells grew to fold-changes in cell number between 14.9 and 18.8. In contrast, under Sorafenib treatment a fold-change in cell number of 3.5 ± 0.2 was determined. Under BIRB 796 treatment, however, the cell proliferation rate was higher and reached a fold-change in cell number of 9.6 ± 0.6. Also, a combinatorial treatment further attenuated the proliferation rate compared to single treatements (fold-change in cell number 2.0 ± 0.2, $p < 0.0016$ combinatorial treatment vs. Sorafenib) (Fig. 21b). These results were also recapitulated by crystal violet staining after 4 days of treatment. It showed a reduced number of cells by treatments with Sorafenib or Mapk14 inhibitors, however, this phenotype was additionally enhanced by simultaneous incubation of Sorafenib with Mapk14 inhibitors (Fig. 21c,d).

The trypan blue staining using SB 202190 as a Mapk14 inhibitor did not reveal by treatment with dmso high percentages of dead cells (8.9 - 16.7 %). Under Sorafenib treatment the number of dead cells increased slightly to 18.0 ± 1.0 %. Interestingly, upon treatment with SB 202190 the number of dead cells increased to 45.3 ± 2.7 % and therefore was higher as under Sorafenib treatment alone.

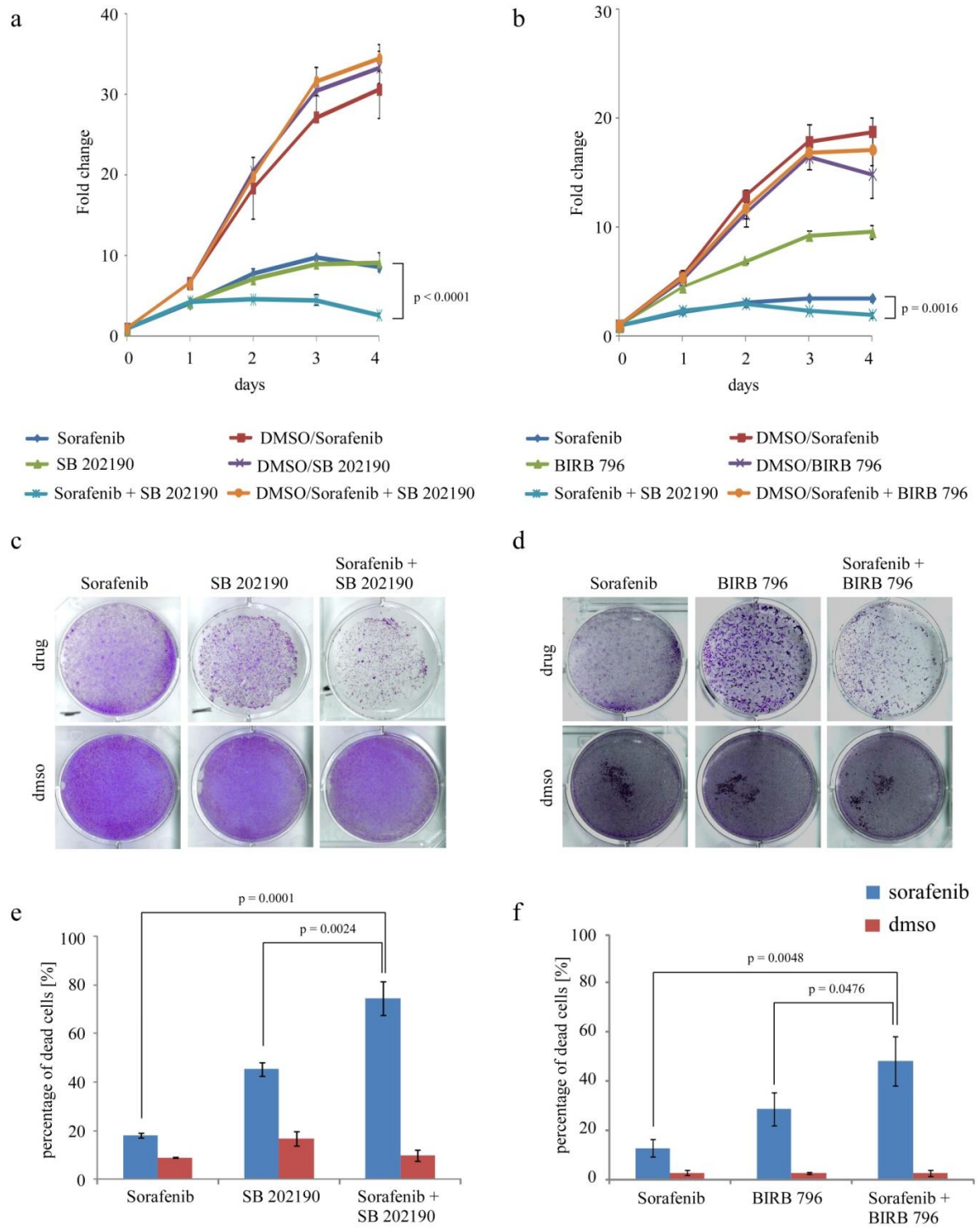

Figure 21 Combinatorial treatment with Sorafenib and chemical inhibitors of Mapk14 decreases cell proliferation and increases cell death of $Nras^{G12V}$; $p19^{Arf-/-}$ cells

Proliferation rates of $Nras^{G12V}$; $p19^{Arf-/-}$ cells upon treatment with 8 µM Sorafenib and 50 µM of the Mapk14 inhibiors SB 202190 or BIRB 796 as well as the combination thereof. Plotted are averages of fold-changes in comparison to the initial point (day 0). The number of cells was determined by Guava FACS measurements (a,b). Visualization of cells by crystal violet staining after 4 days of treatment with 8 µM of Sorafenib and 50 µM of SB 202190 or BIRB 796 or combination thereof. 120,000 cells were plated one day before treatment onset (c,d). Cell death assay with trypan blue staining after 4 days of treatment with above mentioned conditions. Shown are percentages of trypan blue positive cells, counted by the Neubauer hemocytometer. The trypan blue solution was mixed with the cell suspension in a 1:1 ratio (e,f).

Combination treatment further elevated the number of dead cells up to 74.5 ± 6.9 % ($p < 0.0001$ combinatorial treatment vs. Sorafenib alone, $p = 0.0024$ combinatorial treatment vs. SB 202190 alone) (Fig. 21e). In case of treatment with BIRB 796 the results were comparable.

Whereas the percentages of dead, dmso treated cells were comparable (2.6 - 2.9 %), Sorafenib treated cells showed a percentage of 12.9 ± 3.7 % dead cells and BIRB 796 treated cells a percentage of 28.3 ± 6.7 % dead cells. Also in this case the combinatorial treatments increased the percentage of dead cells to 48.1 ± 10.1 % ($p = 0.0048$ combinatorial treatment vs. Sorafenib alone, $p = 0.0476$ combinatorial treatment vs. BIRB 796 alone) (Fig. 21f).

These *in vitro* data showed that the pharmacological inhibition of Mapk14 by SB 202190 or BIRB 796 improves Sorafenib treatment similarly to the shRNA-mediated knockdown. However, the chemical inhibition alone shows already an effect to $Nras^{G12V}$; $p19^{Arf-/-}$ cells by reduced proliferation. Additionally, the pharmacological inhibition of Mapk14 increased cell death, which was enhanced by a combinatorial treatment of Mapk14 inhibitors with Sorafenib. These data indicate that the sensitization towards Sorafenib treatment by Mapk14 inhibition, which is in gerenal linked to a decreased proliferation rate after double treatment is to a minor role also induced by induction of cell death, but only when Mapk14 inhibition is applied by pharmacological inhibitors and not by shRNA-mediated knockdown.

To identify the effect of chemical inhibition of Mapk14 in concert with Sorafenib to tumor development, an *in vivo* double treatment study was conducted using BIRB 796, a pharmacological inhibitor which was already applied in *in vivo* studies. Therefore, $p19^{Arf}$ deficient mice were injected with $Nras^{G12V}$ and subjected to treatment 7 days after injection.

The mice were treated either with Sorafenib or BIRB 796 alone (50 mg/kg) or with combination thereof.

To exclude unspecific effects, the carrier for Sorafenib was added to BIRB 796 monotherapy and also Sorafenib treatment alone was supplemented with the carrier for BIRB 796.

Additionally, carriers of both compounds were combined for a control group. One cohort of mice was harvested 4 weeks after injection to analyze the intrahepatic tumor burden (Fig. 22a) ($n = 4$), and a second cohort of mice was dissected due to critical tumor development to assess the survival of different groups in a Kaplan-Meier curve (Fig. 22b).

Tumor development for carrier treated mice was comparable to the described study of *in vivo* response to Sorafenib treatment and showed a median survival of 28 days. Treatment with Sorafenib or BIRB 796 alone showed a moderate survival advantage to mice with a median survival of 34 days for both Sorafenib and for BIRB 796 treated cohorts of mice.

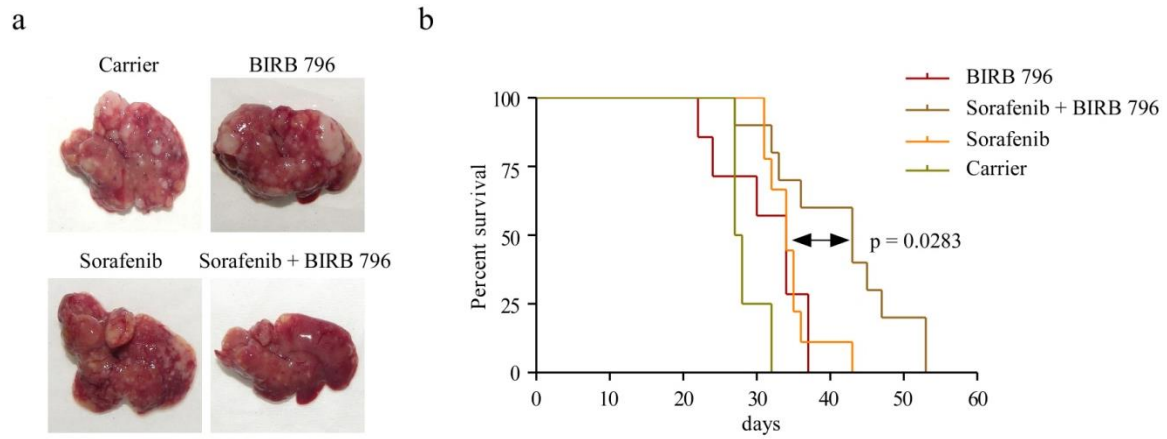

Figure 22 Inhibition of Mapk14 by BIRB 796 causes a survival benefit for mice under Sorafenib treatment

Intrahepatic tumor burden of $p19^{Arf}$ deficient mice at a 4-week timepoint after injection of $Nras^{G12V}$ and treatment onset 7 days upon injection. The mice were treated either with Sorafenib (100 mg/kg) and carrier for BIRB 796, with BIRB 796 (50 mg/kg) and carrier for Sorafenib, with Sorafenib and BIRB 796 combination or treated with both carriers (n = 4) (a). Survival plot of $p19^{Arf}$ deficient mice after single or combinatorial treatments of Sorafenib and BIRB 796 or with the carriers upon injection of $Nras^{G12V}$ (b).

Interestingly, the combinatorial treatment significantly slowed down tumor development and extended the survival period with a median survival of 43 days (p = 0.0283 between Sorafenib and combinatorial treatment).

These data imply that disadvantageous effect of shRNA-mediated knockdown of Mapk14 in concert with Sorafenib treatment to tumor development is reflected by pharmacological inhibition of Mapk14 together with Sorafenib, suggesting a potential for this combinatorial targeted therapy to be used in HCC patients.

Taken together, these data show that therapy resistance of HCC can be overcome by a combination treatment with pharmacological p38 inhibitors and Sorafenib.

4.7. The outcome of combination therapy in different genetic backgrounds

The *in vivo* RNAi screen which identified Mapk14 as a potential target in combination with Sorafenib treatment was conducted in a genetically defined background with expression of oncogenic $Nras^{G12V}$ in $p19^{Arf-/-}$ mice. The expression of $Nras^{G12V}$ activates the MAPK pathway, a frequently upregulated signaling cascade in human HCC. Nevertheless, profiling of human HCCs identified dysregulation in many pathways as potential driver for HCC development [27;34;53;107;141]. The genetic complexity of human HCCs impedes the success of targeted therapies because treatment strategies which are dependent on a genetic background might be only applicable for a small subgroup of human HCC patients.

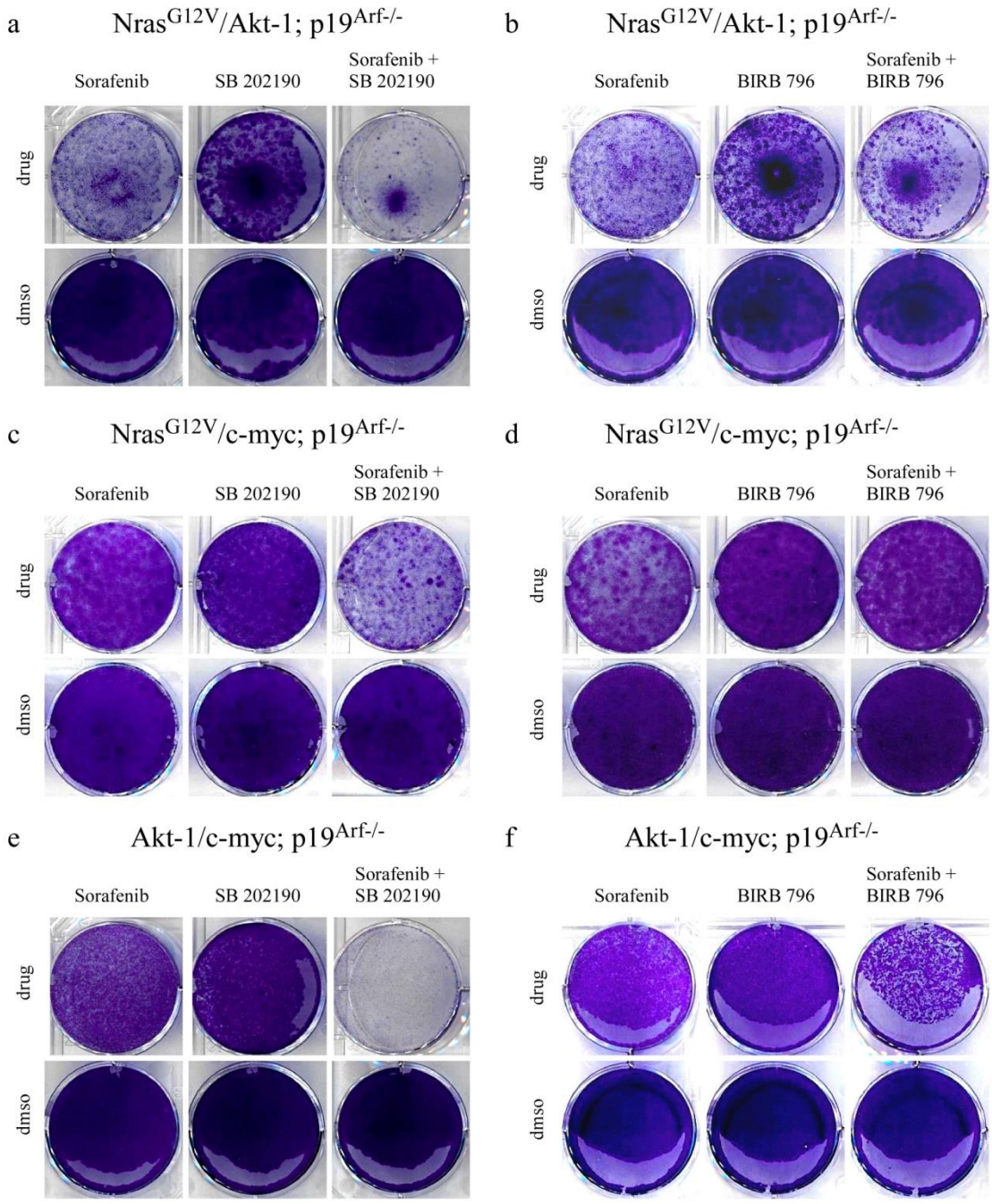

Figure 23 HCCs cell lines with different oncogenic combinations show also an effect to combinatorial therapy

Visualization of cells by crystal violet staining after 4 days of treatment with 8 µM of Sorafenib and 50 µM of SB 202190 or BIRB 796 or combination thereof. Shown are Nras^{G12V}/Akt-1; p19$^{Arf-/-}$ cells treated with SB 202190 (a), Nras^{G12V}/Akt-1; p19$^{Arf-/-}$ cells treated with BIRB 796 (b), Nras^{G12V}/c-myc; p19$^{Arf-/-}$ cells treated with SB 202190 (c), Nras^{G12V}/c-myc; p19$^{Arf-/-}$ cells treated with BIRB 796 (d) Akt-1/c-my; p19$^{Arf-/-}$ cells treated with SB 202190 (e) and Akt-1/c-myc; p19$^{Arf-/-}$ cells treated with BIRB 796 (f).

To investigate whether the outcome of combination therapy is limited to the genetic profile of the RNAi screen or works also in other oncogenic backgrounds, we applied murine HCC cells, which were isolated from tumors driven by different oncogenic combinations in p19^{Arf}

deficient backgrounds using standard collagenase/dispase digestion. These tumors were also induced by transposon based gene transfer of the corresponding oncogenes upon hydrodynamic tail vein injection into $p19^{Arf}$ deficient mice (Dauch, Hohmeyer, Zender, unpublished data). The first tested cell line was driven by oncogenic $Nras^{G12V}$ in combination with activated Akt1 (a constitutively active form of Akt, by attachment of a N-terminally myristoylation signal) [142], another cell line combined the expression of $Nras^{G12V}$ with the oncogene c-myc and a third used cell line was driven by a combination of c-myc and Akt1 and therefore without expression of oncogenic $Nras^{G12V}$.

These cells were now used to test the efficiency of combinatorial effect of Sorafenib and the Mapk14 inhibitors BIRB 796 and SB 202190 in *in vitro* assays. 120,000 cells were plated and after one day the cells were treated either with Sorafenib or Mapk14 inhibitor alone, the combination thereof, or corresponding amounts of carrier (dmso). The same concentrations of Sorafenib and Mapk14 inhibtors were used as in earlier experiments for $Nras^{G12V}$; $p19^{Arf-/-}$ cells. On 4^{th} day of treatment, the attached cells were washed and stained with crystal violet to visualize the abundance of cells under different conditions.

As observed for $Nras^{G12V}$; $p19^{Arf-/-}$ cells, Sorafenib monotherapy reduced the number of $Nras^{G12V}$/Akt-1; $p19^{Arf-/-}$ cells to a low amount. The admistritation of SB202190 and BIRB 796 alone showed only marginal effects. Importantly, due to combinatorial treatment of the Mapk14 inhibitors together with Sorafenib a strong reduction was seen regardless of which Mapk14 inhibitor was used. However, by using SB 202190 the reduction in cell growth was much stronger than using BIRB 796 (Fig. 23a,b).

By testing $Nras^{G12V}$/c-myc; $p19^{Arf-/-}$ cells, it was seen that Sorafenib monotherapy showed a much lower effect than in $Nras^{G12V}$; $p19^{Arf-/-}$ or $Nras^{G12V}$/Akt-1; $p19^{Arf-/-}$ cells. Also administration of the Mapk14 inhibitors alone showed lower effect than in previously tested cells. The combination of Sorafenib and SB 202190 reduced the amount of cells significantly more than individual monotherapies. However, by using BIRB 796 together with Sorafenib no additional effect was seen (Fig. 23c,d).

The administration of Sorafenib monotherapy to Akt-1/c-myc; $p19^{Arf-/-}$ cells showed also lower responses than $Nras^{G12V}$ or $Nras^{G12V}$/Akt-1 driven cells and therefore similarities to $Nras^{G12V}$/c-myc; $p19^{Arf-/-}$ cells. Also the administration of the Mapk14 inhibitors alone did not show strong effects, which was also comparable to $Nras^{G12V}$/c-myc; $p19^{Arf-/-}$ cells. However, the combination of Sorafenib and the Mapk14 inhibitors in these cells showed much stronger effects than in $Nras^{G12V}$/c-myc; $p19^{Arf-/-}$ cells. Especially a strong effect was seen in the presence of SB 202190.

Taken together, these data indicate that HCC cell lines triggered by the oncogenic combinations $Nras^{G12V}$/Akt-1, $Nras^{G12V}$/c-myc and Akt-1/c-myc in $p19^{Arf}$ deficient backgrounds show also responses towards the combinatorial treatment. However, $Nras^{G12V}$/c-myc; $p19^{Arf-/-}$ cells showed a much lower effect than the other tested cell lines and no effect was seen when using BIRB 796 as a Mapk14 inhibitor. In general, SB 202190 showed stronger inhibitory effects than BIRB 796 in combinatorial therapy.

4.8. A combination treatment of Sorafenib with Mapk14 inhibitors decreases proliferation of different human hepatoma cell lines

It could be shown, that the effect of the combinatorial therapy is in general not limited to the genetic background of the RNAi screen, in which Mapk14 was identified as a potential target for combinatorial therapy with Sorafenib, but also showed responses in murine HCC cell lines which were driven by different oncogenic combinations. However, these results indicate differences in the outcome indicating that the genetic background might influence the efficacy of the combinatorial therapy. To see the response of cells to the combinatorial treatment, we applied a panel of human hepatoma cell lines as PLC/PRF/5 (Alexander), Huh7 and Hep3B cells.

These cells were also treated either with Sorafenib monotherapy, the Mapk14 inhibitors SB 202190 and BIRB 796 alone and the combination thereof. Also controls with corresponding dmso concentrations were applied. The different treatment effects on cell proliferation rates were determined by cell doubling assays which were performed, as described before, by daily quantification of the number of attached cells. One day after plating the cells, the number of cells was quantified (initial point) and consecutive cell quantifications over a 4-day period were compared to initial point (fold-changes) to determine cell proliferation rates. Additionally, cell staining using crystal violet were performed upon 4 days of treatment which was also started one day after plating the cells, to visualize the effect of the different conditions.

Furthermore, trypan blue stainings were performed to quantify the number of dead cells (trypan blue positive). As described before, all collected cell fractions were mixed with a trypan blue solution in a 1:1 ratio and cells were counted with Neubauer hemocytometer. To determine the amount of dead cells, the percentage of trypan blue positive cells was calculated with respect to the total number of cells.

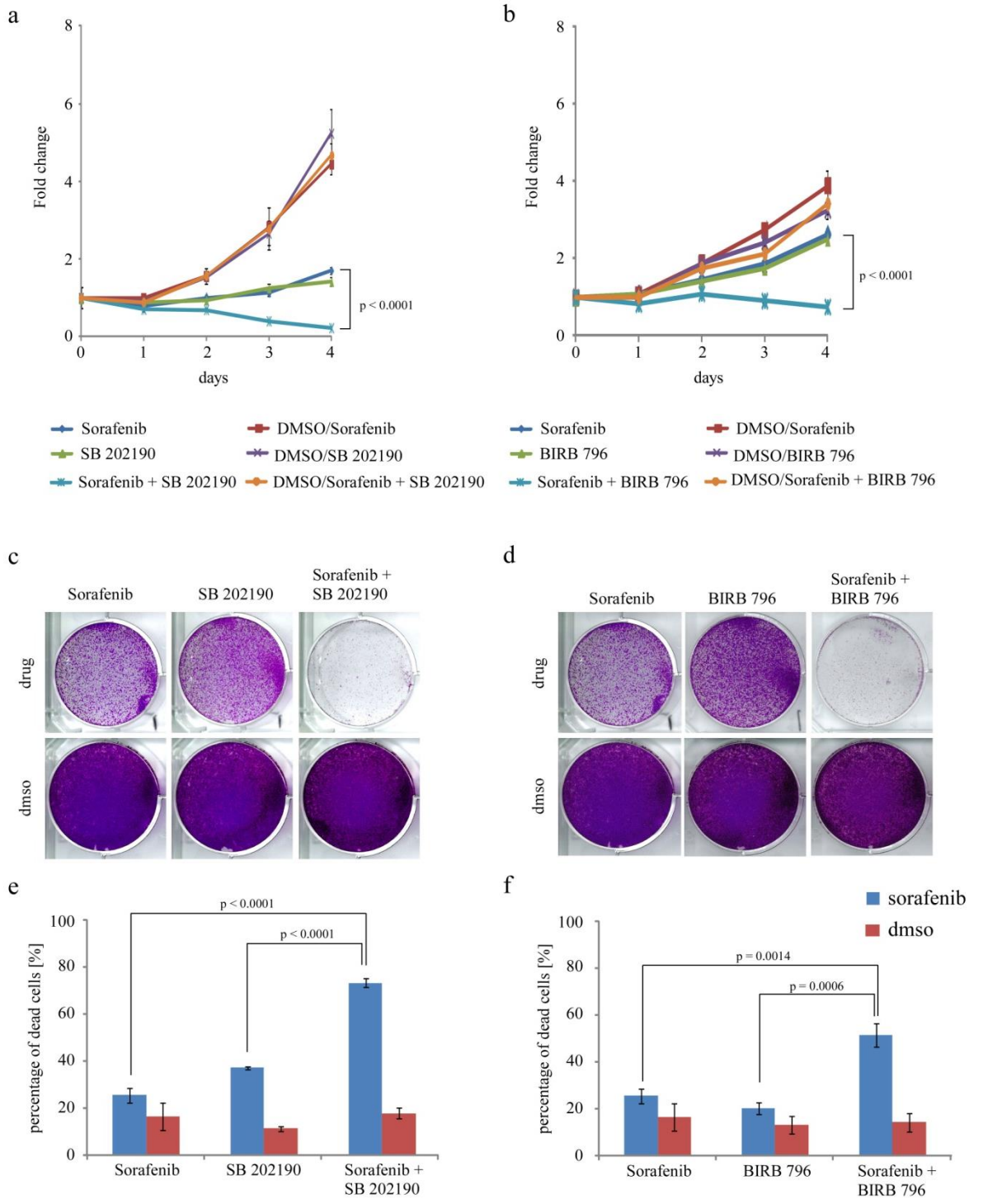

Figure 24 Treatment of PLC/PRF/5 cells with Sorafenib and Mapk14 inhibitors greatly decreases cell proliferation

Proliferation rates of PLC/PRF/5 cells upon treatment with 4 µM Sorafenib and 20 µM of the Mapk14 inhibiors SB 202190 or BIRB 796 as well as the combination thereof. Plotted are averages of fold-changes in comparison to the initial point (day 0). The number of cells was determined by Guava FACS measurements (a,b). Visualization of cells by crystal violet staining after 4 days of treatment with 4 µM of Sorafenib and 20 µM of SB 202190 or BIRB 796 or combination thereof. 80,000 cells were plated one day before treatment onset (c,d). Cell death assay with trypan blue staining after 5 days of treatment with above mentioned conditions. Shown are percentages of trypan blue positive cells, counted by the Neubauer hemocytometer. The trypan blue solution was mixed with the cell suspension in a 1:1 ratio (e,f).

To determine the effect of combinatorial therapy on the proliferation of PLC/PRF/5 cells, first a cell doubling assay was performed using SB 202190 as a Mapk14 inhibitor. The cells were treated either with Sorafenib or SB 202190 alone, with the combination of both medicaments or the corresponding dmso (carrier) concentrations. All three populations of dmso treated cells showed a comparable proliferation rate with a fold-change of cell number between 4.4 and 5.2. The Sorafenib monotherapy reduced the proliferation rate to a fold-change of 1.7 ± 0.1. Also with SB 202190 administration a lower proliferation of cells (fold-change of cell number: 1.4 ± 0.1) was determined.

Interestingly, the combination treatment reduced the number of cells compared to the initial point and a fold-change of 0.2 ± 0.01 was determined. This proliferation rate is significant different to the monotherapies ($p < 0.0001$ Sorafenib vs. Sorafenib/SB 202190) (Fig. 24a).

A similar pattern in cell proliferation rates was recapitulated by cell doubling assay with BIRB 796, as a Mapk14 inhibitor. Also here monotherapies of Sorafenib and BIRB 796 were compared to a combination therapy, where again dmso treated cells served as controls. Similarly, in this assay the different groups of dmso treated cells showed comparable proliferation rates with fold-changes in cell numbers after 4-days between 3.2 and 3.9. The Sorafenib monotherapy reduced the proliferation rate to a fold-change in cell number of 2.6 ± 0.1 whereas treatment with BIRB 796 resulted in a fold-change in cell number of 2.5 ± 0.1. A combinatorial therapy abrogate cell proliferation and a fold-change in the cell number of 0.7 ± 0.02 was measured after 4 days which is significantly different to monotherapies ($p < 0.0001$) (Fig. 24b).

The already described visualization of cells with crystal violet after 4 days of treatment reproduced the results from the cell doubling assays. The Sorafenib monotherapy as well as incubation with the Mapk14 inhibitors reduced the number of cells compared to the DMSO treated cells. However, the combination of Sorafenib and Mapk14 inhibitor induced a much stronger effect in cell reduction than the single treatments (Fig. 24c,d).

To identify the percentage of dead cells, trypan blue stainings were conducted upon combinatorial treatment compared to single treatments and corresponding dmso concentrations (see above). In this assay, using SB 202190 as a Mapk14 inhibitor, the number of DMSO treated cells was in general low, between 11.4 and 18.0 % of dead cells. The application of Sorafenib increased the number of dead cells to 25.5 ± 3 % and the application of SB 202190 to 37.2 ± 0.5 %. Nevertheless, a combinatorial therapy induced a much stronger amount of dead cells (73.2 ± 2.0 %) which was significantly different in comparison to both

monotherapies ($p < 0.0001$) (Fig. 19e). A quantification of trypan blue positive cells using BIRB 796 as a Mapk14 inhibitor, showed similar results. The number of DMSO treated cells was again low between 13.2 and 16.5 % of dead cells. The Mapk14 inhibition by BIRB 796 resulted in 20.2 ± 2.5 % of dead cells and therefore lower than upon SB 202190 treatment. However, a combinatorial treatment with Sorafenib and BIRB 796 increased cell death to 51.5 ± 5.0 %, again significantly higher than monotherapies ($p = 0.0006$ Sorafenib vs. Sorafenib/BIRB 796) (Fig. 4f).

These data illustrate that pharmacological inhibition of Mapk14 can efficiently sensitize also human HCC cells towards treatment with Sorafenib. To investigate whether this effect could be shown in a broader spectrum of human hepatocarcinoma cells, the same assays were performed with the same conditions for Huh7 cells.

Also for these cells the cell doubling assay was performed with SB 202190 as a Mapk14 inhibitor. Due to the fact that these cells grow faster than PLC/PRF/5 cells, dmso treated cells showed higher proliferation rates but they were also very comparable between the different dmso treated groups (fold-changes of cell number after 4 days: ~ 22). Also in Huh7 cells the treatment with Sorafenib dimished cell proliferation and a fold-change in the cell number of 4.5 ± 0.3 was determined. The treatment with SB 202190 resulted also in a reduced proliferation rate displayed by a fold-change in cell number of 8.2 ± 0.8. However, the combinatorial treatment increased further the proliferation rate and amounted to a fold-change in cell number of 1.9 ± 0.1, which is significantly different to Sorafenib monotherapy ($p = 0.0002$) (Fig. 25a).

These results were also confirmed by taking BIRB 796, as a second Mapk14 inhibitor. Here dmso treated cells showed after 4 days fold-changes in the number of cells between 16.0 and 18.0. Sorafenib treatment declined the proliferation rate of cells considerably to a fold-change in the cell number of 6.2 ± 0.4. By administration of BIRB 796 a fold-change in the cell number of 4.9 ± 0.5 was calculated. A double incubation of cells with Sorafenib and BIRB 796 aggravated a reduction in the proliferation rate, determined by a fold-change in cell number of 1.5 ± 0.1 ($p = 0.0003$ Sorafenib vs. Sorafenib/BIRB 796) (Fig. 25b).

Visualization of Huh7 cells by crystal violet recapitulates the results of cell doubling assays. Whereas dmso treated cells showed no impact on proliferation, monotherapies with Sorafenib or the Mapk14 inhibitors SB 202190 or BIRB 796 reduced the number of cells to a small extent. Nevertheless, a combination treatment with Sorafenib and Mapk14 inhibitors reduced the number of cells much stronger than the corresponding monotherapies (Fig. 25c,d).

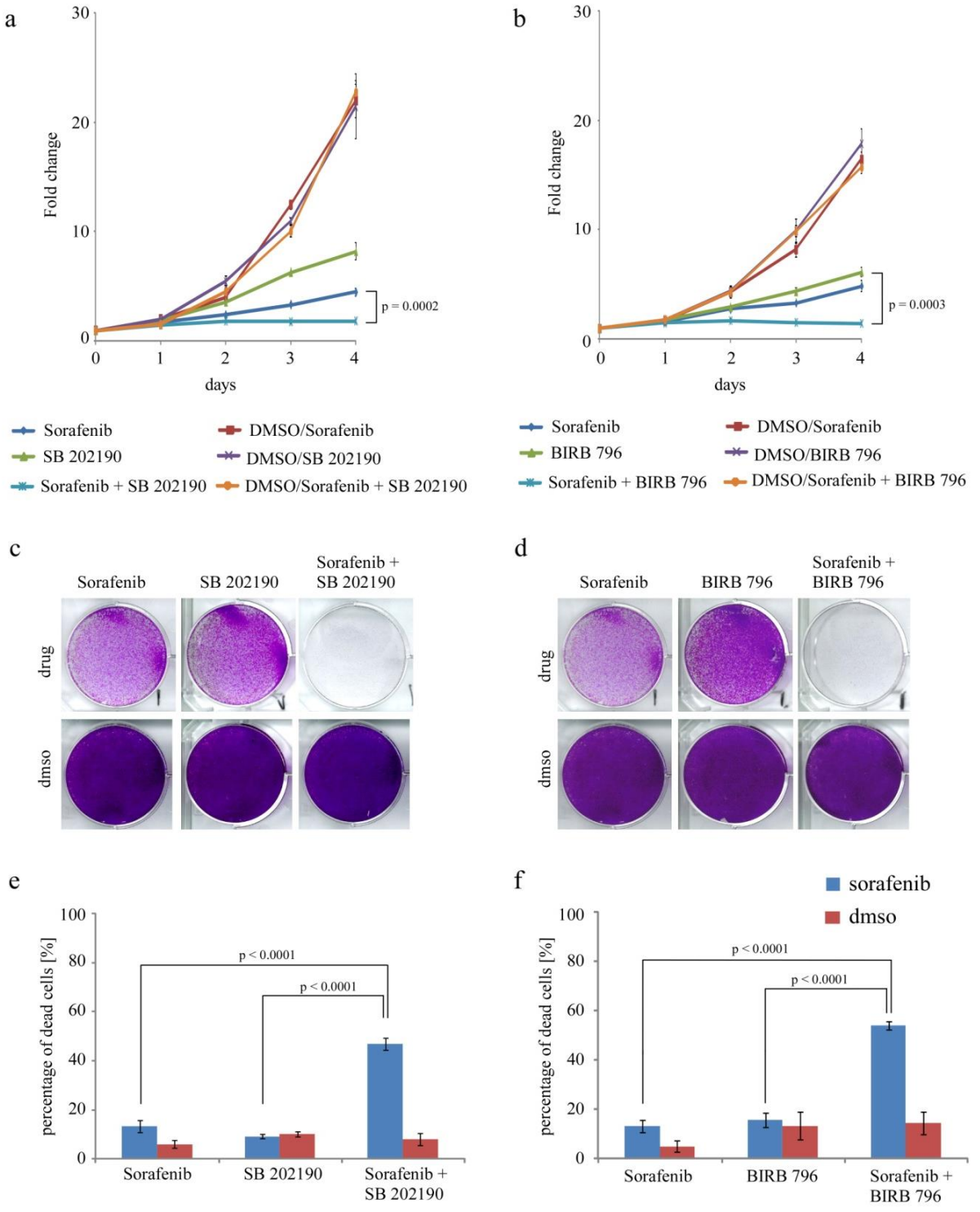

Figure 25 Mapk14 inhibition in Huh7 cells sensitizes cells towards Sorafenib treatment

Cell proliferation rates of Huh7 cells upon treatment with 4 µM Sorafenib and 20 µM of the Mapk14 inhibiors SB 202190 or BIRB 796 as well as the combination thereof. Plotted are averages of fold-changes in comparison to the initial point (day 0). The number of cells was determined by Guava FACS measurements (a,b). 80,000 cells were plated 1 day before treatment onset and above is shown the visualization of cells stained with crystal violet after 4 days of treatment with 4 µM of Sorafenib and 20 µM of SB 202190 or BIRB 796 or combination thereof (c,d). Presented are percentages of trypan blue positive cells, indicative of cell death, counted with Neubauer hemocytometer after 5 days of treatment with above mentioned conditions. The trypan blue solution was mixed with the cell suspension in a 1:1 ratio (e,f).

Quantification of cell death by counting trypan blue positive Huh7 cells indicated a similar response to the different treatment options as it was shown for PLC/PRF/5 cells. Using SB 202190 as a Mapk14 inhibitor the number of dead cells under dmso treatment was in general low between 6.0 and 10.2 %.

Application of Sorafenib increased the number of dead cells to 13.2 ± 2.4 %. Treatment with SB 202190 resulted in 9.2 ± 0.9 % of dead cells and therefore a little bit lower amount than under Sorafenib treatment. However, a combination of Sorafenib and SB 202190 increased the number of dead cells to 47 ± 2.4 %, a significant difference to monotherapies ($p < 0.0001$) (Fig. 25e). These striking differences were also yielded by using BIRB 796 as a Mapk14 inhibitor. Whereas dmso treated cells showed again low amounts of dead cells with 5.0 – 14.5 %, inhibition of Mapk14 increased the number of dead cells to 15.6 ± 2.8 % and therefore comparable to Sorafenib. A combinatorial therapy using Sorafenib and BIRB 796 resulted in 54.0 ± 1.6 % of dead cell, a value which was again significantly different to monotherapies ($p < 0.0001$) (Fig. 25f).

Finally, as a last example of a human HCC cell line Hep3B cells were used for aforementioned experiments. Also for those cells, cell doubling assays were carried out in order to determine the proliferation rate under different conditions.

Using SB 202190 as a Mapk14 inhibitor, the highest proliferation rates were reached by dmso treated cells (fold-changes in cell number after 4 days: ~ 30.0). Treatment with Sorafenib reduced the proliferation rate of the cells to a fold-change in the cell number of 16.0 ± 0.07. The administration of SB 202190 to Hep3B cells changed the proliferation rate of cells only in a marginal way compared to dmso treated cells (fold-change in cell number after 4 days: 24.0 ± 2.0). However, similarly as PLC/PRF/5 and Huh7 cells, Hep3B cells showed also an impact from the combinatorial treatment. Under Sorafenib/SB 202190 treatment, the proliferation rate of cells was lower and a fold-change in the number of cell of 6.5 ± 0.5 was determined ($p < 0.0001$ Sorafenib vs. Sorafenib/SB 202190) (Fig. 26a).

Importantly, a similar pattern in the proliferation rates was shown for BIRB 796. In this assay, all groups of dmso treated cells proliferated in a comparable way. The fold-changes in cell number after 4 days ranged between 21.0 and 26.0. Single treatment with Sorafenib displayed a fold-change in cell number of 14.9 ± 0.3. This proliferation rate was comparable to BIRB 796 treated cells with a fold-change in cell number of 13.5 ± 0.2.

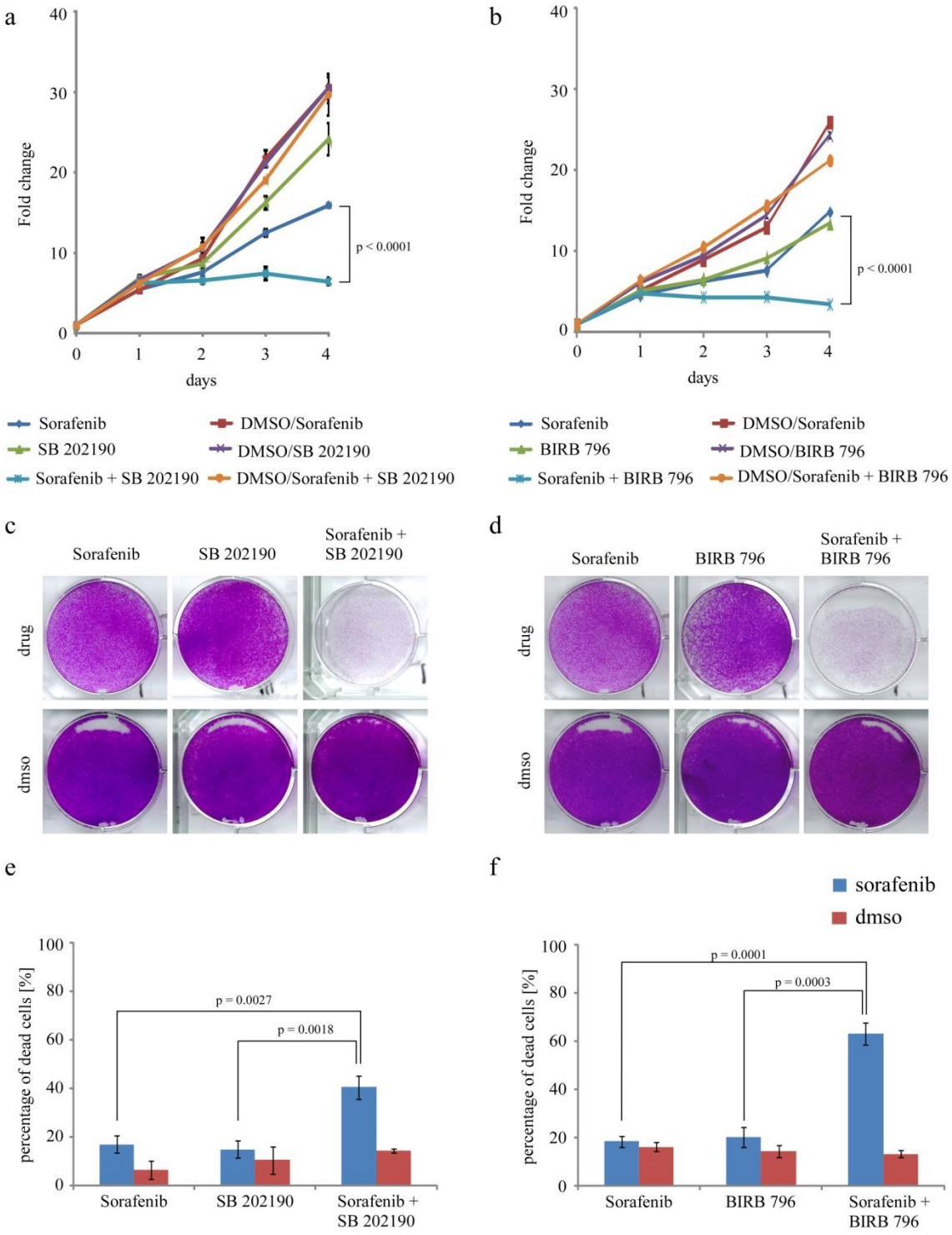

Figure 26 BIRB 796 and SB 202190 enhance response towards Sorafenib in Hep3B cells

Cell proliferation rates for Hep3B cells treated with 2 µM Sorafenib and 12 µM of the Mapk14 inhibitors SB 202190 or BIRB 796 as well as the combinatorial treatment. The number of cells was evaluated by Guava FACS measurements and plotted are averages of fold-changes in comparison to the initial point (day 0) (a,b). Visualization of cells stained with crystal violet after 4 days of treatment with 2 µM of Sorafenib and 12 µM of SB 202190 or BIRB 796 or combination thereof. 80,000 cells were plated one day before treatment onset (c,d). Determination of cell death by counting trypan blue positive cells upon mixing cell supsenstion with trypan blue solution in a 1:1 ratio. Shown are percentages of trypan blue positive cells, counted by the Neubauer hemocytometer after 5 days of treatment with above mentioned conditions (e,f).

A combination treatment with Sorafenib and BIRB 796 further reduced the proliferation rate and a fold-cange in cell number of 3.5 ± 0.1 was determined, which was significantly different compared to monotherapies ($p < 0.0001$) (Fig. 26b).

A visual depiction of crystal violet assay upon 4 days of different treatments also recapitulated a disadvantegous effect of combinatorial treatment. As shown, a significantly reduced number of cells for combinatorial treatment was stained with crystal violet compared to single treatments with Sorafenib or with Mapk14 inhibitors (Fig. 26c,d).

Comparable to Huh7 and PLC/PRF/5 cells, this combinatorial therapy also induced higher percentage of dead cells than for single treatments and for dmso treated (control) groups.

Using SB 202190 as a Mapk14 inhibitor the values for trypan blue positive cells of dmso treated groups ranged from 6.5 % to 14.4 %. Sorafenib treated cells reached a value of 17.1 ± 3.7 % of dead cells which was comparable to SB 202190 treated cells with a value of 15.0 ± 3.6 % of dead cells. The number of dead cells in Hep3B cells was further increased by combination treatment of Sorafenib and SB 202190 and reached a value of 40.6 ± 4.8 % of dead cells. These values were significantly different to monotherapies with a p value of 0.0027 compared to Sorafenib and a p value of 0.0018 compared to SB 202190 treatment (Fig. 26e).

These results were also confirmed by the usage of BIRB 796 as a Mapk14 inhibitor. After trypan blue staining, dmso treated cells showed between 13.3 % and 16.3 % of dead cells. Sorafenib treatment induced 18.4 ± 2.4 % of dead cells and which was comparable to a value of 20.2 ± 4.2 % of dead cells for BIRB 796 monotherapy. The combination of Sorafenib and BIRB 796 further increased the number of dead cells to 63.2 ± 4.5 % and showed a statistical significance in comparison to single treated cell populations (monotherapies) ($p = 0.0001$ to Sorafenib and $p = 0.0003$ to BIRB 796) (Fig. 26f).

Taken together, quantification of cell proliferation rates using a cell doubling assay and crystal violet staning as well as determination of cell death by quantification of trypan blue positive cells in a panel of human HCC cell lines shows a promising, disadvantegous effect on human HCC cell lines by a combinatorial treatment of Sorafenib and different Mapk14 inhibitors. This sensitization effect of the combinatorial therapy is achieved by significantly lower cell proliferation rates and higher amounts of dead cells compared to individual monotherapies. Interestingly, these results in human HCC cells showed an even more potent effect of the combinatorial therapy than the murine $Nras^{G12V;}$ $p19^{Arf-/-}$ cells. These data

indicate that this combination therapy constitutes a strong potential in the treatment of human hepatocellular carcinoma.

4.9. ATF2 plays a role as a downstream target in Mapk14 mediated resistance towards Sorafenib treatment

Our treatment studies of several different rodent and human HCC cell lines indicate the combination of Sorafenib and Mapk14 inhibitor as a potent treatment strategy for human HCC patients. Nevertheless, so far it is not clear how Mapk14 induces resistance towards Sorafenib treatment. In chapter 4.4 (Figure 17 and 18) it could already be shown that knockdown of Mapk14 did not influence the amount of dead cells but reduced the proliferation rate of Sorafenib treated tumors and HCC cells. Although this is different upon pharmacological inhibition of Mapk14 (possible off target effects of compounds), it indicates that Mapk14 is necessary for a signaling cascade which induces proliferation in the absence of Sorafenib targets Raf1, c-Raf, VEGFR-2 and VEGFR-3. To see whether this signaling cascade is upregulated upon Sorafenib treatment, western blot assays of activated Mapk14 (P-Thr-180/Tyr-182) was performed 6 hours, 24 hours and 3 days upon Sorafenib treatment or dmso in murine $Nras^{G12V}$; $p19^{Arf-/-}$ und human Hep3B cells. Interestingly, the amount of phosphorylated Mapk14 in $Nras^{G12V}$; $p19^{Arf-/-}$ cells did not increase upon Sorafenib treatment but was even slightly reduced 3 days after treatment (Fig. 27a) which shows that the Mapk14 pathway is not upregulated upon short-term Sorafenib treatment. Likewise, no difference was seen for phosphorylated Mapk14 at different timepoints after Sorafenib treatment for Hep3B cells (Fig. 27b). Nevertheless, independently of whether Mapk14 is upregulated or not upon Sorafenib administration, previous data showed that this pathway is necessary for proliferation upon Sorafenib treatment.

To identify how the Mapk14 pathway induces resistance towards Sorafenib treatment in more detail, mRNA gene expression analyses were carried out in $Nras^{G12V}$; $p19^{Arf-/-}$ cells harboring Mapk14 or control shRNA upon 3 days of treatment with Sorafenib or dmso, respectively. The analysis was performed with whole cell mRNA extracts using Affymetrix gene chip (in cooperation with Robert Geffers, Helholtz Centre for Infection Research).

The expression data from shcontrol cells treated with Sorafenib, shMapk14 cells treated with dmso and shMapk14 cells treated with Sorafenib were normalized towards the expression data of shcontrol cells treated with dmso and compared (log_2 ratio). Interestingly, the

expression of several genes related to cell proliferation and cell growth were highly reduced in cells carrying the hairpin against Mapk14 and which were treated with Sorafenib, compared to dmso treated shcontrol cells. These data are in line with previous data which showed a lower proliferation rate of Sorafenib treated tumors or cancer cells carrying a Mapk14 hairpin compared to Sorafenib treated tumors/cells with a control hairpin or carrier treated tumors/cells (Figure 17 and 18). To evaluate the underlying signal cascades of this expression pattern, a bioinformatical analysis of the expression data was conducted by using Ingenuity pathway analysis software (Ingenuity Systems, Inc). This software applies a literature based analysis of upstream factors, which activation or deactivation might be causative for the observed gene expression phenotype (illustrated by a positive or negative z-score). This analysis was done for shcontrol cells treated with Sorafenib and shMapk14 cells treated with Sorafenib or dmso, which where previously normalized to dmso treated shcontrol cells. All three groups were compared between each other upon bioinformatical analysis.

Interestingly, several upstream regulators were identified as significantly deactivated in HCC cells upon Sorafenib treatment in combination with knockdown of Mapk14 compared to Sorafenib monotherapy and Mapk14 knockdown alone. In Figure 27c the 50 most depleted upstream factors upon combinatorial therapy are listed (No value = no significant regulation found).

As a proof of principle the activity of the Sorafenib targets Raf and VEGF was analyzed. Importantly, in cells treated with Sorafenib monotherapy (sh-control cells) a deactivation of the major Sorafenib target Raf1 (c-raf) [76] was identified (z-score = -3.05). In line with these data, also deactivation of VEGF (-3.24) and PDGF (-3.16) (together with the PDGF subunit PDGFBB [143] (-4.51)) were seen, which are ligands for Sorafenib targets VEGFR-2, VEGFR-3 or PDGFR, respectively [76]. Moreover, the deactivation of Raf1 and VEGF was even stronger under combinatorial therapy with Mapk14 knockdown, illustrated by z-scores of -6.22 (RAF-1), -5,80 (VEGF). Similar results were observed by analyzing the downstream targets of Raf1, ERK and MAP2K1 (MEK-1). Also here a strong reduction upon Sorafenib monotherapy was seen (z-score of ERK = -2.41/-2,97 and of MAP2K1 = -1,64), however, there was also reduction upon Mapk14 knockdown and a stronger reduction upon combinatorial therapy with z-scores of -4.80/-4.00 (ERK) and -3.64 (Mapk2K1).

Apart from VEGF and PDGF, also the growth factors EGF (-4,85), IGF1 (-3,88) (in combination with Insulin (-4,13)), TGFA (-4,38) and HGF (-4,40) were identified as deactivated upon combinatorial therapy.

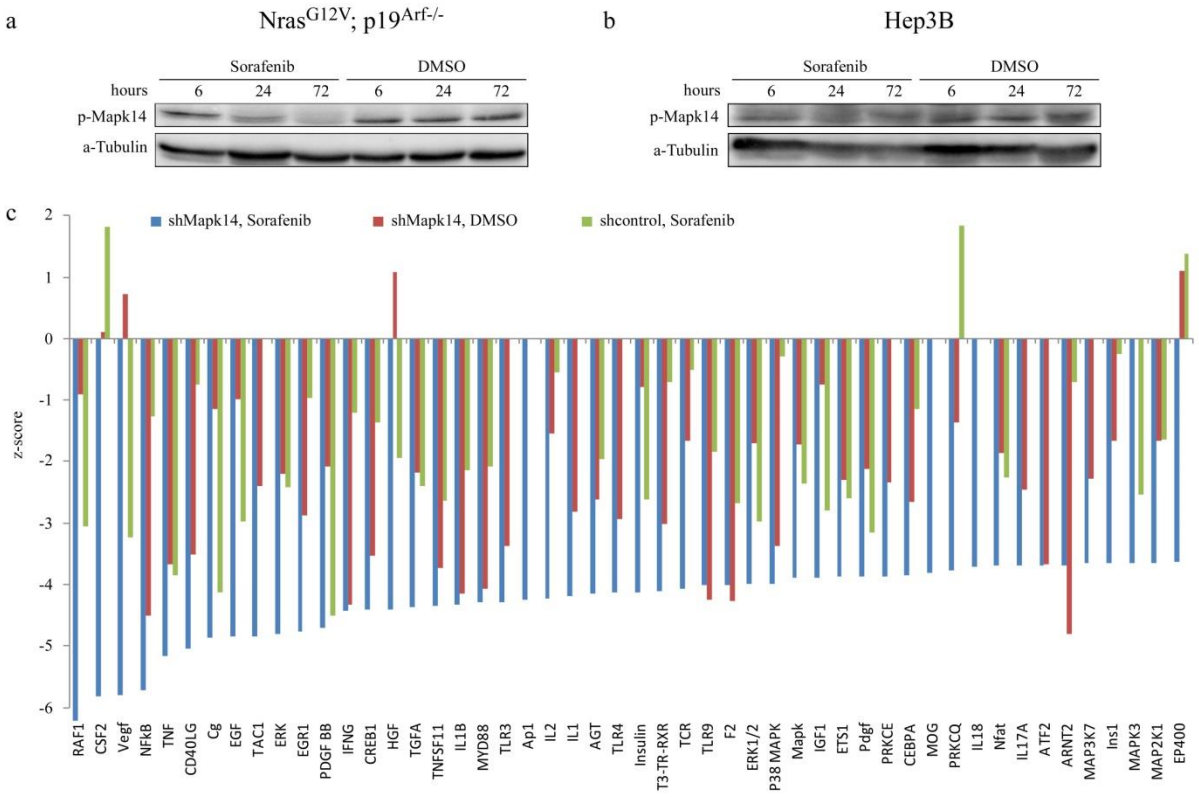

Figure 27 Mapk14 is not activated upon Sorafenib treatment but influences several cell regulatory factors involved in cell proliferation

Western blot assay against activated Mapk14 (p-p38) in Nras^{G12V}; p19$^{Arf-/-}$ cells (a). Western blot assay against activated Mapk14 (p-p38) in human Hep3B cells (b). Bioinformatical analysis of upstream factors (Ingenuity pathway analysis) based on gene expression data which were collected from Nras^{G12V}; p19$^{Arf-/-}$ cells carrying a control shRNA or a shRNA against Mapk14 and which were treated with Sorafenib or carrier for a 3day period. The data from Sorafenib treated cells and dmso treated Mapk14 cells were normalized towards dmso treated shcontrol cells.

Also several cytokines as IL1 (-4.19/-4.32), IL2 (-4.22), IL17A (-3,70), IL18 (3,70), interferon gamma (IFNG -4.42) and TNFSF11 (-4.34) were found deactivated upon combinatorial therapy.

As another proof of principle also activity of Mapk14/p38 was determined and a strong deactivation was seen upon Mapk14 knockdown, independenly of whether the cells were treated with Sorafenib or with carrier (z-score = -3.38 in dmso treated, -3.98 in Sorafenib treated cells). Interestingly, also the activity of Mapk14 downstream target ATF2 (Activating transcription factor 2) was found strongly diminished upon Mapk14 knockdown (-3.67 in dmso treated, -3.69 in Sorafenib treated cells), indicating a putative role of ATF2 in Mapk14 mediated resistance towards Sorafenib treatment.

ATF2 is a transcription factor which binds to a DNA sequence called cAMP-responsive element (CRE). It builds a complex, which is called Ap-1 (activator protein 1) with several

other transcription factors, as members of the Jun, Fos, Maf and ATF/Creb gene families [144]. Interestingly the Ap-1 complex was also found strongly deactivated upon combinatorial therapy (-4.24), but in this case not upon knockdown of Mapk14 alone. Also CREB1, one member of the ATF/Creb gene family which is also a downstream target of Mapk14 [145] and a binding partner of ATF2 [146] was found dimished upon combinatorial therapy (-4.41).

To validate the results from this bioinformatical analyses, western blot analysis were performed for activated ATF2 (phosphorlyated at Thr69 and Thr51) upon combinatorial therapy (using two different Mapk14 shRNAs), as well as upon Sorafenib treatment and Mapk14 knockdown alone. These data showed diminished activation of ATF2 upon combinatorial therapy (Fig. 28a).

To determine whether ATF2 is necessary for Mapk14 mediated resistance towards Sorafenib therapy, genetic validation experiments were performed using two independent shRNAs targeting ATF2 (ATF2.1136 and ATF2.1362). As described before, these hairpins were also ordered as 97base oligos and cloned by PCR cloning using XhoI and EcoRI into MSCV plasmids. $Nras^{G12V}$; $p19^{Arf-/-}$ cells were stably transduced with these hairpins and upon quantitative PCR analysis, using whole cell extracts a clear reduction of ATF2 mRNA (>40%) was seen compared to a control shRNA, indicating a good knockdown efficiency of the ATF2 shRNAs (Fig. 28b).

To allow for conditional expression of these shRNAs, the hairpins were shuttled using XhoI and EcoRI cloning into MSCV plasmids carrying a tetracycline resposive element. $Nras^{G12V}$; $p19^{Arf-/-}$ cells carrying constitutively expressed tetracycline/doxycycline binding protein (rtTA3) were stably transduced with viral particles carrying these constructs, and upon puromycin selection the shRNAs were activated due to doxycycline (5µg/ml medium) administration.

Next, the cells were either treated with Sorafenib or with dmso and subjected to quantification of proliferation rates and colony formation assay, which was visualized by crystal violet staining. For cell doubling assay, 120,000 cells were seeded per plate, subjected to doxycycline and 24 hours later the treatment with Sorafenib or dmso was started. Similar to previous cell doubling assays, the number of attached cells (GFP positive) was subsequently measured everyday for a 4-day time period and again compared to the initial point (day 0) to calculate a fold-change (Fig. 28c).

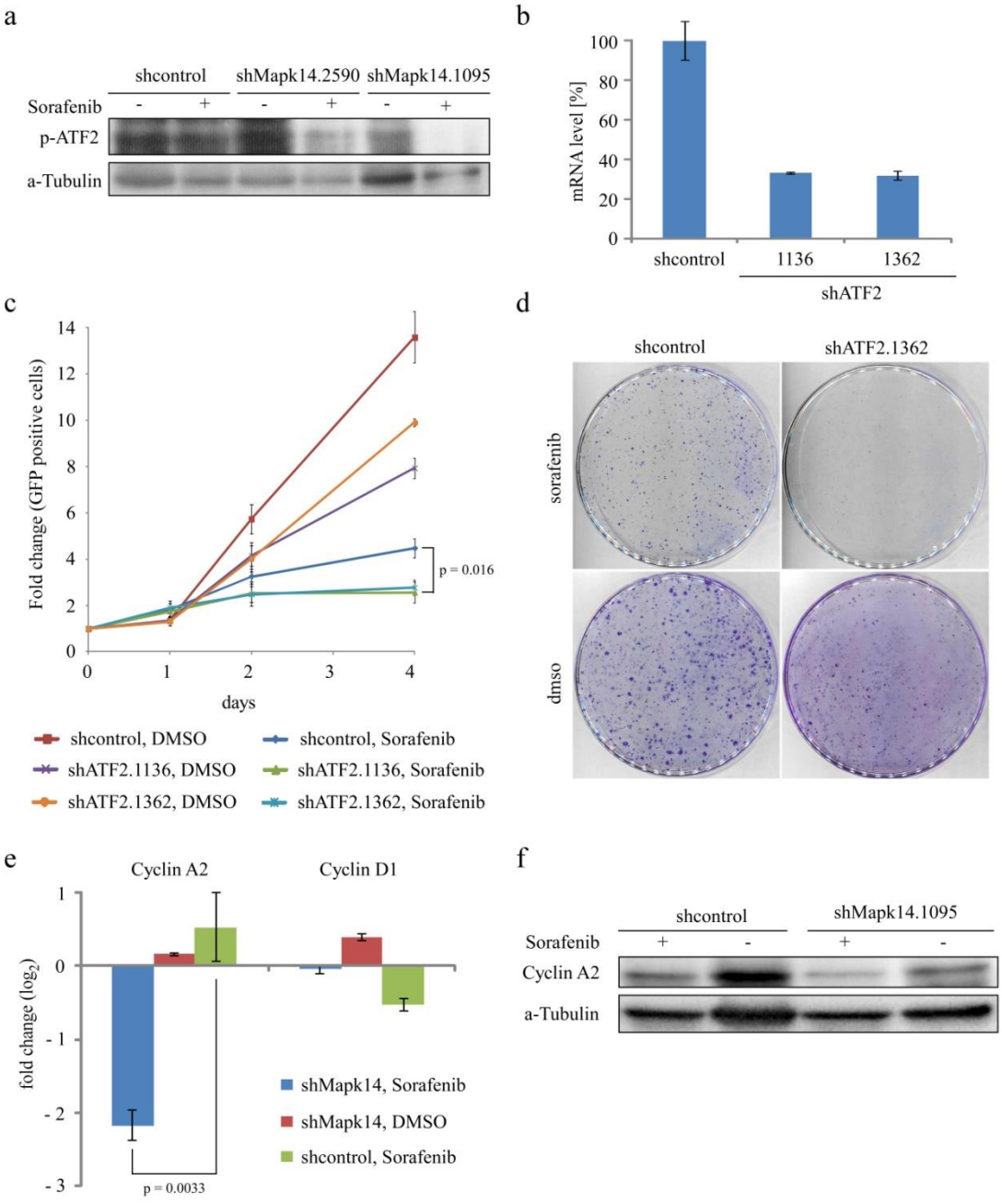

Figure 28 ATF2 is downregulated upon combinatorial treatment and is an important Mapk14 downstream target mediating resistance towards Sorafenib therapy

Western blot assay against activated ATF2 in $Nras^{G12V}$; $p19^{Arf-/-}$ cells carrying a control shRNA or two different shRNAs targeting Mapk14 (a). Quantitative PCR analysis of knockdown efficiency of ATF2.1136 and ATF2.1362 shRNAs compared to a control shRNA after stable transdution of $Nras^{G12V}$; $p19^{Arf-/-}$ cells, measured by mRNA level of whole cell extracts (b). Cell proliferation rates of $Nras^{G12V}$; $p19^{Arf-/-}$ cells carrying a control shRNA or two different shRNAs targeting ATF2 either treated with 8 µM Sorafenib or dmso respectively. The number of cells was evaluated by Guava FACS measurements and plotted as averages of fold-changes in comparison to the initial point (day 0) (c). Cell doubling assay of $Nras^{G12V}$; $p19^{Arf-/-}$ cells carrying a control shRNA or shRNAs targeting ATF2 either treated with 8 µM Sorafenib or dmso. Cells were visualized by crystal violet staining (d). mRNA expression analysis of Cyclin A2 and Cyclin D1 in $Nras^{G12V}$; $p19^{Arf-/-}$ cells carrying a control or a shRNA targeting Mapk14 and which were treated either with Sorafenib or carrier. Microarray data using affymetrix gene chip upon whole cell mRNA extraction. Values were normalized towards the expression data from dmso treated shcontrol cells (e). Western blot analysis of Cyclin A2 in $Nras^{G12V}$; $p19^{Arf-/-}$ cells also carrying a control shRNA or a shRNA targeting Mapk14 upon treatment either with Sorafenib or carrier (f).

Dmso treated shcontrol cells reached after 4 days a fold-change of 13.59 ± 1.1. Due to knockdown of ATF the $Nras^{G12V}$; $p19^{Arf-/-}$ cells grew slower and reached after 4 days fold-changes of 9.90 ± 0.2 (shATF2.1362) and 7.93 ± 0.4 (shATF2.1136), implying that knockdown of ATF2 influences already cell growth of non treated cancer cells. However, Sorafenib treated shcontrol cells reached only a fold-change of 4.48 ± 0.4, indicating that Sorafenib monotherapy dimished cell growth stronger than ATF2 knockdown. Interestingly, cells carrying ATF2 hairpins which were treated with Sorafenib showed a much stronger reduction in cell growth (fold change 2.57 ± 0.5 with ATF2.1136 and 2.77 ± 0.3 with ATF2.1362) than Sorafenib treated shcontrol cells (p=0.016).

The results from the cell doubling assay could be reproduced by colony formation assay, which was also performed as previously described. 5000 cells, carrying a non targeting control shRNA or the previously described shRNAs against ATF2 were plated onto 10-cm dish plates, treated either with Sorafenib or with dmso and subsequently visualized using crystal violet staining. The combination of ATF2 knockdown and Sorafenib treatment reduced the amount of cells much stronger than Sorafenib treated shcontrol cells and dmso treated cells (Fig. 28d).

Taken together, these data illustrate that knockdown of ATF2 can phenocopy the knockdown of Mapk14 implying that ATF2 might play a major role as a downstream target of Mapk14 towards Sorafenib treatment.

Some of the most relevant targets of ATF2 mediated transcriptional activation are the Cyclins A and D [146]. Interestingly, in the mRNA based gene expression microarray analysis, which was used for the Ingenuity based identification of upstream factors, we identified Cyclin A2 (the somatic isoform of Cyclin A [147]) strongly downregulated in Sorafenib treated shMapk14 cells compared to dmso treated control cells (log_2 fold = -2.17 ± 0.2). Moreover, no downregulation was seen in Sorafenib treated shcontrol cells and shMapk14 cells treated with dmso (p = 0.0033 shMapk14 vs. shcontrol, both Sorafenib treated) (Fig. 28e). The expression data of Cyclin D1 were different to Cyclin A2 and upon combinatorial therapy no downregulation was seen compared to dmso treated control cells (log_2 fold = -0.05 ± 0.06) (Fig. 28e). These data indicate a special role of Cyclin A2 as a transriptional target of ATF2 upon Sorafenib treatment. To validate the data from the expression array, western blot analysis of Cyclin A2 was performed in shcontrol and shMapk14 cells, which were again either treated with Sorafenib or with dmso. These data also showed lower amount of Cyclin A2 protein upon combinatorial therapy (Fig. 28f).

Taken together, these data indicate that ATF2 and its transcriptional target Cyclin A2 play a role in Mapk14 mediated resistance towards Sorafenib treatment in hepatocellular carcinoma.

4.10. New Mapk14 inhibitors (Skepinone-L, PH 797804) which are promising candidates for clinical development are effective in combinatorial treatment

In this study there could be shown an effect of combinatorial therapy for Sorafenib and different Mapk14 inhibitors in reducing the growth of murine hepatocellular carcinoma and various murine/human HCC cell lines. This indicates that this combinatorial therapy could be useful in the clinic to treat HCC patients, however, the Mapk14 inhibitors which were tested so far (SB 202190 and BIRB 796) were not approved in clinical studies. SB 202190 was not at all tested in clinical studies and BIRB 796 has been dismissed after phase I of clinical trials due to occurring toxic side effects. Nevertheless, currently different newly designed Mapk14 inhibitors are currently under development or clinical testing, which might have a higher potential for treating patients. Among them is Skepinone-L, which was so far not tested in clinical studies and PH-797804 which completed phase II clinical studies. Both inhibitors showed only marginal side effects and in contrast to BIRB 796 and SB 202190 seem to be more specific for Mapk14 (the α-form of p38) [148;149]. Therefore, the effect of these Inhibitiors should be also tested in combination with Sorafenib treatment (in cooperation with Stefan Laufer, Universitiy of Tübingen).

To determine the efficacy also for those Mapk14 inhibitors in the previously shown *in vitro* setting, murine $Nras^{G12V}$; $p19^{Arf-/-}$ and human Hep3B HCC cells were applied. 120,000 cells were seeded per plate and after 24 hours the cells were treated with Sorafenib, with the corresponding Mapk14 inhibitor alone or in combination thereof. Also controls with corresponding dmso concentrations were performed. Similar to previous assays, the amount of cells upon treatment was visualized by crystal violet staining.

As shown before, the treatment of $Nras^{G12V}$; $p19^{Arf-/-}$ cells with Sorafenib induces only marginal reduction in cell growth. By using Skepinone-L as a Mapk14 inhibitor also a reduction in cell growth was seen, which was even slightly stronger than upon Sorafenib treatment. Importantly, the combination of Sorafenib and Skepinone-L reduced cell growth much stronger than monotherapies (Fig. 29a). By using PH 797804 as a Mapk14 inhibitor nearly no reduction was seen upon PH 797804 monotherapy. In combination with Sorafenib

PH 797804 also reduced cell growth stronger than monotherapies. However, the difference was not as pronounced as for Skepinone-L (Fig. 29b).

By treating the human HCC cell line Hep3B, the effect of Sorafenib monotherapy was again moderate and therefore comparable to previous studies. As shown in $Nras^{G12V}$; $p19^{Arf-/-}$ cells, the application of Skepinone-L monotherapy showed a slightly higher effect in diminishing cell growth than Sorafenib treatment. However, the combination of Sorafenib and Skepinone-L reduced cell growth of Hep3B cells also significantly stronger than monotherapies (Fig. 29c). The treatment of Hep3B cells with PH 797804 alone showed an effect, which was comparable to Sorafenib treatment. However, the combination of Sorafenib and PH 797804 was not as pronounced as for the combination of Sorafenib and Skepinone-L in Hep3B cells or for the combination of Sorafenib and PH 797804 in murine $Nras^{G12V}$; $p19^{Arf-/-}$ cells (Fig. 29d).

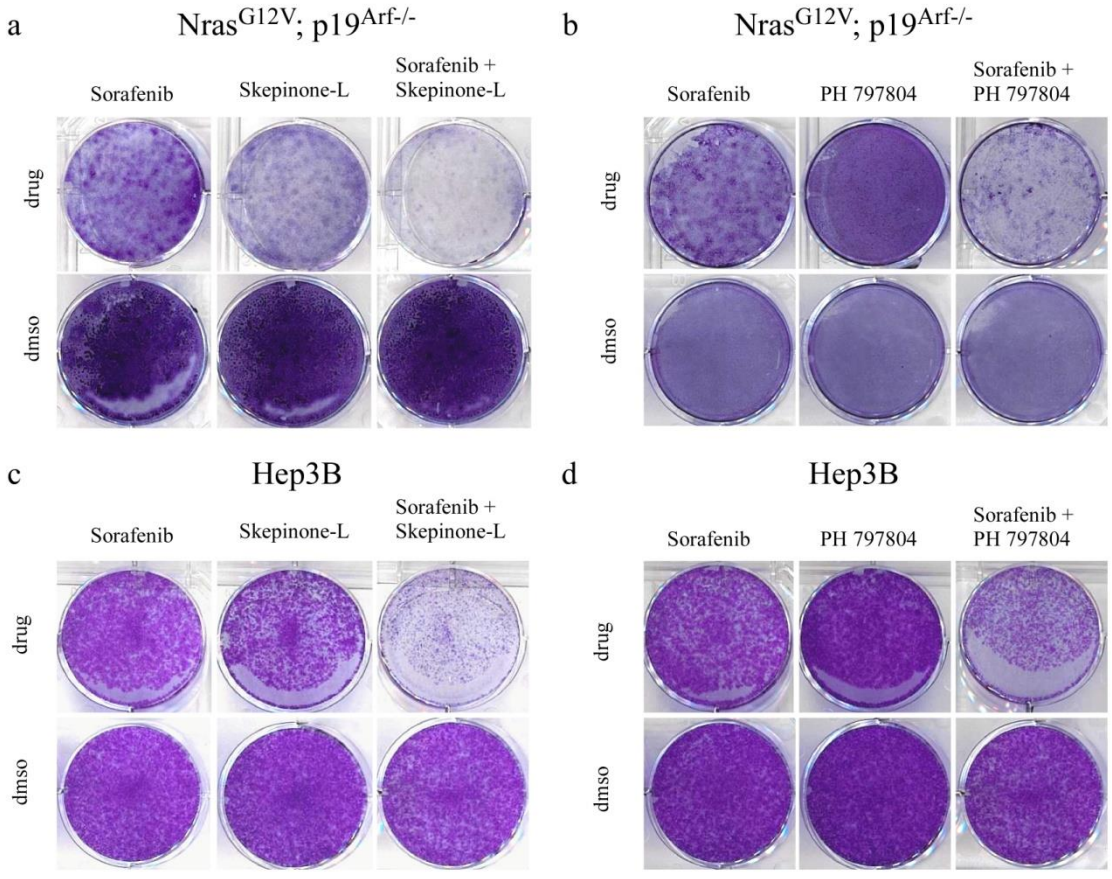

Figure 29 Highly specific Mapk14 inhibitors show enhanced response towards Sorafenib in $Nras^{G12V}$; $p19^{Arf-/-}$ and Hep3B cells

Visualization of $Nras^{G12V}$; $p19^{Arf-/-}$ cells stained with crystal violet after 4 days of treatment with 8 µM of Sorafenib and 20 µM of Skepinone-L or 20 µM PH 797804 or combination thereof (a,b). The respective visualization for Hep3B cells was performed for treatment with 2 µM Sorafenib and 15 µM Skepinone-L or 20 µM PH 797804 or combination thereof (c, d). 120,000 cells were plated one day before treatment onset.

Taken together, both newly developed Mapk14 inhibitors showed a significant effect in combinatorial treatment with Sorafenib in diminishing HCC cell growth. Skepinone-L showed in general stronger effects with Sorafenib than PH-797804, however, small effects were already seen upon Skepinone-L monotherapy. Nevertheless, these Mapk14 inhibitors might be promising compounds to organize clinical studies, which might approve this combinatorial therapy to HCC.

5. Discussion and outlook

Hepatocellular carcinoma represents the sixth most frequent type of cancer and the third leading cause of cancer related death worldwide [1]. This high lethality rate (5 year survival rate of only 8.9 %) is mainly be due to a lack of efficient treatment options. Surgical resection of tumors is only applicable to a small subgroup of patients and chemotherapeutic drugs are often shown to be not effective [56].

As for melecular targeted therapies, only the small kinase inhibitor Sorafenib is approved, however Sorafenib prolongs survival of HCC patients only by 2.8 months. Nevertheless, the tumor inhibitory effect of Sorafenib shows that a targeted therapy in general can be effective to treat HCC [80]. Sorafenib is a multikinase inhibitor with several targets. The main targets are members of the Raf family (C-Raf also known as Raf1, mutant and wild type B-Raf) and the vascular endothelial growth factor receptors (VEGFR-2 and VEGFR-3) [76]. Currently it is under scientific discussion which target plays the major role in tumor inhibition. However, it may be possible that the combinatorial inhibition of both, proliferative and angiogenic targets explains the effectiveness of Sorafenib in HCC treatment as it is known that combinatorial targeting may improve targeted therapies in general. These facts provide the rationale that HCC treatment with Sorafenib may be more effective with addition of other targeted agents [150]. Recently, several combinatorial therapies with Sorafenib are under investigation as for example the combination of Sorafenib with the EGFR inhibitor Erlotinib or the VEGF receptor Bevacizumab (Avastin) [151].

To identify new promising targets for a combinatorial therapy with Sorafenib, either a hypothesis driven approach could be applied, based on the molecular background of HCC development and Sorafenib treatment or an unbiased approach could be chosen. In this study, a combinatorial treatment is described that improves Sorafenib treatment significantly in different experimental setups. This combinatorial treatment is based on the inhibition of the Mitogen activated kinase 14 (Mapk14 or p38α). This candidate was identified by an unbiased approach using an *in vivo* RNAi screen in a mosaic cancer mouse model.

As decribed before, RNAi screens in the presence of drugs were already performed and identified potential new targets for combinatoral therapies. For example, in the presence of PARP inhibitor, a screen in breast cancer cells using siRNAs was performed which identified CDK5 and STK22c as potential drug sensitizing targets [124]. Also in the presence of paclitaxel or gemcitabine, siRNA screens were conducted [125;126]. Genes mediating doxorubicin resistance were identified with a miR30-based shRNA library in lymphoma cells

[127]. These screens showed the utility of drug sensitizing screens; however, these screens are based entirely on cell culture systems.

Although candidates for human treatment were identified by cell culture or xenograft models, it became evident that new treatment strategies that were identified using *in vitro* systems are of limited value for the treatment of human cancer patients due to differences in cell growth and cell environment [96]. A human tumor is influenced by several cell extrinsic factors, as growth factors, angiogenesis and the role of the immune system. These factors are not reflected accurately in an *in vitro* model. Also in transplanted cells in a xenograft model, arising tumors differ strongly to tumors occurring directly in the corresponding organ [96].

To identify possible treatment options for a therapy in humans, a model is requested that mimics human cancer induction and development. In our mosaic cancer mouse model, malignancy is induced in cells which are surrounded by normal tissue cells of the corresponding organ. This resembles carcinogenesis in a better way than a simultaneous, tissue specific expression of transgenes in all cells of the organ. Furthermore, the genomic lesions are induced in adult cells, thus avoiding developmental compensation as seen in germline transgenic mice.

The mosaic cancer mouse model described in this study induces tumor development by transposon-based gene transfer. Therefore, transposable elements carrying oncogenes and marker genes were integrated into adult hepatocytes by hydrodynamic tail vein injection. This is entirely assured of *in vivo* manipulation of hepatocytes, the major target cells for HCC transformation [5]. *Ex vivo* cell manipulation steps which are necessary for previously used mosaic cancer mouse models [107;108] and which can already influence cell behavior are therefore no longer necessary. The described model was already used to characterize liver cancer development and to identify new cell extrinsic or intrinsic tumor suppressive mechanisms in liver cancer ([113;115] and Dauch and Zender, unpublished data). In these studies these model was characterized as highly physiological.

In some of the studies it was shown that transposon-based gene transfer of oncogenic $Nras^{G12V}$ can trigger HCC development in $p19^{Arf}$ deficient mice. Delivery of oncogenic $Nras^{G12V}$ activates the MAPK pathway, a signaling cascade which is frequently upregulated in several human cancers and also in human HCC [14;152]. Mutation in genes of the Ras family occurs in 11 percent of human HCCs (4 % *NRAS*, 7 % *KRAS*) [14]. Additionally, genes which induce Ras activation as the transforming *growth factor α* or *insulin-like growth factor II* are found activated or overexpressed in human HCCs [44]. Furthermore, negative regulatory

factors of Ras as *NF1*, *RPS6KA3* or the Ras GAP genes *RASAL1*, *DAB2IP* are found downregulated or depleted in several human HCCs [16], which induce a higher activity of Ras.

The deficiency of $p19^{Arf}$ in this mouse model is necessary to abrogate tumor suppressive pathways, which are found to be activated due to oncogenic activation [153]. It is an important tumor suppressor protein in different types of cancer, as also in HCC. Although the human counterpart $p14^{Arf}$ is not often mutated in liver cancer it is often found inactivated by promoter methylation in around 15 % of HCC cases [46].

Consequently, this relevant setup was used to identify the response of HCC development to Sorafenib by treatment of mice after $Nras^{G12V}$ injection. Interestingly, only a small survival benefit could be reported upon Sorafenib treatment. This is remarkable, since signaling to Raf is one of the major targets of Sorafenib and this is important for the Ras/MAPK signaling cascade. Nevertheless, this small but significant response mimics closely the Sorafenib response of human HCCs [80] in contrast to experiments *in vitro* or xenograft models, were in general a strong response to Sorafenib treatment was determined [77]. Interestingly, a cell line established from the $Nras^{G12V}$; $p19^{Arf-/-}$ tumor shows a higher response to Sorafenib than the *in vivo* tumors, although the genetic background was identical. This strong effect of Sorafenib in the *in vitro* setup shows further that Sorafenib influences cell intrinsic targets (as Raf).

In contrast to pure transgenic mouse models, an advantage of mosaic cancer mouse models is the ability to perform *in vivo* RNAi screens. For this screen expanded transposable elements were used, where miR30-based shRNAs were combined with expression of oncogenes and marker genes on one construct. The use of shRNAs, wich were embedded into a miR30 context was shown to induce a physiological knockdown of genes [118]. In a recent study it was shown that these expanded transposon constructs induce a good knockdown and are suitable to perform a positive selection screen to identify new tumor suppressor genes in HCC (Dauch and Zender, unpublished data). Additionally, comparable constructs have already been used for a positive non cancer related RNAi screens in the liver [154]. However, to identify putative targets for the treatment options, oncogenic candidates have to be identified and a negative selection screen has to be performed. Due to technical limitations based on the complexity of shRNA screens, negative selection screens are until now restricted to *in vitro* screens and in mouse models only positive selection screens are feasible.

However, because the stable delivery of oncogenic $Nras^{G12V}$ gives rise to hundreds of macroscopically visible tumors and even more microscopic tumors, this setup should allow for negative screens. Since each neutral shRNA is expressed in many tumors a shRNA which

inhibits tumor development can be found depleted, in comparison to the performance of neutral hairpins.

The screen was performed using an shRNA library (designated as ROMA Amplicon Library), targeting genes which were found amplified in human HCCs and therefore may play roles as driver genes in tumor progression. These amplifications were identified via Representational Oligonucleotide Microarray Analysis (ROMA). This method was already used to identify depleted genes in human HCCs and the collected data were applied to conduct a shRNA library which was used for a positive RNAi selection screen to identify possible tumor suppressor genes [108]. This screen showed already that the integration of human data into an *in vivo* screen in mice can identify candidates which can give an insight into human cancer development.

The ROMA Amplicon library consists of 250 shRNAs. In order to define the maximal pool size for the screen, dilution experiments were performed where two individual hairpins were mixed in different ratios and injected with oncogenic $Nras^{G12V}$ into $p19^{Arf}$ deficient mice. The experiments identified that also haipins, which were diluted 1:250 with another hairpin can be found in the arising tumors in the same ratio (Pesic and Zender, unpublished data). These data illustrated that screening with a high complexity pool of 250 shRNAs is possible.

The comparison of the hairpins distribution between Sorafenib and carrier treated mice allows to identify shRNAs whose knockdown of target genes, may improve Sorafenib treatment. Due to the fact that the variability between different mice in one group was relatively high, bigger groups with 8-10 mice per condition were used. This screen identified different hairpins targeting the *Mapk14 (p38α)* gene depleted under Sorafenib treatment compared to the carrier treated group.

The fact that two different hairpins against one target were identified ensured that this target is relevant in the screening context. Therefore, off-target effects, which are in general possible by shRNA-mediated knockdown, can be excluded, a fact which was further confirmed by a knockdown test where both depleted hairpins show a good knockdown efficiency against Mapk14.

In follow-up validation experiments knockdown of Mapk14 using different single shRNAs improved significantly the treatment effectiveness of Sorafenib. This was shown in the *in vivo* model where knockdown of Mapk14 induces a lower tumor burden and a longer survival of Sorafenib treated mice compared to a control hairpin, as well as in an *in vitro* model where

the number of Sorafenib treated $Nras^{G12V}$; $p19^{Arf-/-}$ cells was significantly reduced under Mapk14 knockdown.
Interestingly, the knockdown of Mapk14 without Sorafenib treatments has no or only a marginal effect to tumor development and tumor cell reduction. This indicated that this candidate gene plays a special role under Sorafenib treatment.

One hairpin against Mapk14 was also found depleted, in an *in vitro* RNAi screen, which was performed with cells from an $Nras^{G12V}$; $p19^{Arf-/-}$ driven tumor and therefore in the same genetic background as in the *in vivo* screen. However, the depletion was in general low and hairpins against Mapk14 are not found as strong depleted as in the *in vivo* model. Therefore, the most depleted Mapk14 hairpin ranked only on position 5 of the most depleted hairpins and hence questionable is whether Mapk14 would be chosen as a possible candidate without the information from the *in vivo* screen.
This is an intesting observation, due to the fact that Mapk14 could be validated as a candidate also in the *in vitro* setting. A possible explanation could be that the *in vivo* RNAi screen is in general more selective than the *in vitro* screen, which is also indicated by the in general lower changes in shRNA distribution upon Sorafenib treatment. A higher selectivity in the *in vivo* screens could be explained by the fact, that Sorafenib shows in general a lower effect in the *in vivo* setting. Also the strong amplification of not affected shRNAs in single cell derived tumors might induce a strong selectivity. Taken together these data highlight the need for *in vivo* RNAi screens in relevant models even for investigating cell-intrinsic mechanisms of tumor development.

Mapk14 is a member of the p38 gene family, consisting of p38α (Mapk14), p38β (Mapk11), p38γ (Mapk12) and p38δ (Mapk13) [20]. Although this gene family has similarities, especially in activation, they have different functions due to different downstream targets. Interestingly, Mapk13 which is also included into the ROMA Amplicon library, was not found as much depleted as Mapk14 due to Sorafenib treatment. The Mapk14 kinase activity can phosphorylate many downstream targets and can therefore regulate many different processes in the cell. Intriguingly, it has proliferative as well as anti-proliferate functions and can induce survival and growth of cells as well as apoptosis or cell cycle arrests and senescence. Important downstream targets are p53, ATF2 and Creb1 [155].
Mapk14 is involved in the signaling cascades of the MAPK pathway and can be activated by MKK3, MKK4, MKK6 and MKK7. It can be stimulated by inflammatory cytokines,

environmental stress and growth factors. Interestingly, Mapk14 is also linked to Ras signaling either while it is activated by MKK4 and MKK7 [156] or when it is activated via Rac-MKK3/6 [18;157].

By quantification of cell proliferation rates it was shown that knockdown of Mapk14 reduces the proliferation of Sorafenib treated cells or tumors, which results in a better response towards Sorafenib. Induction of cell death was not identified as beeing relevant for the effect of combinatoral treatment.

To get more mechanistic insight how Mapk14 induces resistance towards Sorafenib treatment bioinformatical analyses of expression profiling data were performed. These analyses identified ATF2 as an important factor in Mapk14 induced resistance towards Sorafenib treatment in hepatocellular carcinoma. ATF2, a known downstream target of Mapk14 influences as a transcription factor the expression of several genes involved in proliferation and cell growth [145;146]. It forms a complex with several other transcription factors as c-Fos, Maf and other members of the ATF gene family which is called AP-1 [144]. The analysis of the expression data indicates that knockdown or inhibition of Mapk14 in HCC cells inhibits also the activation of ATF2 and upon Sorafenib treatment also the AP-1 complex. This could be explained by the fact that beside Mapk14, ATF2 can be also activated by the Raf/Mek/ERK pathway, which is inactivated upon Sorafenib treatment. These results were validated via western blot by analysing the expression of ATF2 phosphorlyated at Thr-69 which is together with Thr-71 the main phosphorylation side for ATF2 activation [146]. ATF2 is known to play also a role in cancer development [144;146]. Therefore, it is not suprising that shRNA-mediated knockdown of ATF2 reduce the proliferation rate of HCC cell lines in general. However, by cell doubling and colony formation assays, it could be shown, that ATF2 knockdown cooperates with Sorafenib in inhibiting HCC cell growth extensively.

Among several genes which are transcriptionally regulated by ATF2, there are also the Cyclins A2 and D1 [146]. Cyclins cooperate with Cyclin dependent kinases (Cdks) to regulate the progression of the cell cycle. Cyclin A2 interacts with cyclin dependent kinase 2 (Cdk2) and its expression induces cell cycle progression in S phase and G2/M phase [147]. Cyclin D1 is important for the transition from G1 into S phase [158]. To the fact, that Mapk14 knockdown did not influence Cyclin D1 expression, other signal cascades might influence its transcription in hepatocellular carcinoma.

Apart from the Mapk14-ATF2 pathway, also several other upstream factors were found deactivated upon combinatorial therapy. Among them are several growth factors as VEGF,

PDGF, EGF IGF1, TGF and HGF. These growth factors might play also a role in Mapk14 mediated resistance, however so far it is not clear which growth factor is relevant for this mechanism. Also several cytokines were found downregulated upon combinatorial therapy. Therefore, it might be interesting to illuminate the role of growth factors and cytokines during Sorafenib therapy in follow-up studies.
An interesting observation was made by looking deeper into the activity of the Sorafenib targets VEGFR and Raf-1 and their downstream targets ERK and MAP2K1. These genes were identified as deactivated upon Sorafenib treatment; however a combination of Sorafenib and Mapk14 knockdown induces a stronger inhibition than Sorafenib monotherapy. So far it is not known, whether this is a direct consequence due to Mapk14 knockdown, or an indirect effect, based on general reduction of growth factors and mitogens. Nevertheless, this effect could be also an interesting topic for ongoing studies.

For the application of Mapk14 as a potential target for a combinatorial therapy with Sorafenib, there is a strong need to clarify, whether the effect of Mapk14 knockdown also affects advanced tumors in an intervention setting. Using regulatable expression of shRNAs, based on a tetracycline/doxycycline responsive system (tet-on), it was shown that indeed knockdown of Mapk14 enhances Sorafenib treatment even when it is induced in already established tumors. Interestingly, in Sorafenib treated mice it was possible to see a tumor-intrinsic selection against cells harboring an active Mapk14 hairpin. These intriguing results imply again the disadvantage of Mapk14 knockdown in Sorafenib treated tumor cells and indicate that the findings from this intervention mouse model might be underestimated.
Due to the fact that this regulatable system needs shRNAs and marker genes expressed by a regulatable promoter (TREtight), in combination with a constitutive active rtTA gene, it is currently difficult to apply this for transposon-based gene transfer. Therefore, $Nras^{G12V}$; $p19^{Arf-/-}$ cells were transduced with the corresponding plasmids and injected into the livers of wildtype mice. Although the effect in the intervention system could be nicely identified with this model, a transposon-based regulatory model would be also desirable due to the fact that it would enable intervention-based *in vivo* RNAi screens to indentify new potential treatment targets.

The observed effect of Mapk14 knockdown under Sorafenib treatment in advanced tumors enables the possibility of using Mapk14 as a therapeutic target. Since RNAi-based therapy is still in its infancy with many physiological obstacles to be solved [159], it was investigated

whether the combinatorial effect of Mapk14 knockdown and Sorafenib treatment can be phenocopied by pharmacological inhibition of Mapk14. Importantly, a handful of p38 inhibitors are known and described but so far none is available for clinical use. Some of these inhibitors are only used for experimental investigations, but some inhibitors have being already investigated in clinical trials [160]. Many of them exert high specificity towards p38α (Mapk14) but target, albeit with a lower affinity, also other members of the p38 gene family (e.g. p38β) [161]. Although, some have yielded promising results in preclinical studies for treating mainly inflammatory diseases, only few have progressed beyond Phase I clinical studies (e.g. BIRB 796 or PH 797804). An important consideration, given the suspension from futher development due to side effects (liver damage), is that side effects could result from off-target effects of the drug [139;162]. Importantly, liver cancer is associated with chronic inflammation which is an important cancer promoting factor [163]. In this process are involved different pro-inflammatory mediators with cancer survival properties (e.g. cytokines) which are regulated by Mapk14. However, Mapk14 inhibition can also activate anti-inflammatory cytokines, and therefore its inhibition can suppress or activate inflammatory reactions. Thus, Mapk14 inhibition can either predispose to cancer or its inhibition can be important for treating inflammation-asscociated cancer, like for example HCC, given its role in the production of pro-inflammatory cytokines [20].

The inhibitors SB 202190 and BIRB 796 that were firstly chosen for here presented studies are relatively specific for Mapk14 and showed a high inhibitory efficiency, although some activity to inhibit p38β cannot be excluded [161]. Both inhibitors were used to investigate the response in combination with Sorafenib in the experimental setups. By targeting $Nras^{G12V}$; $p19^{Arf-/-}$ cells, it was possible to achieve with both inhibitors a significant reduction in cell proliferation under Sorafenib treatment. Using SB 202190 which showed a higher inhibitory efficiency while used alone, showed also a higher effect in the combinatorial treatment with Sorafenib. Although, it was possible to phenocopy the results of shRNA-mediated knockdown, two striking differences in the response between shRNA-mediated and pharmacological inhibition were observed. First, the pharmacological inhibition of Mapk14 reduced the proliferation rate of tumor cells also as a single treatment. Using SB 202190 as an inhibitor, this effect was even comparable with Sorafenib monotherapy. However, a combinatorial therapy showed a much higher effect than Sorafenib monotherapy. Additionally, the application of the Mapk14 inhibitors showed a higher amount of cell death induction than the shRNA-mediated knockdown. The cell death under SB 202190 and BIRB 796 treatment alone was higher, than under Sorafenib treatment. Interestingly, by

combinatorial treatment with Sorafenib a much higher amount of cell death was identified, indicating that this is a specific effect that counts for the combinatorial effect of the Mapk14 inhibitors in combination with Sorafenib. These differences in phenotypes between shRNA-mediated knockdown and pharmacological inhibition could be caused by the different modes of function. Importantly, in case of shRNA-mediated Mapk14 (p38α) knockdown there is a specific inhibition of α isoform, therefore stronger effects conferred by the administration of chemical inhibitors could be attributed to above mentioned lack of specificity. Additionally, a pharmacological inhibition affects the cells in a more direct and immediate way than shRNA mediated knockdown which in turn reduces the protein level of its target gradually and in a more extended time frame.

Since BIRB 796 was already applied in *in vivo* studies, this inhibitor was used to investigate the combinatorial treatment using a pharmacological inhibition in the mosaic cancer mouse model. In this model, the combinatorial therapy induced a survival benefit in comparison to Sorafenib or BIRB 796 monotherapy, indicating that this combination could play a relevant role in HCC therapy. Interestingly, also in this experiment a low surfival benefit was observed upon BIRB 796 monotherapy which was comparable to Sorafenib monotherapy, indicating differences between shRNA mediated knockdown and pharmacological inhibition of Mapk14. Apart from the above mentioned potential explanation for this phenotype, also another reason for these differences could be likely in the presented *in vivo* model. As shown before, the transposon mediated delivery of transgenes and shRNAs is selective for the hepatocytes of the liver, inducing therefore knockdown of Mapk14 only in the hepatocytes. However, a pharmacological inhibition of Mapk14 might target other cell types of the corresponding individual. Therefore, an inhibition of Mapk14 in other cell types might explain the reduced tumor development in mice upon BIRB 796 monotherapy, e.g. by influencing angiogenesis or the immune response.

Mapk14 was identified as a candidate in a genetically defined shRNA screen with expression of oncogenic $Nras^{G12V}$ in a $p19^{Arf}$ deficient background. This constitutively active Nras mutant induces activation of the Ras/MAPK pathway. Although this pathway is frequently upregulated in human HCC [14;152] the geneticaly complexity of this cancer type enables also tumor growth triggered by other or by additional oncogenes as Akt/mTOR, c-myc, Wnt/beta-Catenin or Yap1 [27;34;53;107;141]. To determine, whether the tumor suppressive effect of Mapk14 inhibition is restricted to tumors with are triggered by activated Ras/MAPK

pathway, we took advantage of the flexibility of our transposon-based mouse model and triggered tumor growth by the oncogenic combinations $Nras^{G12V}$/Akt-1, $Nras^{G12V}$/c-myc and Akt-1/c-myc also in an $p19^{Arf}$ deficient background. These tumors were used to isolate additional HCC cell lines, which were also treated either with combinatorial therapy or with Sorafenib or different Mapk14 inhibitors alone. Interestingly, all of these HCC cell lines with different genotypes showed responses to Sorafenib treatment in combination with Mapk14 inhibition. However, the response was dependent on the used Mapk14 inhibitor, indicating that the genetic background can also predict the outcome of combinatorial therapy. Nevertheless, genetic information can be also used for tailored approaches to individual patients and thus used in selection of patients for whom this combinatorial treatment would be the most efficacious. Nevertheless, there might be a need to identify additional candidates, which may improve a Sorafenib therapy also in HCCs were the genetic background might reduce the efficiency of the combinatorial therapy. This could be succeeded by additional *in vivo* RNAi screens were the genetic background is adjusted to a background with a lower treatment response.

To illuminate the potential of this combinatorial therapy in human HCC patients in general, the combination of Sorafenib and Mapk14 inhibitors (using SB 202190 and BIRB 796) was tested in a cohort of different human HCC cell lines (PLC/PRF/5, Huh7 and Hep3B). Importantly a strong effect by this combinatorial therapy was identified in all tested cell lines. Interestingly, in these human cells no difference between SB 202190 and BIRB 796 was observed in improvement of Sorafenib treatment.

The results from human data strongly emphasize a clinical relevance of a combinatorial therapy of Sorafenib and Mapk14 inhibition although this combinatorial treatment may not work against every kind of HCC development. However, the so far used Mapk14 inhibitors (SB 202190 and BIRB 796) are not applicable for human patients and, as mentioned before, also several other available inhitors are limited due to unspecifity or toxic side effects.
Nevertheless, some Mapk14 inhibitors have the potential to be approved as therapeutic targets. As example, ARRY 797 is investigated in phase 3 of clinical trials. At the moment, no relevant side effects are described, although toxic effects in other tissues cannot be excluded. Additionally, this inhibitor shows a high specificity to Mapk14 (p38α) and could be therefore a promising target for a potential therapy in the clinic [164]. However, due to patent procedures, it could not be tested in this study. Another promising candidate is PH 797804

which is currently in Phase II of clinical trials in subjects with rheumatoid arthritis and obstructive pulmonary disease [165]. This inhibitor is shown to have only small side effects, and seems to have less liver toxicity than other Mapk14 inhibtors [149]. PH 797804 could be tested and showed a good response in combination with Sorafenib towards murine and human HCC cell lines. Also the Mapk14 inhibitor Skepinone-L might be a promising candidate. Skepinone-L is also highly specific to Mapk14 and showed only marginal side effects in different studies [148]. However, so far it is not yet tested in clinical trials. Interestingly, Skepinone-L could also be tested in human and murine HCC cell lines and it could be shown that it also cooperates with Sorafenib in reducing cell growth. Interestingly, it showed even a better performance that PH-797804 in human HCC cells.
Taken together these data indicate that a translation in to the clinic might be conceivable by using these newly developed Mapk14 inhibitors. Nevertheless, finally clinical studies have to show, wether such a translation is possible.

Independently of a possible success of this combinatorial therapy in clinical studies, it remains a strong need to further improve HCC treatment. Here shown data present a powerful platform to identify specific drug-sensitizing targets. Beyond this, the same model can be used in a parallel study to identify straight lethal targets in tumors, driven by Ras or other oncogenes.
By further development of mosaic cancer mouse models, a translation to other organs could also be imaginable in order to develop treatment options of other types of cancer.

6. References

Reference List

1. Forner A, Llovet JM, Bruix J: **Hepatocellular carcinoma**. *Lancet* 2012.

2. Yang JD, Roberts LR: **Hepatocellular carcinoma: A global view**. *Nat.Rev.Gastroenterol.Hepatol.* 2010, **7:**448-458.

3. El-Serag HB, Rudolph KL: **Hepatocellular carcinoma: epidemiology and molecular carcinogenesis**. *Gastroenterology* 2007, **132:**2557-2576.

4. Roskams T: **Liver stem cells and their implication in hepatocellular and cholangiocarcinoma**. *Oncogene* 2006, **25:**3818-3822.

5. Lee J., Heo J., Libbrecht L., Chu I., Kaposi-Novak P., Calvisi D.F., Mikaelyan A., Roberts L.R., Demetris A.J., Sun Z., Nevens F., Roskams T., Thorgeirsson S.S.: **A novel prognostic subtype of human hepatocellular carcinoma derived from hepatic progenitor cells**. *Nature medicine* 2006, **12**.

6. Farazi PA, DePinho RA: **Hepatocellular carcinoma pathogenesis: from genes to environment**. *Nat.Rev.Cancer* 2006, **6:**674-687.

7. Shariff MI, Cox IJ, Gomaa AI, Khan SA, Gedroyc W, Taylor-Robinson SD: **Hepatocellular carcinoma: current trends in worldwide epidemiology, risk factors, diagnosis and therapeutics**. *Expert.Rev.Gastroenterol.Hepatol.* 2009, **3:**353-367.

8. Fung J, Lai CL, Yuen MF: **Hepatitis B and C virus-related carcinogenesis**. *Clin.Microbiol.Infect.* 2009, **15:**964-970.

9. Ierardi E, Rosania R, Zotti M, Giorgio F, Prencipe S, Valle ND, Francesco VD, Panella C: **From chronic liver disorders to hepatocellular carcinoma: Molecular and genetic pathways**. *World J.Gastrointest.Oncol.* 2010, **2:**259-264.

10. Hashimoto E, Tokushige K: **Prevalence, gender, ethnic variations, and prognosis of NASH**. *J.Gastroenterol.* 2011, **46 Suppl 1:**63-69.

11. Starley BQ, Calcagno CJ, Harrison SA: **Nonalcoholic fatty liver disease and hepatocellular carcinoma: a weighty connection**. *Hepatology* 2010, **51:**1820-1832.

12. Llovet JM, Bruix J: **Molecular targeted therapies in hepatocellular carcinoma**. *Hepatology* 2008, **48:**1312-1327.

13. Ahearn IM, Haigis K, Bar-Sagi D, Philips MR: **Regulating the regulator: post-translational modification of RAS**. *Nat.Rev.Mol.Cell Biol.* 2012, **13:**39-51.

14. Karreth FA, Tuveson DA: **Modelling oncogenic Ras/Raf signalling in the mouse**. *Curr.Opin.Genet.Dev.* 2009, **19:**4-11.

15. Downward J: **Targeting RAS signalling pathways in cancer therapy**. *Nat.Rev.Cancer* 2003, **3:**11-22.

16. Calvisi DF, Ladu S, Conner EA, Seo D, Hsieh JT, Factor VM, Thorgeirsson SS: **Inactivation of Ras GTPase-activating proteins promotes unrestrained activity of wild-type Ras in human liver cancer**. *J.Hepatol.* 2011, **54:**311-319.

17. Guichard C, Amaddeo G, Imbeaud S, Ladeiro Y, Pelletier L, Maad IB, Calderaro J, Bioulac-Sage P, Letexier M, Degos F, Clement B, Balabaud C, Chevet E, Laurent A, Couchy G, Letouze E, Calvo F, Zucman-Rossi J: **Integrated analysis of somatic mutations and focal copy-number changes identifies key genes and pathways in hepatocellular carcinoma**. *Nat.Genet.* 2012, **44:**694-698.

18. Chen G, Hitomi M, Han J, Stacey DW: **The p38 pathway provides negative feedback for Ras proliferative signaling**. *J.Biol.Chem.* 2000, **275:**38973-38980.

19. McDermott EP, O'Neill LA: **Ras participates in the activation of p38 MAPK by interleukin-1 by associating with IRAK, IRAK2, TRAF6, and TAK-1**. *J.Biol.Chem.* 2002, **277:**7808-7815.

20. Wagner EF, Nebreda AR: **Signal integration by JNK and p38 MAPK pathways in cancer development**. *Nat.Rev.Cancer* 2009, **9:**537-549.

21. Nebreda AR, Porras A: **p38 MAP kinases: beyond the stress response**. *Trends Biochem.Sci.* 2000, **25:**257-260.

22. Recio JA, Merlino G: **Hepatocyte growth factor/scatter factor activates proliferation in melanoma cells through p38 MAPK, ATF-2 and cyclin D1**. *Oncogene* 2002, **21:**1000-1008.

23. Hui L, Bakiri L, Mairhorfer A, Schweifer N, Haslinger C, Kenner L, Komnenovic V, Scheuch H, Beug H, Wagner EF: **p38alpha suppresses normal and cancer cell proliferation by antagonizing the JNK-c-Jun pathway**. *Nat.Genet.* 2007, **39:**741-749.

24. Okamoto K, Neureiter D, Ocker M: **Biomarkers for novel targeted therapies of hepatocellular carcinoma**. *Histol.Histopathol.* 2009, **24:**493-502.

25. El-Assal ON, Yamanoi A, Soda Y, Yamaguchi M, Igarashi M, Yamamoto A, Nabika T, Nagasue N: **Clinical significance of microvessel density and vascular endothelial growth factor expression in hepatocellular carcinoma and surrounding liver: possible involvement of vascular endothelial growth factor in the angiogenesis of cirrhotic liver**. *Hepatology* 1998, **27:**1554-1562.

26. Li XM, Tang ZY, Qin LX, Zhou J, Sun HC: **Serum vascular endothelial growth factor is a predictor of invasion and metastasis in hepatocellular carcinoma**. *J.Exp.Clin.Cancer Res.* 1999, **18:**511-517.

27. Lee JW, Soung YH, Kim SY, Lee HW, Park WS, Nam SW, Kim SH, Lee JY, Yoo NJ, Lee SH: **PIK3CA gene is frequently mutated in breast carcinomas and hepatocellular carcinomas**. *Oncogene* 2005, **24:**1477-1480.

28. Wong KK, Engelman JA, Cantley LC: **Targeting the PI3K signaling pathway in cancer**. *Curr.Opin.Genet.Dev.* 2010, **20:**87-90.

29. Liu P, Cheng H, Roberts TM, Zhao JJ: **Targeting the phosphoinositide 3-kinase pathway in cancer**. *Nat.Rev.Drug Discov.* 2009, **8:**627-644.

30. Schagdarsurengin U, Wilkens L, Steinemann D, Flemming P, Kreipe HH, Pfeifer GP, Schlegelberger B, Dammann R: **Frequent epigenetic inactivation of the RASSF1A gene in hepatocellular carcinoma**. *Oncogene* 2003, **22:**1866-1871.

31. Fujiwara Y, Hoon DS, Yamada T, Umeshita K, Gotoh M, Sakon M, Nishisho I, Monden M: **PTEN / MMAC1 mutation and frequent loss of heterozygosity identified in chromosome 10q in a subset of hepatocellular carcinomas**. *Jpn.J.Cancer Res.* 2000, **91:**287-292.

32. Sears R, Nuckolls F, Haura E, Taya Y, Tamai K, Nevins JR: **Multiple Ras-dependent phosphorylation pathways regulate Myc protein stability**. *Genes Dev.* 2000, **14:**2501-2514.

33. Bachireddy P, Bendapudi PK, Felsher DW: **Getting at MYC through RAS**. *Clin.Cancer Res.* 2005, **11:**4278-4281.

34. Adhikary S, Eilers M: **Transcriptional regulation and transformation by Myc proteins**. *Nat.Rev.Mol.Cell Biol.* 2005, **6:**635-645.

35. Fernandez PC, Frank SR, Wang L, Schroeder M, Liu S, Greene J, Cocito A, Amati B: **Genomic targets of the human c-Myc protein**. *Genes Dev.* 2003, **17:**1115-1129.

36. Nevins JR: **The Rb/E2F pathway and cancer**. *Hum.Mol.Genet.* 2001, **10:**699-703.

37. MacLeod K: **pRb and E2f-1 in mouse development and tumorigenesis**. *Curr.Opin.Genet.Dev.* 1999, **9:**31-39.

38. Sherr CJ, McCormick F: **The RB and p53 pathways in cancer**. *Cancer Cell* 2002, **2:**103-112.

39. Ortega S, Malumbres M, Barbacid M: **Cyclin D-dependent kinases, INK4 inhibitors and cancer**. *Biochim.Biophys.Acta* 2002, **1602:**73-87.

40. Sherr CJ: **Divorcing ARF and p53: an unsettled case**. *Nat.Rev.Cancer* 2006, **6:**663-673.

41. Sherr CJ: **The INK4a/ARF network in tumour suppression**. *Nat.Rev.Mol.Cell Biol.* 2001, **2:**731-737.

42. Campisi J, d'Adda di FF: **Cellular senescence: when bad things happen to good cells**. *Nat.Rev.Mol.Cell Biol.* 2007, **8:**729-740.

43. Hollstein M, Rice K, Greenblatt MS, Soussi T, Fuchs R, Sorlie T, Hovig E, Smith-Sorensen B, Montesano R, Harris CC: **Database of p53 gene somatic mutations in human tumors and cell lines**. *Nucleic Acids Res.* 1994, **22:**3551-3555.

44. Thorgeirsson SS, Grisham JW: **Molecular pathogenesis of human hepatocellular carcinoma**. *Nat.Genet.* 2002, **31:**339-346.

45. Bruix J, Boix L, Sala M, Llovet JM: **Focus on hepatocellular carcinoma**. *Cancer Cell* 2004, **5:**215-219.

46. Tannapfel A, Busse C, Weinans L, Benicke M, Katalinic A, Geissler F, Hauss J, Wittekind C: **INK4a-ARF alterations and p53 mutations in hepatocellular carcinomas**. *Oncogene* 2001, **20:**7104-7109.

47. Edamoto Y, Hara A, Biernat W, Terracciano L, Cathomas G, Riehle HM, Matsuda M, Fujii H, Scoazec JY, Ohgaki H: **Alterations of RB1, p53 and Wnt pathways in hepatocellular carcinomas associated with hepatitis C, hepatitis B and alcoholic liver cirrhosis**. *Int.J.Cancer* 2003, **106:**334-341.

48. Nejak-Bowen KN, Monga SP: **Beta-catenin signaling, liver regeneration and hepatocellular cancer: sorting the good from the bad**. *Semin.Cancer Biol.* 2011, **21:**44-58.

49. Huang H, Fujii H, Sankila A, Mahler-Araujo BM, Matsuda M, Cathomas G, Ohgaki H: **Beta-catenin mutations are frequent in human hepatocellular carcinomas associated with hepatitis C virus infection**. *Am.J.Pathol.* 1999, **155:**1795-1801.

50. Cha MY, Kim CM, Park YM, Ryu WS: **Hepatitis B virus X protein is essential for the activation of Wnt/beta-catenin signaling in hepatoma cells**. *Hepatology* 2004, **39:**1683-1693.

51. Peng SY, Chen WJ, Lai PL, Jeng YM, Sheu JC, Hsu HC: **High alpha-fetoprotein level correlates with high stage, early recurrence and poor prognosis of hepatocellular carcinoma: significance of hepatitis virus infection, age, p53 and beta-catenin mutations**. *Int.J.Cancer* 2004, **112:**44-50.

52. An FQ, Matsuda M, Fujii H, Tang RF, Amemiya H, Dai YM, Matsumoto Y: **Tumor heterogeneity in small hepatocellular carcinoma: analysis of tumor cell proliferation, expression and mutation of p53 AND beta-catenin**. *Int.J.Cancer* 2001, **93:**468-474.

53. Park JY, Park WS, Nam SW, Kim SY, Lee SH, Yoo NJ, Lee JY, Park CK: **Mutations of beta-catenin and AXIN I genes are a late event in human hepatocellular carcinogenesis**. *Liver Int.* 2005, **25:**70-76.

54. Yang B, Guo M, Herman JG, Clark DP: **Aberrant promoter methylation profiles of tumor suppressor genes in hepatocellular carcinoma**. *Am.J.Pathol.* 2003, **163:**1101-1107.

55. Cabibbo G, Latteri F, Antonucci M, Craxi A: **Multimodal approaches to the treatment of hepatocellular carcinoma**. *Nat.Clin.Pract.Gastroenterol.Hepatol.* 2009, **6:**159-169.

56. Llovet JM, Burroughs A, Bruix J: **Hepatocellular carcinoma**. *Lancet* 2003, **362:**1907-1917.

57. Llovet JM, Bru C, Bruix J: **Prognosis of hepatocellular carcinoma: the BCLC staging classification**. *Semin.Liver Dis.* 1999, **19:**329-338.

58. Llovet JM, Bruix J: **Systematic review of randomized trials for unresectable hepatocellular carcinoma: Chemoembolization improves survival**. *Hepatology* 2003, **37:**429-442.

59. Llovet JM, Bruix J: **Novel advancements in the management of hepatocellular carcinoma in 2008**. *J.Hepatol.* 2008, **48 Suppl 1:**S20-S37.

60. Giuliani F, Colucci G: **Treatment of hepatocellular carcinoma**. *Oncology* 2009, **77 Suppl 1:**43-49.

61. Clavien PA, Lesurtel M, Bossuyt PM, Gores GJ, Langer B, Perrier A: **Recommendations for liver transplantation for hepatocellular carcinoma: an international consensus conference report**. *Lancet Oncol.* 2012, **13:**e11-e22.

62. Lencioni R: **Loco-regional treatment of hepatocellular carcinoma**. *Hepatology* 2010, **52:**762-773.

63. Koda M, Murawaki Y, Mitsuda A, Ohyama K, Horie Y, Suou T, Kawasaki H, Ikawa S: **Predictive factors for intrahepatic recurrence after percutaneous ethanol injection therapy for small hepatocellular carcinoma**. *Cancer* 2000, **88:**529-537.

64. Lencioni RA, Allgaier HP, Cioni D, Olschewski M, Deibert P, Crocetti L, Frings H, Laubenberger J, Zuber I, Blum HE, Bartolozzi C: **Small hepatocellular carcinoma in cirrhosis: randomized comparison of radio-frequency thermal ablation versus percutaneous ethanol injection**. *Radiology* 2003, **228:**235-240.

65. Bouza C, Lopez-Cuadrado T, Alcazar R, Saz-Parkinson Z, Amate JM: **Meta-analysis of percutaneous radiofrequency ablation versus ethanol injection in hepatocellular carcinoma**. *BMC.Gastroenterol.* 2009, **9:**31.

66. Popperl G, Helmberger T, Munzing W, Schmid R, Jacobs TF, Tatsch K: **Selective internal radiation therapy with SIR-Spheres in patients with nonresectable liver tumors**. *Cancer Biother.Radiopharm.* 2005, **20:**200-208.

67. Khodjibekova M, Szyszko T, Singh A, Tait P, Rubello D, AL-Nahhas A: **Treatment of primary and secondary liver tumours with selective internal radiation therapy**. *J.Exp.Clin.Cancer Res.* 2007, **26:**561-570.

68. Yau T, Chan P, Epstein R, Poon RT: **Evolution of systemic therapy of advanced hepatocellular carcinoma**. *World J.Gastroenterol.* 2008, **14:**6437-6441.

69. Yeo W, Mok TS, Zee B, Leung TW, Lai PB, Lau WY, Koh J, Mo FK, Yu SC, Chan AT, Hui P, Ma B, Lam KC, Ho WM, Wong HT, Tang A, Johnson PJ: **A randomized phase III study of doxorubicin versus cisplatin/interferon alpha-2b/doxorubicin/fluorouracil (PIAF) combination chemotherapy for unresectable hepatocellular carcinoma**. *J.Natl.Cancer Inst.* 2005, **97:**1532-1538.

70. Taieb J, Bonyhay L, Golli L, Ducreux M, Boleslawski E, Tigaud JM, de BT, Mansourbakht T, Delgado MA, Hannoun L, Poynard T, Boige V: **Gemcitabine plus oxaliplatin for patients with advanced hepatocellular carcinoma using two different schedules**. *Cancer* 2003, **98:**2664-2670.

71. Watanuki A, Ohwada S, Fukusato T, Makita F, Yamada T, Kikuchi A, Morishita Y: **Prognostic significance of DNA topoisomerase IIalpha expression in human hepatocellular carcinoma.** *Anticancer Res.* 2002, **22:**1113-1119.

72. Jiang W, Lu Z, He Y, Diasio RB: **Dihydropyrimidine dehydrogenase activity in hepatocellular carcinoma: implication in 5-fluorouracil-based chemotherapy**. *Clin.Cancer Res.* 1997, **3:**395-399.

73. Soini Y, Virkajarvi N, Raunio H, Paakko P: **Expression of P-glycoprotein in hepatocellular carcinoma: a potential marker of prognosis**. *J.Clin.Pathol.* 1996, **49:**470-473.

74. Lord R, Suddle A, Ross PJ: **Emerging strategies in the treatment of advanced hepatocellular carcinoma: the role of targeted therapies**. *Int.J.Clin.Pract.* 2011, **65:**182-188.

75. Ma WW, Adjei AA: **Novel agents on the horizon for cancer therapy**. *CA Cancer J.Clin.* 2009, **59:**111-137.

76. Wilhelm S, Carter C, Lynch M, Lowinger T, Dumas J, Smith RA, Schwartz B, Simantov R, Kelley S: **Discovery and development of sorafenib: a multikinase inhibitor for treating cancer**. *Nat.Rev.Drug Discov.* 2006, **5:**835-844.

77. Liu L, Cao Y, Chen C, Zhang X, McNabola A, Wilkie D, Wilhelm S, Lynch M, Carter C: **Sorafenib blocks the RAF/MEK/ERK pathway, inhibits tumor angiogenesis, and induces tumor cell apoptosis in hepatocellular carcinoma model PLC/PRF/5**. *Cancer Res.* 2006, **66:**11851-11858.

78. Wilhelm SM, Carter C, Tang L, Wilkie D, McNabola A, Rong H, Chen C, Zhang X, Vincent P, McHugh M, Cao Y, Shujath J, Gawlak S, Eveleigh D, Rowley B, Liu L, Adnane L, Lynch M, Auclair D, Taylor I, Gedrich R, Voznesensky A, Riedl B, Post LE, Bollag G, Trail PA: **BAY 43-9006 exhibits broad spectrum oral antitumor activity and targets the RAF/MEK/ERK pathway and receptor tyrosine kinases involved in tumor progression and angiogenesis**. *Cancer Res.* 2004, **64:**7099-7109.

79. Murphy DA, Makonnen S, Lassoued W, Feldman MD, Carter C, Lee WM: **Inhibition of tumor endothelial ERK activation, angiogenesis, and tumor growth by sorafenib (BAY43-9006)**. *Am.J.Pathol.* 2006, **169:**1875-1885.

80. Llovet JM, Ricci S, Mazzaferro V, Hilgard P, Gane E, Blanc JF, de Oliveira AC, Santoro A, Raoul JL, Forner A, Schwartz M, Porta C, Zeuzem S, Bolondi L, Greten TF, Galle PR, Seitz JF, Borbath I, Haussinger D, Giannaris T, Shan M, Moscovici M, Voliotis D, Bruix J: **Sorafenib in advanced hepatocellular carcinoma**. *N.Engl.J.Med.* 2008, **359:**378-390.

81. Cheng AL, Kang YK, Chen Z, Tsao CJ, Qin S, Kim JS, Luo R, Feng J, Ye S, Yang TS, Xu J, Sun Y, Liang H, Liu J, Wang J, Tak WY, Pan H, Burock K, Zou J, Voliotis D, Guan Z: **Efficacy and safety of sorafenib in patients in the Asia-Pacific region with advanced hepatocellular carcinoma: a phase III randomised, double-blind, placebo-controlled trial**. *Lancet Oncol.* 2009, **10:**25-34.

82. Tanaka S, Arii S: **Molecularly targeted therapy for hepatocellular carcinoma**. *Cancer Sci.* 2009, **100:**1-8.

83. Faivre S, Bouattour M, Raymond E: **Novel molecular therapies in hepatocellular carcinoma**. *Liver Int.* 2011, **31 Suppl 1:**151-160.

84. Semela D, Piguet AC, Kolev M, Schmitter K, Hlushchuk R, Djonov V, Stoupis C, Dufour JF: **Vascular remodeling and antitumoral effects of mTOR inhibition in a rat model of hepatocellular carcinoma**. *J.Hepatol.* 2007, **46:**840-848.

85. Huynh H, Chow KH, Soo KC, Toh HC, Choo SP, Foo KF, Poon D, Ngo VC, Tran E: **RAD001 (everolimus) inhibits tumour growth in xenograft models of human hepatocellular carcinoma**. *J.Cell Mol.Med.* 2009, **13:**1371-1380.

86. Rizell M, Andersson M, Cahlin C, Hafstrom L, Olausson M, Lindner P: **Effects of the mTOR inhibitor sirolimus in patients with hepatocellular and cholangiocellular cancer**. *Int.J.Clin.Oncol.* 2008, **13:**66-70.

87. Faivre S, Demetri G, Sargent W, Raymond E: **Molecular basis for sunitinib efficacy and future clinical development**. *Nat.Rev.Drug Discov.* 2007, **6:**734-745.

88. Huynh H, Ngo VC, Choo SP, Poon D, Koong HN, Thng CH, Toh HC, Zheng L, Ong LC, Jin Y, Song IC, Chang AP, Ong HS, Chung AY, Chow PK, Soo KC: **Sunitinib (SUTENT, SU11248) suppresses tumor growth and induces apoptosis in xenograft models of human hepatocellular carcinoma**. *Curr.Cancer Drug Targets.* 2009, **9:**738-747.

89. Finn RS, Bentley G, Britten CD, Amado R, Busuttil RW: **Targeting vascular endothelial growth factor with the monoclonal antibody bevacizumab inhibits human hepatocellular carcinoma cells growing in an orthotopic mouse model**. *Liver Int.* 2009, **29:**284-290.

90. Siegel AB, Cohen EI, Ocean A, Lehrer D, Goldenberg A, Knox JJ, Chen H, Clark-Garvey S, Weinberg A, Mandeli J, Christos P, Mazumdar M, Popa E, Brown RS, Jr., Rafii S, Schwartz JD: **Phase II trial evaluating the clinical and biologic effects of bevacizumab in unresectable hepatocellular carcinoma**. *J.Clin.Oncol.* 2008, **26:**2992-2998.

91. Philip PA, Mahoney MR, Allmer C, Thomas J, Pitot HC, Kim G, Donehower RC, Fitch T, Picus J, Erlichman C: **Phase II study of Erlotinib (OSI-774) in patients with advanced hepatocellular cancer**. *J.Clin.Oncol.* 2005, **23:**6657-6663.

92. Thomas MB, Chadha R, Glover K, Wang X, Morris J, Brown T, Rashid A, Dancey J, Abbruzzese JL: **Phase 2 study of erlotinib in patients with unresectable hepatocellular carcinoma**. *Cancer* 2007, **110:**1059-1067.

93. Huynh H, Ngo VC, Koong HN, Poon D, Choo SP, Toh HC, Thng CH, Chow P, Ong HS, Chung A, Goh BC, Smith PD, Soo KC: **AZD6244 enhances the anti-tumor activity of sorafenib in ectopic and orthotopic models of human hepatocellular carcinoma (HCC)**. *J.Hepatol.* 2010, **52:**79-87.

94. Olive KP, Jacobetz MA, Davidson CJ, Gopinathan A, McIntyre D, Honess D, Madhu B, Goldgraben MA, Caldwell ME, Allard D, Frese KK, Denicola G, Feig C, Combs C, Winter SP, Ireland-Zecchini H, Reichelt S, Howat WJ, Chang A, Dhara M, Wang L, Ruckert F, Grutzmann R, Pilarsky C, Izeradjene K, Hingorani SR, Huang P, Davies SE, Plunkett W, Egorin M, Hruban RH, Whitebread N, McGovern K, Adams J, Iacobuzio-Donahue C, Griffiths J, Tuveson DA: **Inhibition of Hedgehog signaling enhances delivery of chemotherapy in a mouse model of pancreatic cancer**. *Science* 2009, **324:**1457-1461.

95. Kerbel RS: **Human tumor xenografts as predictive preclinical models for anticancer drug activity in humans: better than commonly perceived-but they can be improved**. *Cancer Biol.Ther.* 2003, **2:**S134-S139.

96. Sharpless NE, DePinho RA: **The mighty mouse: genetically engineered mouse models in cancer drug development**. *Nat.Rev.Drug Discov.* 2006, **5:**741-754.

97. Kile BT, Hilton DJ: **The art and design of genetic screens: mouse**. *Nat.Rev.Genet.* 2005, **6:**557-567.

98. Verna L, Whysner J, Williams GM: **2-Acetylaminofluorene mechanistic data and risk assessment: DNA reactivity, enhanced cell proliferation and tumor initiation**. *Pharmacol.Ther.* 1996, **71:**83-105.

99. Verna L, Whysner J, Williams GM: **N-nitrosodiethylamine mechanistic data and risk assessment: bioactivation, DNA-adduct formation, mutagenicity, and tumor initiation**. *Pharmacol.Ther.* 1996, **71:**57-81.

100. Frese KK, Tuveson DA: **Maximizing mouse cancer models**. *Nat.Rev.Cancer* 2007, **7:**645-658.

101. Sandgren EP, Quaife CJ, Pinkert CA, Palmiter RD, Brinster RL: **Oncogene-induced liver neoplasia in transgenic mice**. *Oncogene* 1989, **4:**715-724.

102. Deane NG, Parker MA, Aramandla R, Diehl L, Lee WJ, Washington MK, Nanney LB, Shyr Y, Beauchamp RD: **Hepatocellular carcinoma results from chronic cyclin D1 overexpression in transgenic mice**. *Cancer Res.* 2001, **61:**5389-5395.

103. Kellendonk C, Opherk C, Anlag K, Schutz G, Tronche F: **Hepatocyte-specific expression of Cre recombinase**. *Genesis.* 2000, **26:**151-153.

104. Tan X, Behari J, Cieply B, Michalopoulos GK, Monga SP: **Conditional deletion of beta-catenin reveals its role in liver growth and regeneration**. *Gastroenterology* 2006, **131:**1561-1572.

105. Manickan E, Satoi J, Wang TC, Liang TJ: **Conditional liver-specific expression of simian virus 40 T antigen leads to regulatable development of hepatic neoplasm in transgenic mice**. *J.Biol.Chem.* 2001, **276:**13989-13994.

106. Heyer J, Kwong LN, Lowe SW, Chin L: **Non-germline genetically engineered mouse models for translational cancer research**. *Nat.Rev.Cancer* 2010, **10:**470-480.

107. Zender L, Spector MS, Xue W, Flemming P, Cordon-Cardo C, Silke J, Fan ST, Luk JM, Wigler M, Hannon GJ, Mu D, Lucito R, Powers S, Lowe SW: **Identification and validation of oncogenes in liver cancer using an integrative oncogenomic approach**. *Cell* 2006, **125:**1253-1267.

108. Zender L, Xue W, Zuber J, Semighini CP, Krasnitz A, Ma B, Zender P, Kubicka S, Luk JM, Schirmacher P, McCombie WR, Wigler M, Hicks J, Hannon GJ, Powers S, Lowe SW: **An oncogenomics-based in vivo RNAi screen identifies tumor suppressors in liver cancer**. *Cell* 2008, **135:**852-864.

109. Hickman MA, Malone RW, Lehmann-Bruinsma K, Sih TR, Knoell D, Szoka FC, Walzem R, Carlson DM, Powell JS: **Gene expression following direct injection of DNA into liver**. *Hum.Gene Ther.* 1994, **5:**1477-1483.

110. Sebestyen MG, Budker VG, Budker T, Subbotin VM, Zhang G, Monahan SD, Lewis DL, Wong SC, Hagstrom JE, Wolff JA: **Mechanism of plasmid delivery by hydrodynamic tail vein injection. I. Hepatocyte uptake of various molecules**. *J.Gene Med.* 2006, **8:**852-873.

111. Yant SR, Meuse L, Chiu W, Ivics Z, Izsvak Z, Kay MA: **Somatic integration and long-term transgene expression in normal and haemophilic mice using a DNA transposon system**. *Nat.Genet.* 2000, **25:**35-41.

112. Bell JB, Podetz-Pedersen KM, Aronovich EL, Belur LR, McIvor RS, Hackett PB: **Preferential delivery of the Sleeping Beauty transposon system to livers of mice by hydrodynamic injection**. *Nat.Protoc.* 2007, **2:**3153-3165.

113. Carlson CM, Frandsen JL, Kirchhof N, McIvor RS, Largaespada DA: **Somatic integration of an oncogene-harboring Sleeping Beauty transposon models liver tumor development in the mouse**. *Proc.Natl.Acad.Sci.U.S.A* 2005, **102:**17059-17064.

114. Tward AD, Jones KD, Yant S, Kay MA, Wang R, Bishop JM: **Genomic progression in mouse models for liver tumors**. *Cold Spring Harb.Symp.Quant.Biol.* 2005, **70:**217-224.

115. Kang TW, Yevsa T, Woller N, Hoenicke L, Wuestefeld T, Dauch D, Hohmeyer A, Gereke M, Rudalska R, Potapova A, Iken M, Vucur M, Weiss S, Heikenwalder M, Khan S, Gil J, Bruder D, Manns M, Schirmacher P, Tacke F, Ott M, Luedde T, Longerich T, Kubicka S, Zender L: **Senescence surveillance of pre-malignant hepatocytes limits liver cancer development**. *Nature* 2011.

116. Meister G, Tuschl T: **Mechanisms of gene silencing by double-stranded RNA**. *Nature* 2004, **431:**343-349.

117. Chapman EJ, Carrington JC: **Specialization and evolution of endogenous small RNA pathways**. *Nat.Rev.Genet.* 2007, **8:**884-896.

118. Dickins RA, Hemann MT, Zilfou JT, Simpson DR, Ibarra I, Hannon GJ, Lowe SW: **Probing tumor phenotypes using stable and regulated synthetic microRNA precursors**. *Nat.Genet.* 2005, **37:**1289-1295.

119. Olson A, Sheth N, Lee JS, Hannon G, Sachidanandam R: **RNAi Codex: a portal/database for short-hairpin RNA (shRNA) gene-silencing constructs**. *Nucleic Acids Res.* 2006, **34:**D153-D157.

120. Seyhan AA, Rya TE: **RNAi screening for the discovery of novel modulators of human disease**. *Curr.Pharm.Biotechnol.* 2010, **11:**735-756.

121. Westbrook TF, Stegmeier F, Elledge SJ: **Dissecting cancer pathways and vulnerabilities with RNAi**. *Cold Spring Harb.Symp.Quant.Biol.* 2005, **70:**435-444.

122. Liu L, Ulbrich J, Muller J, Wustefeld T, Aeberhard L, Kress TR, Muthalagu N, Rycak L, Rudalska R, Moll R, Kempa S, Zender L, Eilers M, Murphy DJ: **Deregulated MYC expression induces dependence upon AMPK-related kinase 5**. *Nature* 2012, **483:**608-612.

123. Luo B, Cheung HW, Subramanian A, Sharifnia T, Okamoto M, Yang X, Hinkle G, Boehm JS, Beroukhim R, Weir BA, Mermel C, Barbie DA, Awad T, Zhou X, Nguyen T, Piqani B, Li C, Golub TR, Meyerson M, Hacohen N, Hahn WC, Lander ES, Sabatini DM, Root DE: **Highly parallel identification of essential genes in cancer cells**. *Proc.Natl.Acad.Sci.U.S.A* 2008, **105:**20380-20385.

124. Turner NC, Lord CJ, Iorns E, Brough R, Swift S, Elliott R, Rayter S, Tutt AN, Ashworth A: **A synthetic lethal siRNA screen identifying genes mediating sensitivity to a PARP inhibitor**. *EMBO J.* 2008, **27:**1368-1377.

125. Swanton C, Marani M, Pardo O, Warne PH, Kelly G, Sahai E, Elustondo F, Chang J, Temple J, Ahmed AA, Brenton JD, Downward J, Nicke B: **Regulators of mitotic arrest and ceramide metabolism are determinants of sensitivity to paclitaxel and other chemotherapeutic drugs**. *Cancer Cell* 2007, **11:**498-512.

126. Giroux V, Iovanna J, Dagorn JC: **Probing the human kinome for kinases involved in pancreatic cancer cell survival and gemcitabine resistance**. *FASEB J.* 2006, **20:**1982-1991.

127. Burgess DJ, Doles J, Zender L, Xue W, Ma B, McCombie WR, Hannon GJ, Lowe SW, Hemann MT: **Topoisomerase levels determine chemotherapy response in vitro and in vivo**. *Proc.Natl.Acad.Sci.U.S.A* 2008, **105:**9053-9058.

128. Bric A, Miething C, Bialucha CU, Scuoppo C, Zender L, Krasnitz A, Xuan Z, Zuber J, Wigler M, Hicks J, McCombie RW, Hemann MT, Hannon GJ, Powers S, Lowe SW: **Functional identification of tumor-suppressor genes through an in vivo RNA interference screen in a mouse lymphoma model**. *Cancer Cell* 2009, **16:**324-335.

129. Meacham CE, Ho EE, Dubrovsky E, Gertler FB, Hemann MT: **In vivo RNAi screening identifies regulators of actin dynamics as key determinants of lymphoma progression**. *Nat.Genet.* 2009, **41:**1133-1137.

130. Kamijo T, Zindy F, Roussel MF, Quelle DE, Downing JR, Ashmun RA, Grosveld G, Sherr CJ: **Tumor suppression at the mouse INK4a locus mediated by the alternative reading frame product p19ARF**. *Cell* 1997, **91:**649-659.

131. McCurrach ME, Lowe SW: **Methods for studying pro- and antiapoptotic genes in nonimmortal cells**. *Methods Cell Biol.* 2001, **66:**197-227.

132. Vert JP, Foveau N, Lajaunie C, Vandenbrouck Y: **An accurate and interpretable model for siRNA efficacy prediction**. *BMC.Bioinformatics.* 2006, **7:**520.

133. Huesken D, Lange J, Mickanin C, Weiler J, Asselbergs F, Warner J, Meloon B, Engel S, Rosenberg A, Cohen D, Labow M, Reinhardt M, Natt F, Hall J: **Design of a genome-wide siRNA library using an artificial neural network**. *Nat.Biotechnol.* 2005, **23:**995-1001.

134. Zuber J, McJunkin K, Fellmann C, Dow LE, Taylor MJ, Hannon GJ, Lowe SW: **Toolkit for evaluating genes required for proliferation and survival using tetracycline-regulated RNAi**. *Nat.Biotechnol.* 2011, **29:**79-83.

135. Zhang J, Shen B, Lin A: **Novel strategies for inhibition of the p38 MAPK pathway**. *Trends Pharmacol.Sci.* 2007, **28:**286-295.

136. Goldstein DM, Kuglstatter A, Lou Y, Soth MJ: **Selective p38alpha inhibitors clinically evaluated for the treatment of chronic inflammatory disorders**. *J.Med.Chem.* 2010, **53:**2345-2353.

137. Dow LE, Premsrirut PK, Zuber J, Fellmann C, McJunkin K, Miething C, Park Y, Dickins RA, Hannon GJ, Lowe SW: **A pipeline for the generation of shRNA transgenic mice**. *Nat.Protoc.* 2012, **7:**374-393.

138. Agha-Mohammadi S, O'Malley M, Etemad A, Wang Z, Xiao X, Lotze MT: **Second-generation tetracycline-regulatable promoter: repositioned tet operator elements optimize transactivator synergy while shorter minimal promoter offers tight basal leakiness**. *J.Gene Med.* 2004, **6:**817-828.

139. Dominguez C, Powers DA, Tamayo N: **p38 MAP kinase inhibitors: many are made, but few are chosen**. *Curr.Opin.Drug Discov.Devel.* 2005, **8:**421-430.

140. Fabian MA, Biggs WH, III, Treiber DK, Atteridge CE, Azimioara MD, Benedetti MG, Carter TA, Ciceri P, Edeen PT, Floyd M, Ford JM, Galvin M, Gerlach JL, Grotzfeld RM, Herrgard S, Insko DE, Insko MA, Lai AG, Lelias JM, Mehta SA, Milanov ZV, Velasco AM, Wodicka LM, Patel HK, Zarrinkar PP, Lockhart DJ: **A small molecule-kinase interaction map for clinical kinase inhibitors**. *Nat.Biotechnol.* 2005, **23:**329-336.

141. Yang Z, Yi J, Li X, Long W: **Correlation between loss of PTEN expression and PKB/AKT phosphorylation in hepatocellular carcinoma**. *J.Huazhong.Univ Sci.Technolog.Med.Sci.* 2005, **25:**45-47.

142. Ono H, Shimano H, Katagiri H, Yahagi N, Sakoda H, Onishi Y, Anai M, Ogihara T, Fujishiro M, Viana AY, Fukushima Y, Abe M, Shojima N, Kikuchi M, Yamada N, Oka Y, Asano T: **Hepatic Akt activation induces marked hypoglycemia, hepatomegaly, and hypertriglyceridemia with sterol regulatory element binding protein involvement**. *Diabetes* 2003, **52:**2905-2913.

143. Heldin CH, Westermark B: **Mechanism of action and in vivo role of platelet-derived growth factor**. *Physiol Rev.* 1999, **79:**1283-1316.

144. Lopez-Bergami P, Lau E, Ronai Z: **Emerging roles of ATF2 and the dynamic AP1 network in cancer**. *Nat.Rev.Cancer* 2010, **10:**65-76.

145. Cuadrado A, Nebreda AR: **Mechanisms and functions of p38 MAPK signalling**. *Biochem.J.* 2010, **429:**403-417.

146. Vlahopoulos SA, Logotheti S, Mikas D, Giarika A, Gorgoulis V, Zoumpourlis V: **The role of ATF-2 in oncogenesis**. *Bioessays* 2008, **30:**314-327.

147. Yam CH, Fung TK, Poon RY: **Cyclin A in cell cycle control and cancer**. *Cell Mol.Life Sci.* 2002, **59:**1317-1326.

148. Koeberle SC, Romir J, Fischer S, Koeberle A, Schattel V, Albrecht W, Grutter C, Werz O, Rauh D, Stehle T, Laufer SA: **Skepinone-L is a selective p38 mitogen-activated protein kinase inhibitor**. *Nat.Chem.Biol.* 2012, **8:**141-143.

149. Macnee W, Allan RJ, Jones I, De Salvo MC, Tan LF: **Efficacy and safety of the oral p38 inhibitor PH-797804 in chronic obstructive pulmonary disease: a randomised clinical trial**. *Thorax* 2013.

150. Takimoto CH, Awada A: **Safety and anti-tumor activity of sorafenib (Nexavar) in combination with other anti-cancer agents: a review of clinical trials**. *Cancer Chemother.Pharmacol.* 2008, **61:**535-548.

151. Kummar S, Chen HX, Wright J, Holbeck S, Millin MD, Tomaszewski J, Zweibel J, Collins J, Doroshow JH: **Utilizing targeted cancer therapeutic agents in combination: novel approaches and urgent requirements**. *Nat.Rev.Drug Discov.* 2010, **9:**843-856.

152. Calvisi DF, Ladu S, Gorden A, Farina M, Conner EA, Lee JS, Factor VM, Thorgeirsson SS: **Ubiquitous activation of Ras and Jak/Stat pathways in human HCC**. *Gastroenterology* 2006, **130:**1117-1128.

153. Sherr CJ: **Tumor surveillance via the ARF-p53 pathway**. *Genes Dev.* 1998, **12:**2984-2991.

154. Wuestefeld T, Pesic M, Rudalska R, Dauch D, Longerich T, Kang TW, Yevsa T, Heinzmann F, Hoenicke L, Hohmeyer A, Potapova A, Rittelmeier I, Jarek M, Geffers R, Scharfe M, Klawonn F, Schirmacher P, Malek NP, Ott M, Nordheim A, Vogel A, Manns MP, Zender L: **A Direct In Vivo RNAi Screen Identifies MKK4 as a Key Regulator of Liver Regeneration**. *Cell* 2013, **153:**389-401.

155. Cuadrado A, Nebreda AR: **Mechanisms and functions of p38 MAPK signalling**. *Biochem.J.* 2010, **429:**403-417.

156. Reddy KB, Nabha SM, Atanaskova N: **Role of MAP kinase in tumor progression and invasion**. *Cancer Metastasis Rev.* 2003, **22:**395-403.

157. Shin I, Kim S, Song H, Kim HR, Moon A: **H-Ras-specific activation of Rac-MKK3/6-p38 pathway: its critical role in invasion and migration of breast epithelial cells**. *J.Biol.Chem.* 2005, **280:**14675-14683.

158. Ortega S, Malumbres M, Barbacid M: **Cyclin D-dependent kinases, INK4 inhibitors and cancer**. *Biochim.Biophys.Acta* 2002, **1602:**73-87.

159. Pecot CV, Calin GA, Coleman RL, Lopez-Berestein G, Sood AK: **RNA interference in the clinic: challenges and future directions**. *Nat.Rev.Cancer* 2011, **11:**59-67.

160. Yong HY, Koh MS, Moon A: **The p38 MAPK inhibitors for the treatment of inflammatory diseases and cancer**. *Expert.Opin.Investig.Drugs* 2009, **18:**1893-1905.

161. Bain J, Plater L, Elliott M, Shpiro N, Hastie CJ, McLauchlan H, Klevernic I, Arthur JS, Alessi DR, Cohen P: **The selectivity of protein kinase inhibitors: a further update**. *Biochem.J.* 2007, **408:**297-315.

162. Lee MR, Dominguez C: **MAP kinase p38 inhibitors: clinical results and an intimate look at their interactions with p38alpha protein**. *Curr.Med.Chem.* 2005, **12:**2979-2994.

163. Mantovani A, Allavena P, Sica A, Balkwill F: **Cancer-related inflammation**. *Nature* 2008, **454:**436-444.

164. Winski SL, Anderson D, Litwiler KS, Munson M, Lee PA, Winkler JD. **Effects of ARRY-797, a potent small molecule p38 MAPK inhibitor, on** *in vivo* **xeno - graft tumor growth, alone and in combination with cytotoxic agents.** 201.
Ref Type: Online Source

165. http://clinicaltrials.gov . 2013.
Ref Type: Electronic Citation

7. Acknowledgements

The work presented here would not be possible without the help and support of many people around me:

First of all, I would like to express my special appreciation and thanks to my supervisor Lars Zender for giving me the opportunity to join his lab, for his guidance and invaluable advice on research.

I am thankful to Christiane Ritter for support and undertaking the mentorship of my PhD thesis.

Special thanks to Scott Lowe and Katharine McJunkin for providing Roma Amplicon shRNA library.

I thank Tae-Won Kang and Torsten Wuestefeld for help with animal experiments.

I would like to thank Stefan Laufer for providing p38 inhibitors.

I thank members of Genome Analytics Facility of HZI, Robert Geffers, Michael Jarek, Maren Scharfe and members of Animal Facility of HZI for their technical assistance.

I thank Thomas Longerich and Peter Schirmacher for histopatological analyses.

I would also like to thank to all present and former members of Zender's group for their support and friendly working atmosphere.

Finally, I would like to say my special thanks to Daniel Dauch and my family for their unlimited support and for letting me through all the difficulties.

8. Appendix

Table 14 Oligonucleotides of the RomaAmplicon library

Hairpin	Oligosequence
Brd3.411	TGCTGTTGACAGTGAGCGCCACCATGTTTACAAACTGTTATAGTGAAGCCACAGATGTATAACAGTTTG TAAACATGGTGTTGCCTACTGCCTCGGA
Cdkn1a.635	TGCTGTTGACAGTGAGCGCCTCCCAGTCTCCAAACTTAAATAGTGAAGCCACAGATGTATTTAAGTTTG GAGACTGGGAGATGCCTACTGCCTCGGA
FGF12.1037	TGCTGTTGACAGTGAGCGCCAGAGGGCTAATTGTAATGAATAGTGAAGCCACAGATGTATTCATTACAA TTAGCCCTCTGTTGCCTACTGCCTCGGA
Hck.420	TGCTGTTGACAGTGAGCGCTACCATTGTGGTCGCACTGTATAGTGAAGCCACAGATGTATACAGTGCGA CCACAATGGTATTGCCTACTGCCTCGGA
LIPH.1203	TGCTGTTGACAGTGAGCGAAAGAGGGTTTATTACAATCAATAGTGAAGCCACAGATGTATTGATTGTAA TAAACCCTCTTCTGCCTACTGCCTCGGA
Mmp7.125	TGCTGTTGACAGTGAGCGCCAGGCTCAGAATTATCTTAGATAGTGAAGCCACAGATGTATCTAAGATAA TTCTGAGCCTGTTGCCTACTGCCTCGGA
Mmp8.1870	TGCTGTTGACAGTGAGCGCAATGAAGATTATAAACACATATAGTGAAGCCACAGATGTATATGTGTTTA TAATCTTCATTTTGCCTACTGCCTCGGA
Neu1.455	TGCTGTTGACAGTGAGCGAAGGGATAGTGTTCCTTATCTATAGTGAAGCCACAGATGTATAGATAAGGA ACACTATCCCTGTGCCTACTGCCTCGGA
Oat.1833	TGCTGTTGACAGTGAGCGCTTGAAGGTTAAGCATATGTAATAGTGAAGCCACAGATGTATTACATATGC TTAACCTTCAATTGCCTACTGCCTCGGA
Oat.216	TGCTGTTGACAGTGAGCGACACGTCTGTTGCCACAAAGAATAGTGAAGCCACAGATGTATTCTTTGTGG CAACAGACGTGGTGCCTACTGCCTCGGA
ORF9.461	TGCTGTTGACAGTGAGCGCTAGCGACAAAGTACTTTGATATAGTGAAGCCACAGATGTATATCAAAGTA CTTTGTCGCTATTGCCTACTGCCTCGGA
PHKB.338	TGCTGTTGACAGTGAGCGCACCGGTCTCTTTCCTACTAAATAGTGAAGCCACAGATGTATTTAGTAGGA AAGAGACCGGTATGCCTACTGCCTCGGA
Pim1.685	TGCTGTTGACAGTGAGCGCCACAGTCTACACGGACTTTGATAGTGAAGCCACAGATGTATCAAAGTCCG TGTAGACTGTGTTGCCTACTGCCTCGGA
Pld1.4536	TGCTGTTGACAGTGAGCGCCAGAGTGACAGTTATATCCAATAGTGAAGCCACAGATGTATTGGATATAA CTGTCACTCTGTTGCCTACTGCCTCGGA
RCE1.1375	TGCTGTTGACAGTGAGCGCTTGGGATATTAAAGAGATTTATAGTGAAGCCACAGATGTATAAATCTCTT TAATATCCCAATTGCCTACTGCCTCGGA
RCE1.1376	TGCTGTTGACAGTGAGCGCTGGGATATTAAAGAGATTTAATAGTGAAGCCACAGATGTATTAAATCTCT TTAATATCCCAATGCCTACTGCCTCGGA
RNASE4.755	TGCTGTTGACAGTGAGCGCCAGATAGTATCTCAACGATTATAGTGAAGCCACAGATGTATAATCGTTGA GATACTATCTGATGCCTACTGCCTCGGA
RNASE4.916	TGCTGTTGACAGTGAGCGACCAGTGGAAGATCTCAGACAATAGTGAAGCCACAGATGTATTGTCTGAGA TCTTCCACTGGGTGCCTACTGCCTCGGA
Rxra.5180	TGCTGTTGACAGTGAGCGCCAGATACGTGATGTCATCTAATAGTGAAGCCACAGATGTATTAGATGACA TCACGTATCTGATGCCTACTGCCTCGGA
SDHA.2420	TGCTGTTGACAGTGAGCGAAAGGAAAGTTTGGATATGGTATAGTGAAGCCACAGATGTATACCATATCC AAACTTTCCTTCTGCCTACTGCCTCGGA
Tnfsf10.3440	TGCTGTTGACAGTGAGCGCATGCTGTGACTTATAAATTAATAGTGAAGCCACAGATGTATTAATTTATA AGTCACAGCATTTGCCTACTGCCTCGGA
UBE2V2.2678	TGCTGTTGACAGTGAGCGAAAAGATGTTCTAAATATTTAATAGTGAAGCCACAGATGTATTAAATATTT AGAACATCTTTGTGCCTACTGCCTCGGA
UBE2V2.3257	TGCTGTTGACAGTGAGCGAACCCTTGATGACTATATGTTATAGTGAAGCCACAGATGTATAACATATAG TCATCAAGGGTCTGCCTACTGCCTCGGA
UCKL1.225	TGCTGTTGACAGTGAGCGACACAAGCAAACGTACCATCTATAGTGAAGCCACAGATGTATAGATGGTAC GTTTGCTTGTGCTGCCTACTGCCTCGGA
BRMS1.1002	TGCTGTTGACAGTGAGCGCCTGCACAACTGTGGCCCTGAATAGTGAAGCCACAGATGTATTCAGGGCCA CAGTTGTGCAGATGCCTACTGCCTCGGA
CLIC1.573	TGCTGTTGACAGTGAGCGACCAGCCCTCAATGACAACCTATAGTGAAGCCACAGATGTATAGGTTGTCA TTGAGGGCTGGGTGCCTACTGCCTCGGA
CYP27B1.1252	TGCTGTTGACAGTGAGCGCTCCGTGTAGGAAACTATGTAATAGTGAAGCCACAGATGTATTACATAGTT TCCTACACGGATTGCCTACTGCCTCGGA
Ehhadh.1876	TGCTGTTGACAGTGAGCGAAGCGTTGCTTATATTCCCTTATAGTGAAGCCACAGATGTATAAGGGAATA TAAGCAACGCTCTGCCTACTGCCTCGGA
Hck.1981	TGCTGTTGACAGTGAGCGCTAGCTGTGATTTAAGTGGAAATAGTGAAGCCACAGATGTATTTCCACTTA AATCACAGCTATTGCCTACTGCCTCGGA
Id1.334	TGCTGTTGACAGTGAGCGAAGCATGTAATCGACTACATCATAGTGAAGCCACAGATGTATGATGTAGTC GATTACATGCTGTGCCTACTGCCTCGGA
Itpr3.5512	TGCTGTTGACAGTGAGCGACCGGCAGATCCTGCCACCAAATAGTGAAGCCACAGATGTATTTGGTGGCA GGATCTGCCGGCTGCCTACTGCCTCGGA
Mapk14.2590	TGCTGTTGACAGTGAGCGACTCCTTTACTATCTTTCTCAATAGTGAAGCCACAGATGTATTGAGAAAGAT AGTAAAGGAGCTGCCTACTGCCTCGGA
Met.6277	TGCTGTTGACAGTGAGCGCATGAAGAGTAGTGCAAATTTATAGTGAAGCCACAGATGTATAAATTTGCA CTACTCTTCATATGCCTACTGCCTCGGA

MMP12.1107	TGCTGTTGACAGTGAGCGCAAGATGAGAAGTACTGGTTAATAGTGAAGCCACAGATGTATTAACCAGTA CTTCTCATCTTTTGCCTACTGCCTCGGA
Neu1.1710	TGCTGTTGACAGTGAGCGCATCGAAATATTTGTAACTTAATAGTGAAGCCACAGATGTATTAAGTTACA AATATTTCGATTTGCCTACTGCCTCGGA
ORF9.772	TGCTGTTGACAGTGAGCGAATCGAAGGATGCATACCCAAATAGTGAAGCCACAGATGTATTTGGGTATG CATCCTTCGATCTGCCTACTGCCTCGGA
Parp2.946	TGCTGTTGACAGTGAGCGCGACATTGAAATTGCCCTTAAATAGTGAAGCCACAGATGTATTTAAGGGCA ATTTCAATGTCTTGCCTACTGCCTCGGA
PHKB.3907	TGCTGTTGACAGTGAGCGCAAGAAGCTTCATTGTTAATAATAGTGAAGCCACAGATGTATTATTAACAA TGAAGCTTCTTATGCCTACTGCCTCGGA
Pim2.674	TGCTGTTGACAGTGAGCGCTCGGGATATCAAGGATGAGAATAGTGAAGCCACAGATGTATTCTCATCCT TGATATCCCGATTGCCTACTGCCTCGGA
Rem1.227	TGCTGTTGACAGTGAGCGACTCACAGAGGATGACTCTTAATAGTGAAGCCACAGATGTATTAAGAGTCA TCCTCTGTGAGGTGCCTACTGCCTCGGA
Rpl15.483	TGCTGTTGACAGTGAGCGCGGCTATGTCATTTACAGGATTTAGTGAAGCCACAGATGTAAATCCTGTAA ATGACATAGCCTTGCCTACTGCCTCGGA
Rpo1-1.158	TGCTGTTGACAGTGAGCGCCACCACGGACTTTCCCGGTAATAGTGAAGCCACAGATGTATTACCGGGAA AGTCCGTGGTGTTGCCTACTGCCTCGGA
Stk32c.2014	TGCTGTTGACAGTGAGCGACTGATATGTTATTGAGGGTAATAGTGAAGCCACAGATGTATTACCCTCAA TAACATATCAGGTGCCTACTGCCTCGGA
Stk32c.791	TGCTGTTGACAGTGAGCGAAACAAGGACATGCACACCTTATAGTGAAGCCACAGATGTATAAGGTGTGC ATGTCCTTGTTCTGCCTACTGCCTCGGA
Tnfsf10.3258	TGCTGTTGACAGTGAGCGCCTGCTGTTAATTCTATAGTAATAGTGAAGCCACAGATGTATTACTATAGA ATTAACAGCAGATGCCTACTGCCTCGGA
Trfp.642	TGCTGTTGACAGTGAGCGAAGCAGATACCATGATACAGTATAGTGAAGCCACAGATGTATACTGTATCA TGGTATCTGCTGTGCCTACTGCCTCGGA
Trp53.1224	TGCTGTTGACAGTGAGCGCGTGTAATACATCTGTGGCTTCTAGTGAAGCCACAGATGTAGAAGCCACAG ATGTATTACACATGCCTACTGCCTCGGA
ATOX1.420	TGCTGTTGACAGTGAGCGCAAAGTCAAGCTGAGTTTGTTATAGTGAAGCCACAGATGTATAACAAACTC AGCTTGACTTTATGCCTACTGCCTCGGA
Brd3.298	TGCTGTTGACAGTGAGCGAAACCTGCCTGATTATCATAAATAGTGAAGCCACAGATGTATTTATGATAA TCAGGCAGGTTCTGCCTACTGCCTCGGA
Cdk4.402	TGCTGTTGACAGTGAGCGAACCCTAGTGTTTGAGCATATATAGTGAAGCCACAGATGTATATATGCTCA AACACTAGGGTGTGCCTACTGCCTCGGA
Cdk4.950	TGCTGTTGACAGTGAGCGCACTGGAAATGCTGACCTTTAATAGTGAAGCCACAGATGTATTAAAGGTCA GCATTTCCAGTATGCCTACTGCCTCGGA
CYP27B1.190	TGCTGTTGACAGTGAGCGACTGGCTGAACTCTTCTGCAAATAGTGAAGCCACAGATGTATTTGCAGAAG AGTTCAGCCAGGTGCCTACTGCCTCGGA
Dusp15.514	TGCTGTTGACAGTGAGCGCATCTTTGTACGTGCTACTTAATAGTGAAGCCACAGATGTATTAAGTAGCA CGTACAAAGATTTGCCTACTGCCTCGGA
FGF12.2885	TGCTGTTGACAGTGAGCGCTACGGTGAGATGTTTACTCAATAGTGAAGCCACAGATGTATTGAGTAAAC ATCTCACCGTAATGCCTACTGCCTCGGA
Fkbp5.2813	TGCTGTTGACAGTGAGCGCCAGTCTCATGTCAGGCATTAATAGTGAAGCCACAGATGTATTAATGCCTG ACATGAGACTGTTGCCTACTGCCTCGGA
Hck.1204	TGCTGTTGACAGTGAGCGACTGGACTTTCTCAAGAGTGAATAGTGAAGCCACAGATGTATTCACTCTTG AGAAAGTCCAGCTGCCTACTGCCTCGGA
Hsp90ab1.735	TGCTGTTGACAGTGAGCGCCACCCTCTATTTGGAGAAGGATAGTGAAGCCACAGATGTATCCTTCTCCA AATAGAGGGTGATGCCTACTGCCTCGGA
Mmp3.953	TGCTGTTGACAGTGAGCGACAGCTCTACTTTGTTCTTTGATAGTGAAGCCACAGATGTATCAAAGAACA AAGTAGAGCTGCTGCCTACTGCCTCGGA
Oat.1792	TGCTGTTGACAGTGAGCGCCAGAACAGTTAAATCATTATATAGTGAAGCCACAGATGTATATAATGATT TAACTGTTCTGTTGCCTACTGCCTCGGA
Parp2.1677	TGCTGTTGACAGTGAGCGCATGGTGAATGTTGATCAGACATAGTGAAGCCACAGATGTATGTCTGATCA ACATTCACCATATGCCTACTGCCTCGGA
Parp2.574	TGCTGTTGACAGTGAGCGAAGCACGCAGGATGAAAGTAAATAGTGAAGCCACAGATGTATTTACTTTCA TCCTGCGTGCTGTGCCTACTGCCTCGGA
Pim2.1911	TGCTGTTGACAGTGAGCGACAGTGGTTGAAATGTAAATAATAGTGAAGCCACAGATGTATTATTTACAT TTCAACCACTGGTGCCTACTGCCTCGGA
Pld1.3807	TGCTGTTGACAGTGAGCGCCAGGAAGGCATTAAATCCTAATAGTGAAGCCACAGATGTATTAGGATTTA ATGCCTTCCTGTTGCCTACTGCCTCGGA
Rhod.380	TGCTGTTGACAGTGAGCGCCAGCTTTGACAACGTCTCCAATAGTGAAGCCACAGATGTATTGGAGACGT TGTCAAAGCTGTTGCCTACTGCCTCGGA
Rpo1-1.982	TGCTGTTGACAGTGAGCGACCCGGGTTCGGGACCATTATATAGTGAAGCCACAGATGTATATAATGGTC CCGAACCCGGGCTGCCTACTGCCTCGGA
SDHA.2231	TGCTGTTGACAGTGAGCGCCTGGCATAATTCTTAAGTGAATAGTGAAGCCACAGATGTATTCACTTAAG AATTATGCCAGTTGCCTACTGCCTCGGA
SLC35A2.1390	TGCTGTTGACAGTGAGCGATCCCATAATTCTAGAGGGATATAGTGAAGCCACAGATGTATATCCCTCTA GAATTATGGGAGTGCCTACTGCCTCGGA
SLC35A2.2366	TGCTGTTGACAGTGAGCGAAACAAATGTCAGGATACCCAATAGTGAAGCCACAGATGTATTGGGTATCC TGACATTTGTTCTGCCTACTGCCTCGGA
Srpk1.1217	TGCTGTTGACAGTGAGCGAAAGCAGGAACCTAGTTTCCTATAGTGAAGCCACAGATGTATAGGAAACTA GGTTCCTGCTTCTGCCTACTGCCTCGGA
Trfp.2013	TGCTGTTGACAGTGAGCGAAAGAGAAGCATAAACAATCTATAGTGAAGCCACAGATGTATAGATTGTTT ATGCTTCTCTTCTGCCTACTGCCTCGGA

UCKL1.1330	TGCTGTTGACAGTGAGCGAAAGGATATCAGTGATGACCATTAGTGAAGCCACAGATGTAATGGTCATCA CTGATATCCTTGTGCCTACTGCCTCGGA
Acy3.1464	TGCTGTTGACAGTGAGCGACAGACAACTGATCTCATTATATAGTGAAGCCACAGATGTATATAATGAGA TCAGTTGTCTGGTGCCTACTGCCTCGGA
Ctbp2.2774	TGCTGTTGACAGTGAGCGCTAGATTTGTATCAGCTAGTTATAGTGAAGCCACAGATGTATAACTAGCTG ATACAAATCTAATGCCTACTGCCTCGGA
Dusp15.493	TGCTGTTGACAGTGAGCGCCAGTCTATCTTTCACCTCAAATAGTGAAGCCACAGATGTATTTGAGGTGA AAGATAGACTGTTGCCTACTGCCTCGGA
LIPH.1204	TGCTGTTGACAGTGAGCGCAGAGGGTTTATTACAATCAAATAGTGAAGCCACAGATGTATTTGATTGTA ATAAACCCTCTTTGCCTACTGCCTCGGA
Luciferase.1309	TGCTGTTGACAGTGAGCGCCCGCCTGAAGTCTCTGATTAATAGTGAAGCCACAGATGTATTAATCAGAG ACTTCAGGCGGTTGCCTACTGCCTCGGA
Mapk13.445	TGCTGTTGACAGTGAGCGATACCAGATGCTCAAAGGTCTATAGTGAAGCCACAGATGTATAGACCTTTG AGCATCTGGTACTGCCTACTGCCTCGGA
Mapk7.753	TGCTGTTGACAGTGAGCGAACCGTGATCTTAAACCCTCTATAGTGAAGCCACAGATGTATAGAGGGTTT AAGATCACGGTGTGCCTACTGCCTCGGA
Mfap4.676	TGCTGTTGACAGTGAGCGACTGCCATTTCGCCAATCTCAATAGTGAAGCCACAGATGTATTGAGATTGG CGAAATGGCAGCTGCCTACTGCCTCGGA
MMP12.2109	TGCTGTTGACAGTGAGCGCAACTGTGGTCTTCTAAATAAATAGTGAAGCCACAGATGTATTTATTTAGA AGACCACAGTTATGCCTACTGCCTCGGA
Mmp7.170	TGCTGTTGACAGTGAGCGCACAAAGAAGGTCAATAGTCTATAGTGAAGCCACAGATGTATAGACTATTG ACCTTCTTTGTTTGCCTACTGCCTCGGA
Mmp7.352	TGCTGTTGACAGTGAGCGCCACCTACAGAATTGTATCCTATAGTGAAGCCACAGATGTATAGGATACAA TTCTGTAGGTGATGCCTACTGCCTCGGA
Mmp8.2236	TGCTGTTGACAGTGAGCGACAGAGGTATGGGCACATGATATAGTGAAGCCACAGATGTATATCATGTGC CCATACCTCTGCTGCCTACTGCCTCGGA
NDUFS8.354	TGCTGTTGACAGTGAGCGAAACGTACAAGTATGTGAATAATAGTGAAGCCACAGATGTATTATTCACAT ACTTGTACGTTGTGCCTACTGCCTCGGA
NUDT3.2107	TGCTGTTGACAGTGAGCGATAGCCAAGATGTGAATTGAAATAGTGAAGCCACAGATGTATTTCAATTCA CATCTTGGCTACTGCCTACTGCCTCGGA
PCNA.538	TGCTGTTGACAGTGAGCGCGGAGTACAGCTGTGTAATAAATAGTGAAGCCACAGATGTATTTATTACAC AGCTGTACTCCTTGCCTACTGCCTCGGA
PMPCA.2124	TGCTGTTGACAGTGAGCGAAAGCCTAAAGGTATTTCACAATAGTGAAGCCACAGATGTATTGTGAAATA CCTTTAGGCTTGTGCCTACTGCCTCGGA
Renilla.713	TGCTGTTGACAGTGAGCGCAGGAATTATAATGCTTATCTATAGTGAAGCCACAGATGTATAGATAAGCA TTATAATTCCTATGCCTACTGCCTCGGA
Rpa3.278	TGCTGTTGACAGTGAGCGCAAGGAAGATACTAATCGCTTTTAGTGAAGCCACAGATGTAAAAGCGATTA GTATCTTCCTTATGCCTACTGCCTCGGA
Rpa3.431	TGCTGTTGACAGTGAGCGCAAGGAAGACTCCTGCAGTTTATAGTGAAGCCACAGATGTATAAACTGCAG GAGTCTTCCTTATGCCTACTGCCTCGGA
Rpa3.457	TGCTGTTGACAGTGAGCGCGCGACTCCTATAATTTCTAATTAGTGAAGCCACAGATGTAATTAGAAATT ATAGGAGTCGCTTGCCTACTGCCTCGGA
Senp2.2928	TGCTGTTGACAGTGAGCGACATATGAAAGTTTGTATTTAATAGTGAAGCCACAGATGTATTAAATACAA ACTTTCATATGCTGCCTACTGCCTCGGA
Srpk1.504	TGCTGTTGACAGTGAGCGCCAGGCGTTAATGGAACACATATAGTGAAGCCACAGATGTATATGTGTTCC ATTAACGCCTGATGCCTACTGCCTCGGA
UBE2V2.2103	TGCTGTTGACAGTGAGCGAAAGGATAGGTTTCTTGACATATAGTGAAGCCACAGATGTATATGTCAAGA AACCTATCCTTGTGCCTACTGCCTCGGA
UBE2V2.2582	TGCTGTTGACAGTGAGCGAAAGGCTGGAATTATAGCCTTATAGTGAAGCCACAGATGTATAAGGCTATA ATTCCAGCCTTGTGCCTACTGCCTCGGA
Bcl2l1.1099	TGCTGTTGACAGTGAGCGCCTCAGTTCTCTTGGCCTCAAATAGTGAAGCCACAGATGTATTTGAGGCCA AGAGAACTGAGATGCCTACTGCCTCGGA
Ccnd1.1856	TGCTGTTGACAGTGAGCGCAGGGATGAAATAGTGACATAATAGTGAAGCCACAGATGTATTATGTCACT ATTTCATCCCTATGCCTACTGCCTCGGA
Cdkn1a.639	TGCTGTTGACAGTGAGCGACAGTCTCCAAACTTAAAGTTATAGTGAAGCCACAGATGTATAACTTTAAG TTTGGAGACTGGTGCCTACTGCCTCGGA
Grhpr.628	TGCTGTTGACAGTGAGCGCCAGGCAGAGTTTGTGCCTATTTAGTGAAGCCACAGATGTAAATAGGCACA AACTCTGCCTGATGCCTACTGCCTCGGA
Hck.1554	TGCTGTTGACAGTGAGCGCCCCAGGTATGTCAAACCCAGATAGTGAAGCCACAGATGTATCTGGGTTTG ACATACCTGGGTTGCCTACTGCCTCGGA
Inpp5e.1484	TGCTGTTGACAGTGAGCGACAGGTACTTCCCAGACCGAAATAGTGAAGCCACAGATGTATTTCGGTCTG GGAAGTACCTGGTGCCTACTGCCTCGGA
Itpr3.6963	TGCTGTTGACAGTGAGCGACACCTTCATCCGAGGCTATAATAGTGAAGCCACAGATGTATTATAGCCTC GGATGAAGGTGCTGCCTACTGCCTCGGA
LIPH.291	TGCTGTTGACAGTGAGCGCCTCCGTGAGACTGATGCTCTATAGTGAAGCCACAGATGTATAGAGCATCA GTCTCACGGAGATGCCTACTGCCTCGGA
Mapk14.1095	TGCTGTTGACAGTGAGCGAAAGATGAACTTCGCAAATGTATAGTGAAGCCACAGATGTATACATTTGCG AAGTTCATCTTCTGCCTACTGCCTCGGA
Mfap4.759	TGCTGTTGACAGTGAGCGCAAGGCTTCTATTACTCCCTCATAGTGAAGCCACAGATGTATGAGGGAGTA ATAGAAGCCTTTTGCCTACTGCCTCGGA
MMP12.3571	TGCTGTTGACAGTGAGCGACTGAGACAGAATAACAAATAATAGTGAAGCCACAGATGTATTATTTGTTA TTCTGTCTCAGGTGCCTACTGCCTCGGA
NDUFS8.810	TGCTGTTGACAGTGAGCGCCAAGGAGAAGCTACTCAACAATAGTGAAGCCACAGATGTATTGTTGAGTA GCTTCTCCTTGTTGCCTACTGCCTCGGA

NUDT3.1284	TGCTGTTGACAGTGAGCGAAACGAGGAGCTCAACTGTTCATAGTGAAGCCACAGATGTATGAACAGTTG AGCTCCTCGTTCTGCCTACTGCCTCGGA
NUDT3.1789	TGCTGTTGACAGTGAGCGACACGACGTCCTGAGAATACATTAGTGAAGCCACAGATGTAATGTATTCTC AGGACGTCGTGGTGCCTACTGCCTCGGA
PHKB.2084	TGCTGTTGACAGTGAGCGAAAAGTTCATGTTGATCGTTTATAGTGAAGCCACAGATGTATAAACGATCA ACATGAACTTTGTGCCTACTGCCTCGGA
Rhod.218	TGCTGTTGACAGTGAGCGACACAGTGTTTGAGCGCTATAATAGTGAAGCCACAGATGTATTATAGCGCT CAAACACTGTGGTGCCTACTGCCTCGGA
Rxra.2109	TGCTGTTGACAGTGAGCGACTGGGTCATAGCTAACCTATATAGTGAAGCCACAGATGTATATAGGTTAG CTATGACCCAGGTGCCTACTGCCTCGGA
Rxra.4414	TGCTGTTGACAGTGAGCGACAGGGAGTAAAGATAGAGGAATAGTGAAGCCACAGATGTATTCCTCTATC TTTACTCCCTGCTGCCTACTGCCTCGGA
Slc29a2.1849	TGCTGTTGACAGTGAGCGCTCGACTGTCTATGGAAGAGTATAGTGAAGCCACAGATGTATACTCTTCCA TAGACAGTCGAATGCCTACTGCCTCGGA
Slc29a2.2001	TGCTGTTGACAGTGAGCGACTGCTCCTGCATCCAATTAAATAGTGAAGCCACAGATGTATTTAATTGGA TGCAGGAGCAGGTGCCTACTGCCTCGGA
Sparc.1898	TGCTGTTGACAGTGAGCGACAGAACATCACTCAACTGCAATAGTGAAGCCACAGATGTATTGCAGTTGA GTGATGTTCTGGTGCCTACTGCCTCGGA
Stk32c.2134	TGCTGTTGACAGTGAGCGAACCTCTGAGAATTACAGTCTATAGTGAAGCCACAGATGTATAGACTGTAA TTCTCAGAGGTGTGCCTACTGCCTCGGA
Tnfsf10.693	TGCTGTTGACAGTGAGCGCAAGGACAAGGTGAGAACCAAATAGTGAAGCCACAGATGTATTTGGTTCTC ACCTTGTCCTTTTGCCTACTGCCTCGGA
Trfp.1593	TGCTGTTGACAGTGAGCGACTCGGGAAAGCTGTTAATCTATAGTGAAGCCACAGATGTATAGATTAACA GCTTTCCCGAGCTGCCTACTGCCTCGGA
Acy3.782	TGCTGTTGACAGTGAGCGCCTGCCTCATCTCTGAATCCAATAGTGAAGCCACAGATGTATTGGATTCAG AGATGAGGCAGATGCCTACTGCCTCGGA
BAK1.1809	TGCTGTTGACAGTGAGCGACCGGAACCTATGATTACTTGATAGTGAAGCCACAGATGTATCAAGTAATC ATAGGTTCCGGGTGCCTACTGCCTCGGA
BAK1.720	TGCTGTTGACAGTGAGCGCTTGGCTGATATCATACTGCATTAGTGAAGCCACAGATGTAATGCAGTATG ATATCAGCCAAATGCCTACTGCCTCGGA
Bcl2l1.974	TGCTGTTGACAGTGAGCGACAGGAGAACCACTACATGCAATAGTGAAGCCACAGATGTATTGCATGTAG TGGTTCTCCTGGTGCCTACTGCCTCGGA
Ccnd1.1847	TGCTGTTGACAGTGAGCGCCACAGCGGTAGGGATGAAATATAGTGAAGCCACAGATGTATATTTCATCC CTACCGCTGTGTTGCCTACTGCCTCGGA
Cdk4.401	TGCTGTTGACAGTGAGCGCCACCCTAGTGTTTGAGCATATTAGTGAAGCCACAGATGTAATATGCTCAA ACACTAGGGTGATGCCTACTGCCTCGGA
Ctbp2.1895	TGCTGTTGACAGTGAGCGCATGCCTGAAGCTAATCCGATATAGTGAAGCCACAGATGTATATCGGATTA GCTTCAGGCATTTGCCTACTGCCTCGGA
CYP27B1.1244	TGCTGTTGACAGTGAGCGCCAGAGACATCCGTGTAGGAAATAGTGAAGCCACAGATGTATTTCCTACAC GGATGTCTCTGTTGCCTACTGCCTCGGA
Ehhadh.528	TGCTGTTGACAGTGAGCGCCTGGATGTAGTTGTAAAGTCATAGTGAAGCCACAGATGTATGACTTTACA ACTACATCCAGATGCCTACTGCCTCGGA
GPT2.3560	TGCTGTTGACAGTGAGCGACTGGGAAGCTCTGAACAATAATAGTGAAGCCACAGATGTATTATTGTTCA GAGCTTCCCAGCTGCCTACTGCCTCGGA
Grhpr.361	TGCTGTTGACAGTGAGCGACTGACAGATGCCACTGCAGAATAGTGAAGCCACAGATGTATTCTGCAGTG GCATCTGTCAGGTGCCTACTGCCTCGGA
Itfg1.1897	TGCTGTTGACAGTGAGCGCCACTTGATTAGTGAAACATTATAGTGAAGCCACAGATGTATAATGTTTCA CTAATCAAGTGATGCCTACTGCCTCGGA
Itfg1.1947	TGCTGTTGACAGTGAGCGCTGGATCTGAGATATTTATAAATAGTGAAGCCACAGATGTATTTATAAATA TCTCAGATCCATTGCCTACTGCCTCGGA
Itpr3.424	TGCTGTTGACAGTGAGCGCCTGCATATGAAGAGCAACAAATAGTGAAGCCACAGATGTATTTGTTGCTC TTCATATGCAGATGCCTACTGCCTCGGA
Mapk13.417	TGCTGTTGACAGTGAGCGCCAGCGAGGATAAGGTCCAGTATAGTGAAGCCACAGATGTATACTGGACCT TATCCTCGCTGATGCCTACTGCCTCGGA
Mfap4.760	TGCTGTTGACAGTGAGCGCAGGCTTCTATTACTCCCTCAATAGTGAAGCCACAGATGTATTGAGGGAGT AATAGAAGCCTTTGCCTACTGCCTCGGA
Mmp8.708	TGCTGTTGACAGTGAGCGCAACGTGGACTCAAGATTCCAATAGTGAAGCCACAGATGTATTGGAATCTT GAGTCCACGTTTTGCCTACTGCCTCGGA
Ndufv1.916	TGCTGTTGACAGTGAGCGCCAGGTACCAAATTGTTTAACATAGTGAAGCCACAGATGTATGTTAAACAA TTTGGTACCTGATGCCTACTGCCTCGGA
Neu1.441	TGCTGTTGACAGTGAGCGAAACGATGTAGACACAGGGATATAGTGAAGCCACAGATGTATATCCCTGTG TCTACATCGTTCTGCCTACTGCCTCGGA
Pim1.882	TGCTGTTGACAGTGAGCGCCAGAGTGTCAGCACCTTATTATAGTGAAGCCACAGATGTATAATAAGGTG CTGACACTCTGATGCCTACTGCCTCGGA
Pim2.1464	TGCTGTTGACAGTGAGCGACACAAACCACGTAGACACTTATAGTGAAGCCACAGATGTATAAGTGTCTA CGTGGTTTGTGGTGCCTACTGCCTCGGA
SDHA.2825	TGCTGTTGACAGTGAGCGACAGCAATTGTAAGCCAAATAATAGTGAAGCCACAGATGTATTATTTGGCT TACAATTGCTGGTGCCTACTGCCTCGGA
Tmprss2.1223	TGCTGTTGACAGTGAGCGCCCCATCCAAATTACGACTCTATAGTGAAGCCACAGATGTATAGAGTCGTA ATTTGGATGGGATGCCTACTGCCTCGGA
Tmprss2.1667	TGCTGTTGACAGTGAGCGCCAGATTGGATCTACCAGCAAATAGTGAAGCCACAGATGTATTTGCTGGTA GATCCAATCTGTTGCCTACTGCCTCGGA
Acy3.902	TGCTGTTGACAGTGAGCGCCAGCGTGGAATCTATATCCAATAGTGAAGCCACAGATGTATTGGATATAG ATTCCACGCTGATGCCTACTGCCTCGGA

BAK1.1345	TGCTGTTGACAGTGAGCGATACATTGGCTCCCAAGACCAATAGTGAAGCCACAGATGTATTGGTCTTGG GAGCCAATGTAGTGCCTACTGCCTCGGA
Cdk4.377	TGCTGTTGACAGTGAGCGACCGAACTGATCGGGACATCAATAGTGAAGCCACAGATGTATTGATGTCCC GATCAGTTCGGGTGCCTACTGCCTCGGA
CLIC1.614	TGCTGTTGACAGTGAGCGACCTGAAGGTTCTAGACAATTATAGTGAAGCCACAGATGTATAATTGTCTA GAACCTTCAGGGTGCCTACTGCCTCGGA
Ehhadh.582	TGCTGTTGACAGTGAGCGAACGGTTATAGGTAAACCCATATAGTGAAGCCACAGATGTATATGGGTTTA CCTATAACCGTCTGCCTACTGCCTCGGA
FGF12.1241	TGCTGTTGACAGTGAGCGACAGGGTATTCTTTCAATCATATAGTGAAGCCACAGATGTATATGATTGAA AGAATACCCTGGTGCCTACTGCCTCGGA
Fkbp5.1219	TGCTGTTGACAGTGAGCGCCTGGACAGTGCCAATGAGAAATAGTGAAGCCACAGATGTATTTCTCATTG GCACTGTCCAGTTGCCTACTGCCTCGGA
GPT2.911	TGCTGTTGACAGTGAGCGCCAGGCCAGGTACAAAGCAGAATAGTGAAGCCACAGATGTATTCTGCTTTG TACCTGGCCTGTTGCCTACTGCCTCGGA
Hsp90ab1.1308	TGCTGTTGACAGTGAGCGCCCGCAAGAACATCGTCAAGAATAGTGAAGCCACAGATGTATTCTTGACGA TGTTCTTGCGGATGCCTACTGCCTCGGA
Id1.299	TGCTGTTGACAGTGAGCGACCAGAACCGCAAAGTGAGCAATAGTGAAGCCACAGATGTATTGCTCACTT TGCGGTTCTGGGTGCCTACTGCCTCGGA
Itfg1.698	TGCTGTTGACAGTGAGCGCCACGACATTGACTGCCTCTAATAGTGAAGCCACAGATGTATTAGAGGCAG TCAATGTCGTGATGCCTACTGCCTCGGA
Mapk7.2760	TGCTGTTGACAGTGAGCGCCAGACCCACCTTTCAGCCTTATAGTGAAGCCACAGATGTATAAGGCTGAA AGGTGGGTCTGATGCCTACTGCCTCGGA
Met.3642	TGCTGTTGACAGTGAGCGACTGGACAATGACGGAAAGAAATAGTGAAGCCACAGATGTATTTCTTTCCG TCATTGTCCAGCTGCCTACTGCCTCGGA
Mettl1.259	TGCTGTTGACAGTGAGCGACAAGTGGAGTTTGCAGACATATAGTGAAGCCACAGATGTATATGTCTGCA AACTCCACTTGGTGCCTACTGCCTCGGA
MMP12.1110	TGCTGTTGACAGTGAGCGAATGAGAAGTACTGGTTAATAATAGTGAAGCCACAGATGTATTATTAACCA GTACTTCTCATCTGCCTACTGCCTCGGA
Mmp3.1478	TGCTGTTGACAGTGAGCGCGACCCACATATTGAAGAGCAATAGTGAAGCCACAGATGTATTGCTCTTCA ATATGTGGGTCATGCCTACTGCCTCGGA
Mmp7.256	TGCTGTTGACAGTGAGCGCCATCATGGAAATAATGCAGAATAGTGAAGCCACAGATGTATTCTGCATTA TTTCCATGATGTTGCCTACTGCCTCGGA
Neu1.452	TGCTGTTGACAGTGAGCGCCACAGGGATAGTGTTCCTTATTAGTGAAGCCACAGATGTAATAAGGAACA CTATCCCTGTGTTGCCTACTGCCTCGGA
ORF9.566	TGCTGTTGACAGTGAGCGAATGATGGAAGTTCCAAACTGATAGTGAAGCCACAGATGTATCAGTTTGGA ACTTCCATCATCTGCCTACTGCCTCGGA
Pld1.2050	TGCTGTTGACAGTGAGCGCCACGAAGATTATGAAGCCAAATAGTGAAGCCACAGATGTATTTGGCTTCA TAATCTTCGTGATGCCTACTGCCTCGGA
PMPCA.1841	TGCTGTTGACAGTGAGCGAAAGGCTGGGAAAGATTAGAAATAGTGAAGCCACAGATGTATTTCTAATCT TTCCCAGCCTTCTGCCTACTGCCTCGGA
Rem1.1284	TGCTGTTGACAGTGAGCGCAAGGATGAATAGGCAGACTATTAGTGAAGCCACAGATGTAATAGTCTGCC TATTCATCCTTTTGCCTACTGCCTCGGA
Rpo1-1.947	TGCTGTTGACAGTGAGCGCCCGGCATGAGAAACTCAAGAATAGTGAAGCCACAGATGTATTCTTGAGTT TCTCATGCCGGATGCCTACTGCCTCGGA
Sparc.1733	TGCTGTTGACAGTGAGCGAATGGCAAGTCTTAGTAGCCTATAGTGAAGCCACAGATGTATAGGCTACTA AGACTTGCCATGTGCCTACTGCCTCGGA
Acy3.69	TGCTGTTGACAGTGAGCGCAGGCATTGGCTTTACCATCTATAGTGAAGCCACAGATGTATAGATGGTAA AGCCAATGCCTATGCCTACTGCCTCGGA
Bcl2l1.101	TGCTGTTGACAGTGAGCGAATCCTGGAAGAGAATCGCTAATAGTGAAGCCACAGATGTATTAGCGATTC TCTTCCAGGATCTGCCTACTGCCTCGGA
BRMS1.485	TGCTGTTGACAGTGAGCGCCAGGAATAAGTATGAGTGTGATAGTGAAGCCACAGATGTATCACACTCAT ACTTATTCCTGATGCCTACTGCCTCGGA
Ccs.1009	TGCTGTTGACAGTGAGCGACAGATAAGTGCTGTAGCCTGATAGTGAAGCCACAGATGTATCAGGCTACA GCACTTATCTGCTGCCTACTGCCTCGGA
Ccs.914	TGCTGTTGACAGTGAGCGCACAGAGCCTCATGTCAGGTTATAGTGAAGCCACAGATGTATAACCTGACA TGAGGCTCTGTTTGCCTACTGCCTCGGA
FGF12.1933	TGCTGTTGACAGTGAGCGCAAGCAGAAGGTAACTAGTTAATAGTGAAGCCACAGATGTATTAACTAGTT ACCTTCTGCTTTTGCCTACTGCCTCGGA
Grhpr.1009	TGCTGTTGACAGTGAGCGACCCAGCGAACTCAAGCTGTAATAGTGAAGCCACAGATGTATTACAGCTTG AGTTCGCTGGGCTGCCTACTGCCTCGGA
Grhpr.771	TGCTGTTGACAGTGAGCGCCAGCAGAGGAGATGTGGTAAATAGTGAAGCCACAGATGTATTTACCACAT CTCCTCTGCTGATGCCTACTGCCTCGGA
Mapk13.261	TGCTGTTGACAGTGAGCGCCCGCGAGCTTCTGCTCTTGAATAGTGAAGCCACAGATGTATTCAAGAGCA GAAGCTCGCGGTTGCCTACTGCCTCGGA
Mapk14.2964	TGCTGTTGACAGTGAGCGCCAGGTCTTGTGTTTAGGTCAATAGTGAAGCCACAGATGTATTGACCTAAA CACAAGACCTGTTGCCTACTGCCTCGGA
Mettl1.182	TGCTGTTGACAGTGAGCGACAGAGTTCTTTGCTCCGCTTATAGTGAAGCCACAGATGTATAAGCGGAGC AAAGAACTCTGGTGCCTACTGCCTCGGA
Ndufv1.221	TGCTGTTGACAGTGAGCGCCCGGATCTTTACCAACCTGTATAGTGAAGCCACAGATGTATACAGGTTGG TAAAGATCCGGTTGCCTACTGCCTCGGA
Parp2.1429	TGCTGTTGACAGTGAGCGAGAGGCCAATCCTAAAGCACAATAGTGAAGCCACAGATGTATTGTGCTTTA GGATTGGCCTCCTGCCTACTGCCTCGGA
Pip5k2c.3201	TGCTGTTGACAGTGAGCGACAGTGTTGCCATCTTTACTTATAGTGAAGCCACAGATGTATAAGTAAAGA TGGCAACACTGCTGCCTACTGCCTCGGA

Rhod.732	TGCTGTTGACAGTGAGCGCCCGGTTTACTCCGCTGCAGAATAGTGAAGCCACAGATGTATTCTGCAGCG GAGTAAACCGGATGCCTACTGCCTCGGA
RNASE4.499	TGCTGTTGACAGTGAGCGCCCCAGTGCACTTTGACAGATATAGTGAAGCCACAGATGTATATCTGTCAA AGTGCACTGGGATGCCTACTGCCTCGGA
RNASE4.610	TGCTGTTGACAGTGAGCGACTCGTGCCTTATACTCACATATAGTGAAGCCACAGATGTATATGTGAGTA TAAGGCACGAGCTGCCTACTGCCTCGGA
Rpa3.431	TGCTGTTGACAGTGAGCGCAAGGAAGACTCCTGCAGTTTATAGTGAAGCCACAGATGTATAAACTGCAG GAGTCTTCCTTATGCCTACTGCCTCGGA
Rpa3.457	TGCTGTTGACAGTGAGCGCGCGACTCCTATAATTTCTAATTAGTGAAGCCACAGATGTAATTAGAAATT ATAGGAGTCGCTTGCCTACTGCCTCGGA
Rpo1-1.311	TGCTGTTGACAGTGAGCGCCCGGAGAATCCTGTTAGCTGATAGTGAAGCCACAGATGTATCAGCTAACA GGATTCTCCGGATGCCTACTGCCTCGGA
Rxra.2278	TGCTGTTGACAGTGAGCGACAGGGTTAGCCAACTATAGTATAGTGAAGCCACAGATGTATACTATAGTT GGCTAACCCTGGTGCCTACTGCCTCGGA
Senp2.1668	TGCTGTTGACAGTGAGCGCCAGGATGAAAGCAAGACCAAATAGTGAAGCCACAGATGTATTTGGTCTTG CTTTCATCCTGTTGCCTACTGCCTCGGA
Stk32c.724	TGCTGTTGACAGTGAGCGACTGGACTACCTGCGTAGCCAATAGTGAAGCCACAGATGTATTGGCTACGC AGGTAGTCCAGGTGCCTACTGCCTCGGA
UCKL1.1081	TGCTGTTGACAGTGAGCGACGGCTGCTTATTGAACATGCATAGTGAAGCCACAGATGTATGCATGTTCA ATAAGCAGCCGCTGCCTACTGCCTCGGA
Bcl2l1.2091	TGCTGTTGACAGTGAGCGCCCTTGTGAAGATGATATACTATAGTGAAGCCACAGATGTATAGTATATCA TCTTCACAAGGATGCCTACTGCCTCGGA
BRMS1.888	TGCTGTTGACAGTGAGCGACAGGATTAACATTTCTCTGCATAGTGAAGCCACAGATGTATGCAGAGAAA TGTTAATCCTGCTGCCTACTGCCTCGGA
Ccnd1.3415	TGCTGTTGACAGTGAGCGCTACAGCATTGTGCTAATGTAATAGTGAAGCCACAGATGTATTACATTAGC ACAATGCTGTAATGCCTACTGCCTCGGA
Ccs.625	TGCTGTTGACAGTGAGCGATACCTTCCGGATAGAGGATAATAGTGAAGCCACAGATGTATTATCCTCTA TCCGGAAGGTAGTGCCTACTGCCTCGGA
GPT2.3284	TGCTGTTGACAGTGAGCGCTTAGCTGTTCTAAGAGATTAATAGTGAAGCCACAGATGTATTAATCTCTTA GAACAGCTAAATGCCTACTGCCTCGGA
Gstp1.491	TGCTGTTGACAGTGAGCGCCCAGATCTCCTTTGCCGATTATAGTGAAGCCACAGATGTATAATCGGCAA AGGAGATCTGGTTGCCTACTGCCTCGGA
Inpp5e.2892	TGCTGTTGACAGTGAGCGCCAGGCAACCTCTGGTATCCTATAGTGAAGCCACAGATGTATAGGATACCA GAGGTTGCCTGATGCCTACTGCCTCGGA
Itfg1.503	TGCTGTTGACAGTGAGCGCACCACTGATTATGGACTTCAATAGTGAAGCCACAGATGTATTGAAGTCCA TAATCAGTGGTTTGCCTACTGCCTCGGA
Itpr3.2907	TGCTGTTGACAGTGAGCGCCAGAAGCAAATTTGAGGACAATAGTGAAGCCACAGATGTATTGTCCTCAA ATTTGCTTCTGTTGCCTACTGCCTCGGA
Mapk14.2364	TGCTGTTGACAGTGAGCGACTCCAGCTACTTTGTGTTGAATAGTGAAGCCACAGATGTATTCAACACAA AGTAGCTGGAGGTGCCTACTGCCTCGGA
Met.6602	TGCTGTTGACAGTGAGCGCCTGATGAATCATACAGTTGAATAGTGAAGCCACAGATGTATTCAACTGTA TGATTCATCAGATGCCTACTGCCTCGGA
Mfap4.1356	TGCTGTTGACAGTGAGCGCCGGCTACTGCTCAACTCTGAATAGTGAAGCCACAGATGTATTCAGAGTTG AGCAGTAGCCGTTGCCTACTGCCTCGGA
Mmp3.249	TGCTGTTGACAGTGAGCGAGACAGTAGTCTTATTGTCAAATAGTGAAGCCACAGATGTATTTGACAATA AGACTACTGTCCTGCCTACTGCCTCGGA
NDUFS8.807	TGCTGTTGACAGTGAGCGCCAACAAGGAGAAGCTACTCAATAGTGAAGCCACAGATGTATTGAGTAGCT TCTCCTTGTTGTTGCCTACTGCCTCGGA
Ndufv1.914	TGCTGTTGACAGTGAGCGCTTCAGGTACCAAATTGTTTAATAGTGAAGCCACAGATGTATTAAACAATT TGGTACCTGAATTGCCTACTGCCTCGGA
Npr3.2769	TGCTGTTGACAGTGAGCGCCACAGTGGTGATACGTTTAAATAGTGAAGCCACAGATGTATTTAAACGTA TCACCACTGTGTTGCCTACTGCCTCGGA
PHKB.131	TGCTGTTGACAGTGAGCGAAACGCTTATGATAAGAATCAATAGTGAAGCCACAGATGTATTGATTCTTA TCATAAGCGTTGTGCCTACTGCCTCGGA
Pim1.602	TGCTGTTGACAGTGAGCGAATCAAGGACGAGAACATCTTATAGTGAAGCCACAGATGTATAAGATGTTC TCGTCCTTGATGTGCCTACTGCCTCGGA
Pim2.1471	TGCTGTTGACAGTGAGCGACACGTAGACACTTAGTTCAAATAGTGAAGCCACAGATGTATTTGAACTAA GTGTCTACGTGGTGCCTACTGCCTCGGA
Senp2.590	TGCTGTTGACAGTGAGCGCTACGCTGAAATCGGAAGGCTATAGTGAAGCCACAGATGTATAGCCTTCCG ATTTCAGCGTAATGCCTACTGCCTCGGA
Sparc.1196	TGCTGTTGACAGTGAGCGAAACAAGGATCTGGTGATCTAATAGTGAAGCCACAGATGTATTAGATCACC AGATCCTTGTTGTGCCTACTGCCTCGGA
Srpk1.349	TGCTGTTGACAGTGAGCGAAAAGAAGTTTGTAGCAATGAATAGTGAAGCCACAGATGTATTCATTGCTA CAAACTTCTTTCTGCCTACTGCCTCGGA
Srpk1.350	TGCTGTTGACAGTGAGCGCAAGAAGTTTGTAGCAATGAAATAGTGAAGCCACAGATGTATTTCATTGCT ACAAACTTCTTTTGCCTACTGCCTCGGA
UCKL1.1661	TGCTGTTGACAGTGAGCGATCCGAGCTACTCTTATTTCTATAGTGAAGCCACAGATGTATAGAAATAAG AGTAGCTCGGACTGCCTACTGCCTCGGA
Brd3.1245	TGCTGTTGACAGTGAGCGCCTCGAATTGTTATAAGTACAATAGTGAAGCCACAGATGTATTGTACTTAT AACAATTCGAGATGCCTACTGCCTCGGA
Cdkn1a.643	TGCTGTTGACAGTGAGCGCCTCCAAACTTAAAGTTATTTATAGTGAAGCCACAGATGTATAAATAACTTT AAGTTTGGAGATGCCTACTGCCTCGGA
CLIC1.1126	TGCTGTTGACAGTGAGCGATAGGACAACGCATTTCAGTAATAGTGAAGCCACAGATGTATTACTGAAAT GCGTTGTCCTACTGCCTACTGCCTCGGA

CLIC1.1130	TGCTGTTGACAGTGAGCGAACAACGCATTTCAGTAATAAATAGTGAAGCCACAGATGTATTTATTACTGAAATGCGTTGTCTGCCTACTGCCTCGGA
Dusp15.491	TGCTGTTGACAGTGAGCGACACAGTCTATCTTTCACCTCATAGTGAAGCCACAGATGTATGAGGTGAAAGATAGACTGTGGTGCCTACTGCCTCGGA
Fkbp5.3272	TGCTGTTGACAGTGAGCGCCTCAGACGATTTACACGGAAATAGTGAAGCCACAGATGTATTTCCGTGTAAATCGTCTGAGATGCCTACTGCCTCGGA
Fkbp5.628	TGCTGTTGACAGTGAGCGCATCCGTAGAATCAAACGGAAATAGTGAAGCCACAGATGTATTTCCGTTTGATTCTACGGATATGCCTACTGCCTCGGA
GPT2.3193	TGCTGTTGACAGTGAGCGCCAGATTATAAATAACCCTCCATAGTGAAGCCACAGATGTATGGAGGGTTATTTATAATCTGATGCCTACTGCCTCGGA
HP_141864_Mfap4	TGCTGTTGACAGTGAGCGCCCTCCTGACACTGAAGCAGAATAGTGAAGCCACAGATGTATTCTGCTTCAGTGTCAGGAGGTTGCCTACTGCCTCGGA
HP_235196_Brms1	TGCTGTTGACAGTGAGCGCCGGACCCTGACCCTGCATTTATAGTGAAGCCACAGATGTATAAATGCAGGGTCAGGGTCCGTTGCCTACTGCCTCGGA
HP_239339_Trfp	TGCTGTTGACAGTGAGCGCGCTGTTAATCTACAAAGTGTATAGTGAAGCCACAGATGTATACACTTTGTAGATTAACAGCTTGCCTACTGCCTCGGA
HP_268893_Gstp1	TGCTGTTGACAGTGAGCGAGCCCAGATGGATATGGTGAATTAGTGAAGCCACAGATGTAATTCACCATATCCATCTGGGCGTGCCTACTGCCTCGGA
HP_273644_Pmpca	TGCTGTTGACAGTGAGCGCCCTAGTAGAATGTGCCAGAAATAGTGAAGCCACAGATGTATTTCTGGCACATTCTACTAGGTTGCCTACTGCCTCGGA
HP_273729_Gstp1	TGCTGTTGACAGTGAGCGCCCTCACCCTTTACCAATCTAATAGTGAAGCCACAGATGTATTAGATTGGTAAAGGGTGAGGTTGCCTACTGCCTCGGA
HP_281235_Srpk1	TGCTGTTGACAGTGAGCGCGGCATAAAGAGGATCTGCATATAGTGAAGCCACAGATGTATATGCAGATCCTCTTTATGCCTTGCCTACTGCCTCGGA
HP_295174_Senp2	TGCTGTTGACAGTGAGCGCCGCTGAAATCGGAAGGCTATATAGTGAAGCCACAGATGTATATAGCCTTCCGATTTCAGCGTTGCCTACTGCCTCGGA
HP_304374_Id1	TGCTGTTGACAGTGAGCGCCGTCCTGCTCTACGACATGAATAGTGAAGCCACAGATGTATTCATGTCGTAGAGCAGGACGTTGCCTACTGCCTCGGA
Inpp5e.1796	TGCTGTTGACAGTGAGCGAACGCATCGTGTCTCAGATCAATAGTGAAGCCACAGATGTATTGATCTGAGACACGATGCGTGTGCCTACTGCCTCGGA
Met.4214	TGCTGTTGACAGTGAGCGCCACATTTGATATCACTATCTATAGTGAAGCCACAGATGTATAGATAGTGATATCAAATGTGTTGCCTACTGCCTCGGA
NPR3.871	TGCTGTTGACAGTGAGCGATACGCTTTCTTCAACATTGAATAGTGAAGCCACAGATGTATTCAATGTTGAAGAAAGCGTAGTGCCTACTGCCTCGGA
Pip5k2c.3266	TGCTGTTGACAGTGAGCGCTACTCCCGATATCACAATAAATAGTGAAGCCACAGATGTATTTATTGTGATATCGGGAGTAATGCCTACTGCCTCGGA
Pld1.3383	TGCTGTTGACAGTGAGCGATACGTTCTTGTCGATAGCATATAGTGAAGCCACAGATGTATATGCTATCGACAAGAACGTAGTGCCTACTGCCTCGGA
Sparc.1758	TGCTGTTGACAGTGAGCGAAAGGAAAGACAGAATAATCCATAGTGAAGCCACAGATGTATGGATTATTCTGTCTTTCCTTGTGCCTACTGCCTCGGA
Tmprss2.846	TGCTGTTGACAGTGAGCGAAACGAGCTTTATGAAGCTGAATAGTGAAGCCACAGATGTATTCAGCTTCATAAAGCTCGTTGTGCCTACTGCCTCGGA
ATOX1.64	TGCTGTTGACAGTGAGCGCCTCCGTGGACATGACCTGTGATAGTGAAGCCACAGATGTATCACAGGTCATGTCCACGGAGATGCCTACTGCCTCGGA
Ehhadh.2855	TGCTGTTGACAGTGAGCGCCACATTGAGTTCAATGGTTCATAGTGAAGCCACAGATGTATGAACCATTGAACTCAATGTGTTGCCTACTGCCTCGGA
Gstp1.14	TGCTGTTGACAGTGAGCGACTCTGTCTACGCAGCACTGAATAGTGAAGCCACAGATGTATTCAGTGCTGCGTAGACAGAGGTGCCTACTGCCTCGGA
Gstp1.377	TGCTGTTGACAGTGAGCGCCACCAACTATGAGAATGGTAATAGTGAAGCCACAGATGTATTACCATTCTCATAGTTGGTGTTGCCTACTGCCTCGGA
HP_234766_Slc29a2	TGCTGTTGACAGTGAGCGCCGACTGTCTATGGAAGAGTAATAGTGAAGCCACAGATGTATTACTCTTCCATAGACAGTCGATGCCTACTGCCTCGGA
HP_265487_Dusp15	TGCTGTTGACAGTGAGCGACCGGAATAAGATCACACATATTAGTGAAGCCACAGATGTAATATGTGTGATCTTATTCCGGCTGCCTACTGCCTCGGA
HP_303160_Ctbp2	TGCTGTTGACAGTGAGCGCGGTCCTGCAGAGCTTGTTCTATAGTGAAGCCACAGATGTATAGAACAAGCTCTGCAGGACCTTGCCTACTGCCTCGGA
HP_320788_Cyp27b1	TGCTGTTGACAGTGAGCGACCTTGCCTAATTTACAGCGTTTAGTGAAGCCACAGATGTAAACGCTGTAAATTAGGCAAGGGTGCCTACTGCCTCGGA
HP_328142_Ccs	TGCTGTTGACAGTGAGCGAGGTTTATTAATGCTGGGTATTTAGTGAAGCCACAGATGTAAATACCCAGCATTAATAAACCCTGCCTACTGCCTCGGA
Luciferase.1309	TGCTGTTGACAGTGAGCGCCCGCCTGAAGTCTCTGATTAATAGTGAAGCCACAGATGTATTAATCAGAGACTTCAGGCGGTTGCCTACTGCCTCGGA
NUDT3.1654	TGCTGTTGACAGTGAGCGAGAGATTCTTTCTGTAATGCTATAGTGAAGCCACAGATGTATAGCATTACAGAAAGAATCTCCTGCCTACTGCCTCGGA
Oat.136	TGCTGTTGACAGTGAGCGACACACGATGCTTTCTAAACTATAGTGAAGCCACAGATGTATAGTTTAGAAAGCATCGTGTGGTGCCTACTGCCTCGGA
Pip5k2c.796	TGCTGTTGACAGTGAGCGAAAAGTGTATATTGGTGAAGAATAGTGAAGCCACAGATGTATTCTTCACCAATATACACTTTCTGCCTACTGCCTCGGA
RCE1.1385	TGCTGTTGACAGTGAGCGCAAAGAGATTTAACTTGGGTAATAGTGAAGCCACAGATGTATTACCCAAGTTAAATCTCTTTATGCCTACTGCCTCGGA
Renilla.713	TGCTGTTGACAGTGAGCGCAGGAATTATAATGCTTATCTATAGTGAAGCCACAGATGTATAGATAAGCATTATAATTCCTATGCCTACTGCCTCGGA
Rpa3.278	TGCTGTTGACAGTGAGCGCAAGGAAGATACTAATCGCTTTTAGTGAAGCCACAGATGTAAAAGCGATTAGTATCTTCCTTATGCCTACTGCCTCGGA

Rpa3.431	TGCTGTTGACAGTGAGCGCAAGGAAGACTCCTGCAGTTTATAGTGAAGCCACAGATGTATAAACTGCAG GAGTCTTCCTTATGCCTACTGCCTCGGA
Rpa3.457	TGCTGTTGACAGTGAGCGCGCGACTCCTATAATTTCTAATTAGTGAAGCCACAGATGTAATTAGAAATT ATAGGAGTCGCTTGCCTACTGCCTCGGA
Senp2.604	TGCTGTTGACAGTGAGCGAAAGGCTATAATAGAAGGCCAATAGTGAAGCCACAGATGTATTGGCCTTCT ATTATAGCCTTCTGCCTACTGCCTCGGA

Table 15 Resuls from *in vivo* and *in vitro* screen in Nras^{G12V}; p19$^{Arf-/-}$ genetic background

in vivo	
short hairpin	depletion (fold-change)
ATOX1.420	511,462
PHKB.3907	330,690
Ehhadh.2855	157,339
Id1.334	143,573
UBE2V2.2103	121,975
Itfg1.1897	117,601
Cdk4.377	106,746
Rhod.380	63,976
Srpk1.1217	34,276
Neu1.441	31,598
Ccnd1.1856	29,170
Sparc.1733	27,802
Ctbp2.1895	27,443
FGF12.1241	22,494
RNASE4.916	22,306
SLC35A2.1390	21,752
NPR3.871	20,916
CYP27B1.1244	17,105
Oat.1792	14,246
273644_Pmpca	13,881
NUDT3.1284	13,502
Ehhadh.1876	13,265
Itfg1.698	11,130
Senp2.590	10,465
Mmp7.125	10,336
Slc29a2.2001	10,335
Fkbp5.3272	10,172
Itpr3.6963	10,074
Parp2.574	9,997
Pip5k2c.3201	9,919
Fkbp5.628	9,884
Ehhadh.582	9,456
ORF9.566	9,366
Senp2.2928	8,797
Inpp5e.2892	8,780
PHKB.2084	8,746

in vitro	
short hairpin	depletion (fold-change)
BAK1.1809	199,770
Mettl1.182	86,587
NPR3.871	65,000
Neu1.452	42,236
SLC35A2.2366	36,687
Rhod.732	20,385
MMP12.3571	17,964
Inpp5e.1484	16,087
235196_Brms1	10,972
Pip5k2c.3201	10,683
CYP27B1.1252	9,883
RCE1.1385	9,001
GPT2.911	8,815
UBE2V2.3257	8,071
SDHA.2420	7,338
Tmprss2.1667	6,797
Grhpr.771	6,350
Mapk14.2964	6,044
Hck.1981	5,964
UBE2V2.2103	5,964
Srpk1.1217	5,860
Cdkn1a.635	5,765
GPT2.3560	5,654
Pim2.1911	5,238
273644_Pmpca	5,227
Inpp5e.2892	5,121
Mapk13.261	4,685
Hck.420	4,632
Ctbp2.1895	4,343
UCKL1.1661	3,937
Sparc.1733	3,858
Mapk14.2590	3,626
CLIC1.614	3,572
Tmprss2.1223	3,461
Inpp5e.1796	3,222
Mmp7.125	3,203

Pld1.4536	8,020
PMPCA.2124	7,730
FGF12.1037	7,273
Ndufv1.221	7,271
Mapk14.2964	7,129
Brd3.1245	7,066
ATOX1.64	7,062
Pim1.685	6,616
Brd3.298	6,475
Hsp90ab1.735	6,473
BAK1.720	6,434
Itfg1.1947	6,434
Met.4214	6,434
Mmp8.1870	6,434
RCE1.1385	6,434
RNASE4.610	6,434
Rpo1-1.947	6,434
SLC35A2.2366	6,434
ORF9.772	6,405
Fkbp5.1219	6,167
Bcl2l1.2091	5,971
Senp2.1668	5,683
Rpo1-1.158	5,606
Stk32c.791	5,346
UBE2V2.3257	4,898
Gstp1.377	4,822
273729_Gstp1	4,815
UBE2V2.2678	4,758
235196_Brms1	4,721
Pip5k2c.796	4,621
Parp2.1677	4,319
Ctbp2.2774	4,273
SDHA.2825	4,191
Rem1.227	4,171
Hck.1204	4,164
Tnfsf10.3258	4,135
Mfap4.1356	4,094
LIPH.291	4,072
NDUFS8.807	3,912
Oat.1833	3,896
Rxra.4414	3,894
Cdkn1a.643	3,665
Ndufv1.916	3,616
281235_Srpk1	3,597
UCKL1.1081	3,596

Id1.334	3,060
ORF9.461	3,059
Pld1.4536	3,003
Mmp3.249	2,971
141864_Mfap4	2,934
PHKB.3907	2,898
Senp2.604	2,846
Ccnd1.3415	2,618
Acy3.1464	2,540
NDUFS8.810	2,444
Mmp7.352	2,422
Mettl1.259	2,415
Oat.216	2,335
Itfg1.698	2,304
Ndufv1.916	2,233
320788_Cyp27b1	2,131
Rem1.1284	2,063
Rxra.5180	2,034
SDHA.2231	2,031
Renilla.713	2,011
Itpr3.2907	1,933
UBE2V2.2678	1,907
Grhpr.628	1,864
Dusp15.514	1,846
304374_Id1	1,836
Fkbp5.628	1,809
Mapk14.2364	1,779
UCKL1.1330	1,742
Met.6602	1,711
MMP12.2109	1,707
Hsp90ab1.735	1,700
PMPCA.2124	1,640
LIPH.1203	1,628
LIPH.1204	1,628
Mmp3.953	1,626
CYP27B1.190	1,623
RNASE4.499	1,618
Id1.299	1,535
Brd3.411	1,522
Pim2.674	1,502
Tnfsf10.3440	1,501
Pip5k2c.796	1,451
Hsp90ab1.1308	1,439
Ccs.914	1,435
Sparc.1758	1,434

Tmprss2.1223	3,502
Tmprss2.846	3,410
Ccnd1.1847	3,194
Itpr3.5512	3,182
CLIC1.573	3,127
Gstp1.14	3,033
295174_Senp2	2,988
Hsp90ab1.1308	2,945
BAK1.1345	2,933
234766_Slc29a2	2,717
Slc29a2.1849	2,717
Mfap4.759	2,673
Mfap4.760	2,673
Bcl2l1.1099	2,577
Rpo1-1.311	2,529
Met.6277	2,520
Rhod.218	2,509
Cdk4.950	2,462
NDUFS8.810	2,453
Dusp15.514	2,435
UCKL1.1330	2,429
Cdkn1a.635	2,362
CLIC1.614	2,309
Acy3.782	2,215
Itfg1.503	2,084
CYP27B1.190	2,080
Mapk7.753	2,041
Parp2.1429	1,978
MMP12.2109	1,967
UCKL1.225	1,960
Grhpr.628	1,897
Mapk14.2364	1,849
Itpr3.424	1,806
304374_Id1	1,802
Ehhadh.528	1,787
Rem1.1284	1,775
Rpl15.483	1,746
SDHA.2231	1,735
Mmp3.953	1,715
Ndufv1.914	1,689
Tnfsf10.3440	1,662
BRMS1.1002	1,586
RNASE4.755	1,515
Mfap4.676	1,493
CLIC1.1130	1,484

MMP12.1110	1,433
Npr3.2769	1,344
Itpr3.424	1,333
ORF9.566	1,327
Mfap4.760	1,311
Mfap4.759	1,311
Parp2.1429	1,301
239339_Trfp	1,296
Mfap4.1356	1,232
Slc29a2.2001	1,013
Tmprss2.846	-0,836
Brd3.298	-0,841
268893_Gstp1	-0,841
Stk32c.2014	-0,854
Tnfsf10.3258	-0,860
Gstp1.14	-0,924
Cdk4.402	-0,929
Cdk4.401	-0,929
295174_Senp2	-0,931
Trfp.642	-0,937
BRMS1.888	-0,947
NUDT3.1789	-0,950
Dusp15.491	-0,953
Rpo1-1.158	-0,976
BAK1.720	-0,979
Itfg1.1947	-0,979
Mapk13.417	-0,979
RNASE4.610	-0,979
Rpo1-1.947	-0,979
Mapk13.445	-0,980
Bcl2l1.101	-1,005
Gstp1.491	-1,015
265487_Dusp15	-1,027
Stk32c.2134	-1,039
234766_Slc29a2	-1,042
Slc29a2.1849	-1,042
Ehhadh.582	-1,063
328142_Ccs	-1,070
Fkbp5.3272	-1,076
Pip5k2c.3266	-1,093
Met.3642	-1,097
Ccs.625	-1,113
303160_Ctbp2	-1,117
Rem1.227	-1,123
FGF12.1037	-1,168

Grhpr.1009	1,483
GPT2.3284	1,464
GPT2.3560	1,457
PCNA.538	1,446
Luciferase.1309	1,437
NUDT3.1789	1,404
RCE1.1375	1,402
RCE1.1376	1,402
Pim2.674	1,354
Inpp5e.1796	1,353
Neu1.455	1,324
Rxra.5180	1,315
Grhpr.771	1,297
BRMS1.485	1,282
Dusp15.491	1,261
Mettl1.182	1,260
ORF9.461	1,233
Rpa3.431	1,221
Dusp15.493	1,128
Pim1.882	1,101
Trfp.642	1,095
Pim2.1471	1,073
Acy3.69	1,072
Rpo1-1.982	1,047
Grhpr.361	1,046
Brd3.411	1,042
FGF12.1933	1,001
Mapk13.261	-1,005
Ccs.914	-1,010
Parp2.946	-1,019
MMP12.1110	-1,024
Rhod.732	-1,038
Gstp1.491	-1,049
GPT2.911	-1,050
Sparc.1196	-1,087
320788_Cyp27b1	-1,143
Renilla.713	-1,150
Pim2.1911	-1,170
Mmp7.170	-1,189
MMP12.3571	-1,240
303160_Ctbp2	-1,283
NUDT3.1654	-1,336
NDUFS8.354	-1,352
PHKB.131	-1,386
PHKB.338	-1,401

Oat.1833	-1,174
Neu1.455	-1,176
Oat.136	-1,189
Rhod.218	-1,242
NUDT3.1654	-1,254
Mfap4.676	-1,271
Mmp8.1870	-1,275
Senp2.1668	-1,302
Rpa3.431	-1,302
Pld1.3807	-1,314
Itpr3.6963	-1,326
Trfp.2013	-1,326
Rpa3.278	-1,362
Rhod.380	-1,365
PHKB.131	-1,378
Acy3.902	-1,392
RNASE4.755	-1,416
Pim2.1464	-1,417
Acy3.69	-1,447
Ccs.1009	-1,502
Itfg1.503	-1,510
NUDT3.2107	-1,520
UCKL1.1081	-1,531
Mapk7.2760	-1,540
SLC35A2.1390	-1,543
281235_Srpk1	-1,577
Srpk1.504	-1,597
UBE2V2.2582	-1,635
Mmp3.1478	-1,654
Met.4214	-1,661
FGF12.2885	-1,668
RCE1.1376	-1,722
RCE1.1375	-1,722
Dusp15.493	-1,723
PMPCA.1841	-1,736
Pim2.1471	-1,791
Pld1.2050	-1,800
Parp2.1677	-1,834
NDUFS8.354	-1,859
Neu1.441	-1,872
Itpr3.5512	-1,901
Hck.1554	-1,902
PCNA.538	-1,932
Fkbp5.2813	-1,946
Bcl2l1.1099	-2,044

NUDT3.2107	-1,405
SDHA.2420	-1,437
Senp2.604	-1,454
BRMS1.888	-1,480
Hck.1981	-1,543
Trfp.2013	-1,561
Acy3.1464	-1,712
Bcl2l1.974	-1,723
Pld1.3383	-1,765
Rpa3.278	-1,788
Npr3.2769	-1,868
Sparc.1898	-1,872
UBE2V2.2582	-1,920
328142_Ccs	-1,942
Pip5k2c.3266	-2,083
Cdkn1a.639	-2,115
239339_Trfp	-2,203
Mmp7.352	-2,210
Ccs.1009	-2,237
Trfp.1593	-2,379
Srpk1.349	-2,531
Srpk1.350	-2,531
Mmp3.249	-2,541
Met.6602	-2,645
Ccs.625	-2,795
CLIC1.1126	-2,823
Mapk13.445	-2,838
Cdk4.402	-2,900
Cdk4.401	-2,900
Pld1.3807	-2,973
Tnfsf10.693	-3,005
Itpr3.2907	-3,164
LIPH.1203	-3,255
LIPH.1204	-3,255
Stk32c.724	-3,284
UCKL1.1661	-3,546
Pim1.602	-3,556
MMP12.1107	-3,611
GPT2.3193	-3,674
Oat.216	-3,808
Inpp5e.1484	-3,843
Id1.299	-3,861
Hck.1554	-4,046
Rpa3.457	-4,126
Mapk7.2760	-4,162

Gstp1.377	-2,057
GPT2.3193	-2,094
GPT2.3284	-2,118
BRMS1.485	-2,124
PHKB.2084	-2,143
Senp2.590	-2,283
BAK1.1345	-2,341
ATOX1.64	-2,379
Ctbp2.2774	-2,392
CLIC1.1130	-2,402
Luciferase.1309	-2,466
ATOX1.420	-2,506
Hck.1204	-2,548
CLIC1.573	-2,562
MMP12.1107	-2,589
Pld1.3383	-2,617
Rxra.4414	-2,675
Ndufv1.914	-2,786
ORF9.772	-3,120
Ccnd1.1847	-3,135
Senp2.2928	-3,149
Grhpr.1009	-3,209
273729_Gstp1	-3,214
Fkbp5.1219	-3,360
Acy3.782	-3,405
Neu1.1710	-3,453
Ehhadh.528	-3,505
Rpa3.457	-3,603
Rxra.2109	-3,655
Pim1.882	-3,788
RNASE4.916	-3,867
Parp2.946	-3,881
Rpl15.483	-3,950
Cdk4.377	-4,004
Tnfsf10.693	-4,062
Rxra.2278	-4,109
SDHA.2825	-4,141
Srpk1.349	-4,340
Srpk1.350	-4,340
Cdk4.950	-4,397
Oat.1792	-4,654
Trfp.1593	-4,701
Rpo1-1.982	-5,049
Cdkn1a.643	-5,175
UCKL1.225	-5,192

FGF12.2885	-4,605		Met.6277	-5,316
265487_Dusp15	-4,729		PHKB.338	-5,388
Srpk1.504	-5,172		Stk32c.791	-5,467
141864_Mfap4	-5,547		Mapk7.753	-5,642
Stk32c.2014	-5,599		Bcl2l1.974	-5,729
268893_Gstp1	-5,671		Itfg1.1897	-5,825
Bcl2l1.101	-5,912		Ndufv1.221	-6,117
Fkbp5.2813	-6,088		NUDT3.1284	-6,360
Pim2.1464	-6,508		FGF12.1241	-6,457
Neu1.452	-6,710		Stk32c.724	-6,932
Rxra.2278	-6,874		Rpo1-1.311	-6,995
Mmp8.2236	-7,385		CLIC1.1126	-7,069
Stk32c.2134	-7,611		Mmp7.256	-7,097
CYP27B1.1252	-9,698		Mmp8.2236	-8,070
Mmp3.1478	-9,836		Ehhadh.1876	-8,702
Mmp7.256	-10,405		NDUFS8.807	-8,772
Ccnd1.3415	-10,711		FGF12.1933	-8,870
Sparc.1758	-10,861		BRMS1.1002	-9,205
Pld1.2050	-12,052		Pim1.602	-9,501
RNASE4.499	-12,578		Mmp7.170	-10,762
Tmprss2.1667	-13,777		Brd3.1245	-11,871
Oat.136	-15,116		Sparc.1196	-11,937
Rxra.2109	-15,450		Cdkn1a.639	-12,339
Neu1.1710	-20,524		Sparc.1898	-12,347
Acy3.902	-20,606		Ehhadh.2855	-14,082
Mapk13.417	-23,589		LIPH.291	-15,123
Mettl1.259	-37,513		CYP27B1.1244	-20,959
Met.3642	-44,385		Grhpr.361	-22,233
Hck.420	-69,178		Pim1.685	-24,115
Mmp8.708	-76,167		Mapk14.1095	-49,379
BAK1.1809	-79,266		Ccnd1.1856	-50,624
Mapk14.1095	-138,285		Parp2.574	-58,230
PMPCA.1841	-163,065		Bcl2l1.2091	-81,355
Mapk14.2590	-324,163		Mmp8.708	-101,143